INVESTIGATING MYOENDOTHELIAL SIGNALLING MECHANISMS IN RESISTANCE ARTERIES



Hamish Andrew Lachlan Lemmey

Magdalen College

University of Oxford

A thesis submitted for the degree of

Doctor of Philosophy

Trinity 2019

…all we know is still infinitely less than all that still remains unknown…

— *William Harvey, De Motu Cordis (1628)*

ABSTRACT

The regulation of resistance artery tone is a key determinant of blood pressure and tissue perfusion. It is well-established that endothelial cells (ECs) cause vasodilation by producing nitric oxide (NO) and endothelium-dependent hyperpolarization (EDH) in response to circulating vasoactive factors and flow. However, recent evidence has elucidated an intrinsic signalling mechanism, termed myoendothelial feedback, whereby ECs are activated during contraction independently of direct stimulation. The investigations presented in this thesis aimed to characterise myoendothelial feedback in isolated resistance arteries under isobaric and isometric conditions using pressure and wire myography, respectively. Most significantly, the profile of myoendothelial feedback differed between the two experimental approaches. In arteries studied isometrically, inhibition of NO and EDH production increased sensitivity to contractile agonists. On the other hand, blockade of endothelium-dependent vasodilation in pressurised arteries had no effect on submaximal contraction during sympathetic perivascular nerve stimulation and only augmented the maximum contractile response to agonists. Furthermore, arteries in the pressure myograph were less sensitive to NO, which may reflect pressure-induced smooth muscle Ca^{2+} sensitization and an abrogated influence of EC-dependent signalling. Additionally, a role for transient receptor potential cation channel subfamily V member 4 (TRPV4) in myoendothelial feedback was probed. However, while promising, this line of investigation was complicated by the observation that TRPV4 inhibition attenuated depolarization-dependent and -independent contraction, as well as endothelium-dependent vasodilation. The findings reported here have significant implications for the study of isolated resistance artery physiology and identify novel avenues of future research.

ACKNOWLEDGEMENTS

I am immensely grateful to my supervisors and mentors Professor Kim Dora and Professor Christopher Garland. I can say with absolute certainty I would not have made it through my doctorate without their expert guidance.

I wish to thank my colleagues Dr Lyudmyla Borysova and Dr Xi Ye, whose commitment to research was a constant source of inspiration, and my fellow DPhil student Joshua Smith, whose sense of humour was also a constant source of inspiration. I couldn't have asked for a better team to work with every day.

I am indebted to the British Heart Foundation for funding my studentship and providing me with the opportunity of a lifetime.

A very special thank you to my parents, Rosalind and Ian, and my sister Annabel, for their unwavering support — being away from them has without a doubt been the hardest part of my DPhil.

And finally, to my dear friends who have stood beside me throughout this journey; James Eaton, Joshua Fellowes, Lukas Lange, Adam Kenny, Tess Cooper, Sam Griffiths, Serban Ilca, Tim Sudmeier, Sophia Epstein, Alistair Inglis, and Ethan Cunningham, without whom this thesis would have been completed a year earlier.

PUBLICATIONS

Garland, C.J., Bagher, P., Powell, C., Ye, X., Lemmey, H.A.L., Borysova, L., and Dora, K.A. (2017). Voltage-dependent Ca^{2+} entry into smooth muscle during contraction promotes endothelium-mediated feedback vasodilation in arterioles. *Sci. Signal. 10*: eaal3806.

Lemmey, H.A.L., Ye, X., Ding, H.C., Triggle, C.R., Garland, C.J., and Dora, K.A. (2018). Hyperglycaemia disrupts conducted vasodilation in the resistance vasculature of db/db mice. *Vascul. Pharmacol. 103–105*: 29–35.

Pinkney, A.M.H., Lemmey, H.A.L., Dora, K.A., and Garland, C.J. (2017). Vasorelaxation to the nitroxyl donor isopropylamine NONOate in resistance arteries does not require perivascular calcitonin gene–related peptide. *Hypertension 70*: 587–593.

CONFERENCE COMMUNICATIONS

Lemmey, H. A. L, Ye, X., Garland, C. J., and Dora, K. A. Conducted dilation in the resistance vasculature in a mouse model of chronic hyperglycaemia. Poster presented at: Pharmacological aspects of microvascular cell-cell signalling and CVS disease; 2016 September 21-22; Oxford, England.

Lemmey, H. A. L., Ye, X., Garland, C. J., and Dora, K. A. Conducted dilation in the resistance vasculature in a mouse model of chronic hyperglycaemia. Poster presented at: 18th World Congress of Pharmacology; 2018 July 1-6; Kyoto, Japan.

Lemmey, H. A. L., Ye, X., Garland, C. J., and Dora, K. A. Hyperglycaemia disrupts conducted vasodilation in the resistance vasculature of db/db mice. Poster presented at: Europhysiology 2018; 2018 Sep 14-16; London, England.

Lemmey, H. A. L., Garland, C. J., and Dora, K. A. Nerve-mediated responses in isolated myogenic and non-myogenic arteries. Poster presented at: Experimental Biology 2019; 2019 April 6-9; Orlando, FL.

Lemmey, H. A. L., Garland, C. J., and Dora, K. A. Investigating myoendothelial feedback in resistance arteries under isometric and isobaric conditions. Poster presented at: Combined 13th International Symposium on Mechanisms of Vasodilatation and 7th International Symposium on Endothelium-Dependent Hyperpolarization; 2019 May 20-22; Rotterdam, The Netherlands.

CONTENTS

1.0 INTRODUCTION 1

1.1 MORPHOLOGY OF RESISTANCE ARTERIES 2

1.1.1 Myoendothelial junctions and vascular heterogeneity 2

1.2 INTRINSIC VASCULAR SMOOTH MUSCLE CONTRACTION AND RELAXATION 6

1.2.1 Depolarization-dependent contraction 6

1.2.2 Depolarization-independent contraction 8

1.2.3 Endothelium-independent relaxation 10

1.3 ENDOTHELIAL MODULATION OF VASCULAR TONE 12

1.3.1 Endothelium-dependent vasodilation 12

1.3.2 Myoendothelial feedback 14

1.4 THESIS AIM AND OBJECTIVES 16

2.0 MATERIALS AND METHODS 19

2.1 ANIMALS AND TISSUE PREPARATION 20

2.2 PRESSURE MYOGRAPHY 21

2.2.1 Artery cannulation and pressurization 21

2.2.2 Studying mesenteric arteries under isobaric conditions 24

2.2.3 Studying cremasteric and coronary arteries under isobaric conditions 26

2.2.4 EFS of pressurised arteries 29

2.2.5 Analysis of mesenteric artery diameter recordings 29

2.2.6 Analysis of cremasteric and coronary artery diameter recordings 30

2.3 WIRE MYOGRAPHY 31

2.3.1 Mounting of mesenteric arteries in a wire myograph 31

2.3.2 Studying mesenteric arteries under isometric conditions 33

2.3.3 Analysis of isometric tension recordings 33

2.4 IMMUNOHISTOCHEMISTRY 35

2.4.1 Immunostaining of pressurised arteries..... 35

2.4.2 Imaging immunohistochemistry preparations..... 35

2.5 SOLUTIONS AND DRUGS..... 36

2.6 STATISTICAL ANALYSES 39

3.0 INFLUENCE OF THE ENDOTHELIUM ON NEUROGENIC VASOCONSTRICTION IN PRESSURISED RESISTANCE ARTERIES..... 40

3.1 INTRODUCTION 41

3.1.1 Aims and hypotheses..... 42

3.2 MATERIALS AND METHODS..... 43

3.2.1 Pressure myography..... 43

3.2.2 EFS parameters 43

3.2.3 Inhibitors 43

3.2.4 Immunohistochemistry 47

3.3 RESULTS 48

3.3.1 EFS-induced vasoconstriction is attenuated during Ca_V and Na_V blockade 48

3.3.2 EFS-induced vasoconstriction is attenuated during α_1-AR and $P2X_1R$ antagonism 50

3.3.3 Blockade of endothelium-dependent vasodilation does not modulate EFS-induced vasoconstriction 54

3.3.4 EFS does not cause vasoconstriction of pressurised cremasteric arteries 56

3.3.5 Pressurised cremasteric arteries exhibit vasoconstriction to exogenously added PE and ATP 58

3.3.6 Mesenteric arteries are more densely innervated with sympathetic nerve varicosities than cremasteric arteries 60

3.4 DISCUSSION 63

3.5 CONCLUSIONS 71

4.0 MYOENDOTHELIAL FEEDBACK IN RESISTANCE ARTERIES UNDER ISOBARIC AND ISOMETRIC CONDITIONS 72

4.1 INTRODUCTION 73

4.1.1 Aims and hypotheses 76

4.2 MATERIALS AND METHODS 77

4.2.1 Pressure myography 77

4.2.2 Wire myography 77

4.2.3 Inhibitors 77

4.3 RESULTS 78

4.3.1 PE-mediated contraction is limited by the endothelium to a greater degree in arteries under isometric conditions than isobaric 78

4.3.2 NO and EDH limit contraction to ATP in arteries mounted in the wire myograph, but not pressure myograph..... 81

4.3.3 The mechanism of ACh-mediated vasodilation differs between arteries under isobaric and isometric conditions..... 84

4.3.4 Arteries mounted in the wire myograph are more responsive to NO donors than pressurised arteries..... 88

4.3.5 PE-mediated vasoconstriction is sensitive to Ca_V blockade in arteries under isometric and isobaric conditions..... 90

4.3.6 ROCKII inhibition in pressurised arteries decreases contraction to PE and increases relaxation to ACh and exogenously-added NO 93

4.4 DISCUSSION 96

4.5 CONCLUSIONS 106

5.0 THE ROLE OF TRPV4 DURING RELAXATION AND CONTRACTION OF RESISTANCE ARTERIES 107

5.1 INTRODUCTION 108

5.1.1 Aims and hypotheses..... 111

5.2 MATERIALS AND METHODS 112

5.2.1 Pressure myography 112

5.2.2 Wire myography 112

5.2.3 Inhibitors 112

5.3 RESULTS 113

5.3.1 Endothelium-dependent vasodilation is facilitated by activation of eNOS, IK_{Ca} and SK_{Ca} 113

5.3.2 IK_{Ca}-mediated EDH is dependent on TRPV4 opening 116

5.3.3 Ca_V and TRPV4 activation facilitate PE-induced contraction 119

5.3.4 Myoendothelial feedback during α_1-AR stimulation is not prevented by TRPV4 blockade 122

5.3.5 Myoendothelial feedback during α_1-AR stimulation is not prevented by Ca_V blockade 125

5.3.6 RyR activation limits contraction but does not contribute to relaxation 128

5.3.7 TRPV4 mediates Ca_V activation during VSM depolarization 131

5.3.8 TRPV4 activation causes contraction during blockade of endothelium-dependent relaxation 133

5.3.9 Myogenic tone and endothelium-dependent vasodilation in coronary arteries are not modulated by NOS inhibition 135

5.3.10 TRPV4 activation contributes to myogenic tone in coronary arteries 137

5.4 DISCUSSION 139

5.5 CONCLUSION 147

6.0 FUTURE DIRECTIONS 148

7.0 REFERENCES 154

FIGURES

Figure 1.1.1 A myoendothelial gap junction in the rat middle cerebral artery 4

Figure 1.2.2 Mechanisms of depolarization-dependent and -independent VSM contraction in resistance arteries 9

Figure 1.3.2 Mechanisms of endothelium-dependent relaxation and myoendothelial feedback in resistance arteries 17

Figure 2.2.1 Pressure myography apparatus 23

Figure 2.2.2 Excised mesentery and pressurised mesenteric artery 25

Figure 2.2.3 Excised cremaster muscle and pressurised cremasteric artery 27

Figure 2.2.4 Excised heart and pressurised coronary artery 28

Figure 2.3.1 Wire myograph apparatus 32

Figure 3.2.1 EFS apparatus 45

Figure 3.2.2 EFS-induced vasoconstriction in pressurised mesenteric arteries 46

Figure 3.3.1 Effect of Ca_V and Na_V blockers on EFS-induced vasoconstriction in pressurised mesenteric arteries 49

Figure 3.3.2 Effect of α_1-AR and $P2X_1R$ antagonism on EFS-induced vasoconstriction in pressurised mesenteric arteries 51

Figure 3.3.3 Summary of the effect of antagonists on EFS-induced vasoconstriction in pressurised mesenteric arteries 53

Figure 3.3.4 Effect of inhibition of NO and EDH production on EFS-induced vasoconstriction 55

Figure 3.3.5 Effect of EFS in pressurised cremasteric arteries 57

Figure 3.3.6 PE- and ATP-induced vasoconstriction in pressurised cremasteric arteries 59

Figure 3.3.7 Tyrosine hydroxylase staining in mesenteric arteries 61

Figure 3.3.8 Tyrosine hydroxylase staining in cremasteric arteries 62
Figure 3.4.1 Proposed mechanism of EFS-induced vasoconstriction in the current investigation 66
Figure 4.3.1 Effect of blockade of NO and EDH production on PE-induced contraction in mesenteric arteries under isobaric and isometric conditions..... 79
Figure 4.3.2 Effect of blockade of NO and EDH production on ATP-induced contraction in mesenteric arteries under isobaric and isometric conditions..... 82
Figure 4.3.3 Effect of inhibition of NO and EDH production on ACh-induced relaxation in mesenteric arteries under isobaric and isometric conditions..... 86
Figure 4.3.4 DEA/NO- and SNOG-induced relaxation in mesenteric arteries under isobaric and isometric conditions 89
Figure 4.3.5 Effect of Ca_V blockade on PE-induced contraction in mesenteric arteries under isobaric and isometric conditions 91
Figure 4.3.6 Effect of Glycyl-H 1152 on PE-induced vasoconstriction in pressurised mesenteric arteries..... 94
Figure 4.3.7 Effect of Glycyl-H 1152 on DEA/NO- and ACh-induced vasodilation in pressurised mesenteric arteries 95
Figure 4.4.1 Proposed mechanism of pressure-induced ROCKII activation in current investigation 103
Figure 5.3.1 Effect of NOS, IK_{Ca} and SK_{Ca} inhibition on ACh-induced relaxation in mesenteric arteries..... 114

Figure 5.3.2 Effect of TRPV4, NOS and SK_{Ca} inhibition on ACh-induced relaxation in mesenteric arteries 117
Figure 5.3.3 Effect of Ca_v and TRPV4 blockade on PE-induced contraction in mesenteric arteries 120
Figure 5.3.4 Effect of TRPV4, NOS, SK_{Ca} and IK_{Ca} inhibition on PE-induced contraction in mesenteric arteries 123
Figure 5.3.5 Effect of Cav, NOS, IK_{Ca} and SK_{Ca} inhibition on PE-induced contraction in mesenteric arteries 126
Figure 5.3.6 Effect of RyR and TRPV4 blockade on PE-induced contraction and ACh-induced relaxation in mesenteric arteries 129
Figure 5.3.7 Effect of Ca_v, TRPV4, NOS, IK_{Ca} and SK_{Ca} inhibition on 45 mM K_+-induced contraction in mesenteric arteries 132
Figure 5.3.8 Effect of TRPV4 and Ca_v blockade on GSK 1016790A-induced contraction during inhibition of endothelium-dependent relaxation 134
Figure 5.3.9 Effect of NOS inhibition on ACh- and GSK 1016790A-induced relaxation in coronary arteries 136
Figure 5.3.10 Effect of TRPV4 and Ca_v blockade on coronary artery myogenic tone 138
Figure 5.4.1 Proposed mechanism of TRPV4-dependent relaxation and contraction in the current investigation 146

TABLES

Table 1.3.1 Chronological summary of published studies into myoendothelial feedback in isolated resistance arteries 18

Table 2.5.1 List of drugs and compounds used in the current investigations..... 38

ABBREVIATIONS

ACh	Acetylcholine
AKAP150	A-kinase anchoring protein 150
AngII	Angiotensin II
AP	Apamin
AR	Adrenoceptor
ATP	Adenosine triphosphate
BK_{Ca}	Large-conductance Ca^{2+}-activated K^+ channel
CaCC	Ca^{2+}-activated Cl^- channel
Ca_v	L-type voltage-gated Ca^{2+} channel
EC	Endothelial cell
DEA/NO	Diethylamine NONOate
EDH	Endothelium-dependent hyperpolarization
EET	Epoxyeicosatrienoic acid
EFS	Electrical field stimulation
eNOS	Endothelial nitric oxide synthase
GPCR	G protein-coupled receptor
IK_{Ca}	Intermediate-conductance Ca^{2+}-activated K^+ channel
IP_3	Inositol trisphosphate
IP_3R	Inositol trisphosphate receptor
K_{Ca}	Ca^{2+}-activated K^+ channel
L-NAME	N_G-nitro-L-arginine methyl ester
mAChR	Muscarinic acetylcholine receptor
MEGJ	Myoendothelial gap junction
MEP	Myoendothelial projections

MLCP	Myosin light-chain phosphatase
NAD	Noradrenaline
Na_v	Voltage-gated Na^+ channel
Nif	Nifedipine
NO	Nitric oxide
NOS	Nitric oxide synthase
P2XR	ATP-gated purinoceptor, subclass X
P2YR	ATP- gated purinoceptor, subclass Y
PE	Phenylephrine
PKC	Protein kinase C
RhoA	Ras homolog gene family, member A
RN	RN 1734
ROC	Receptor-operated channel
ROCK	Rho-associated protein kinase
RyR	Ryanodine receptor
SK_{Ca}	Small-conductance Ca^{2+}-activated K^+ channel
SR	Sarcoplasmic reticulum
SNOG	S-Nitrosoglutathione
TR	TRAM-34
TRP	Transient receptor potential
TRPV4	Transient receptor potential cation channel subfamily V member 4
TTX	Tetrodotoxin
VSM	Vascular smooth muscle
VSMC	Vascular smooth muscle cell

1.0 INTRODUCTION

1.1 MORPHOLOGY OF RESISTANCE ARTERIES

Terminal resistance arteries, arteries of diameter < 500 µm, represent the region along the vascular tree where the largest drop in blood pressure occurs. They are characterised by a large wall to lumen ratio, dynamic vascular tone and rich perivascular nerve innervation. Furthermore, resistance artery vascular smooth muscle cells (VSMCs) are intimately coupled with the underlying endothelial cells (ECs) allowing for efficient and robust heterocellular communication (Garland et al., 2011a; Straub et al., 2014). Many intrinsic and extrinsic factors regulate the contractile state of these arteries and ensure blood flow and pressure meet the demands of the surrounding tissue. Furthermore, abnormal resistance artery vasoconstriction and vasodilation contribute to the onset and progression of several cardiovascular diseases and, subsequently, the signalling pathways which govern their function are the subject of much research (Westcott and Segal, 2013).

1.1.1 Myoendothelial junctions and vascular heterogeneity

A physical interaction between VSMCs and ECs was first observed in canine coronary arteries and arterioles by Moore and Ruska (1957) in the form of endothelial extensions that made contact with the vascular smooth muscle (VSM) by penetrating the internal elastic lamina that separates them. These cellular extensions, later termed myoendothelial projections (MEPs), allow for bidirectional signalling between ECs and VSMCs within resistance arteries. MEPs have since been observed with electron microscopy in several species and vascular beds including rat (Sandow et al., 2002), mouse (Dora et al., 2003) and

human (Chadha et al., 2011) mesenteric arteries, hamster retractor muscle feed arteries (Tran et al., 2012), and rat cremasteric (McSherry et al., 2006) and middle cerebral arteries (McNeish et al., 2006) (see Figure 1.1.1). Heterocellular communication is facilitated by myoendothelial gap junctions (MEGJs) localised to MEPs, which are permeable to various ions, second messengers and electrical signals. MEPs are a unique structural trait of resistance vessels, and their abundance is inversely proportional to artery diameter. Such a trend was reported during a direct comparison of the physical contacts between VSMCs and ECs in rat mesenteric and femoral arteries (Sandow et al., 2002). MEGJs were observed in mesenteric arteries, which contained ~5 layers of VSM, but were absent in larger femoral arteries, which had roughly twice the number of VSM layers. The presence of MEPs conveyed an ability for hyperpolarization to spread from ECs to VSMCs, which didn't occur in femoral arteries. The conduction of electrical signals within and between the endothelial and smooth muscle layers in resistance arteries is a pivotal aspect of their physiology and considered to play an essential role in the maintenance of blood pressure and supply (Garland et al., 2011a).

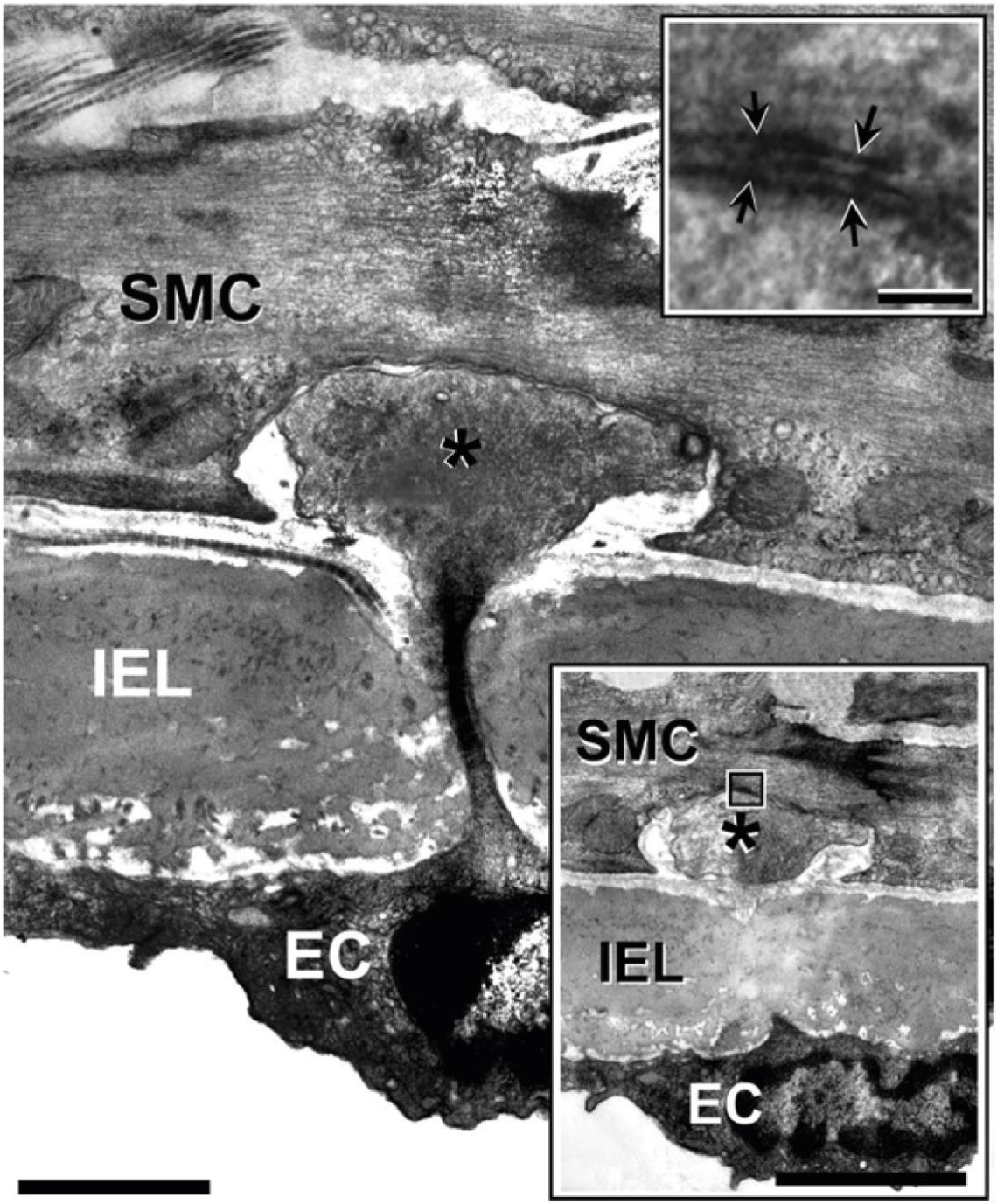

SMC
IEL
EC
SMC
IEL
EC

Figure 1.1.1 A myoendothelial gap junction in the rat middle cerebral artery. Transmission electron micrograph of a rat middle cerebral artery wall with a projection arising from an EC indicated by an asterisk. The stalk of the projection is ~0.1 µm across and the bulbous enlargement at the end of the projection is ~1.2 µm across at the widest point. The lower inset is a micrograph 4 serial sections (~0.4 µm) past the larger micrograph. The box in the lower inset indicates the region magnified in the upper inset. The pentalaminar structure at the interface between the EC projection and the SMC, characteristic of a gap junction, is indicated by the arrows in the upper inset. SMC, smooth muscle cell; IEL, internal elastic lamina; EC, endothelial cell. Scale bar = 0.5 µm; scale bar in upper inset = 0.025 µm; scale bar in lower inset = 1 µm. Adapted from McNeish et al. (2006).

1.2 INTRINSIC VASCULAR SMOOTH MUSCLE CONTRACTION AND RELAXATION

Regulation of resistance artery tone is multi-faceted and involves several intracellular signalling pathways that integrate input from different sources including ECs, perivascular nerves, circulating blood and the surrounding local tissue. Contraction is primarily driven by a rise in intracellular Ca^{2+} following influx from the extracellular space or release from intracellular stores, such as the sarcoplasmic reticulum (SR). Ca^{2+} forms a complex with cytosolic calmodulin to activate myosin light chain kinase (MLCK), which phosphorylates myosin light chain and facilities crossbridge formation between myosin and actin filaments, generating tension. $[Ca^{2+}]_i$ declines when the VSM is hyperpolarized, resulting in the closure of L-type voltage-gated Ca^{2+} channels (Ca_Vs) which represent the main mechanism of Ca^{2+} entry, or intracellular Ca^{2+} is actively removed from the cytosol by plasmalemmal and sarcolemmal pumps. In the absence of intracellular Ca^{2+} MLCK activity declines, allowing its regulatory counterpart, myosin light chain phosphatase (MLCP), to dominate and detach the crossbridges, thus promoting relaxation (Brozovich et al., 2016).

1.2.1 Depolarization-dependent contraction

The VSM plasma membrane contains a range of voltage-sensitive ion channels which play a central role in dictating vascular contractility. Stimulation of metabotropic receptors coupled to G proteins containing the G_q α-subunit, such as the α_1-adrenoceptor (AR), causes the production of diacylglycerol (DAG) and

inositol trisphosphate (IP_3). DAG opens receptor-operated channels (ROCs), which conduct an inward cation current and depolarize the VSMC. The decrease in membrane potential activates Ca_Vs and, subsequently, Ca^{2+} entry (Brozovich et al., 2016). Examples of ROCs include members of the transient receptor potential (TRP) cation channel superfamily, of which over a dozen have been shown to be expressed in vascular myocytes (Earley and Brayden, 2015). VSM membrane potential is also controlled by Ca^{2+}-activated Cl^--channels (CaCCs), through which an efflux of Cl- mediates a positive inward current, and ionotropic adenosine triphosphate (ATP)-gated purinoceptors, subclass X (P2XR), which facilitate a rapid and localised influx of cations (Lamont et al., 2003; Nausch et al., 2012) (see Figure 1.2.2A).

In addition to agonist-mediated voltage-dependent contraction, resistance arteries exhibit a basal level of depolarization in response to intraluminal pressure, which causes Ca_V-dependent vasoconstriction. This phenomenon, known as myogenic tone, was first observed over a century ago and was hypothesised to facilitate the maintenance of blood flow over a range of perfusion pressures (Bayliss, 1902). Later investigations demonstrated pressure-induced contraction is modulated by, but not dependent on, luminal flow, perivascular nerve activation and factors arising from the endothelium (Anschütz and Schubert, 2005; Brozovich et al., 2016; Garland et al., 2017). The exact mechanism, or mechanosensor, responsible for the development of myogenic tone remains to be elucidated, but recent evidence has demonstrated a role for

TRP channels in pressure-induced Ca_V activation (Earley and Brayden, 2015). (see Figure 1.2.2A).

1.2.2 Depolarization-independent contraction

Artery contraction can also occur independent of a change in membrane potential, but this is thought to be more typical of larger arteries which have relatively few voltage-sensitive channels (Godfraind, 1983; Bowles et al., 1997). The opening of plasmalemmal TRP channels and P2XRs can contribute to the rise in $[Ca^{2+}]_i$ without opening Ca_Vs, whilst IP_3 causes Ca^{2+} release from intracellular stores by activating its receptor in the SR membrane (Earley and Brayden, 2015; Brozovich et al., 2016). Furthermore, a role for Ras homolog gene family, member A (RhoA) signalling in depolarization-independent contraction has also been demonstrated. G protein-coupled receptors (GPCRs) linked to G proteins containing the G_{12} α-subunit sensitise the VSM to Ca^{2+} by activating RhoA and, thereafter, Rho-associated protein kinase (ROCK), which phosphorylates and inhibits MLCP. Thus, increased RhoA activity shifts the balance between MLCP and MLCK to favour contraction. VSM Ca^{2+} sensitization is also mediated by protein kinase C (PKC), which is activated by cytosolic Ca^{2+} and DAG. PKC, along with ROCK, activates CPI-17 which is an inhibitor of MLCP (Swärd et al., 2003). Overall, second messengers of VSMC GPCRs and Ca^{2+} influx through plasmalemmal cation channels can increase contractility in the absence of depolarization and Ca_V opening (see Figure 1.2.2B).

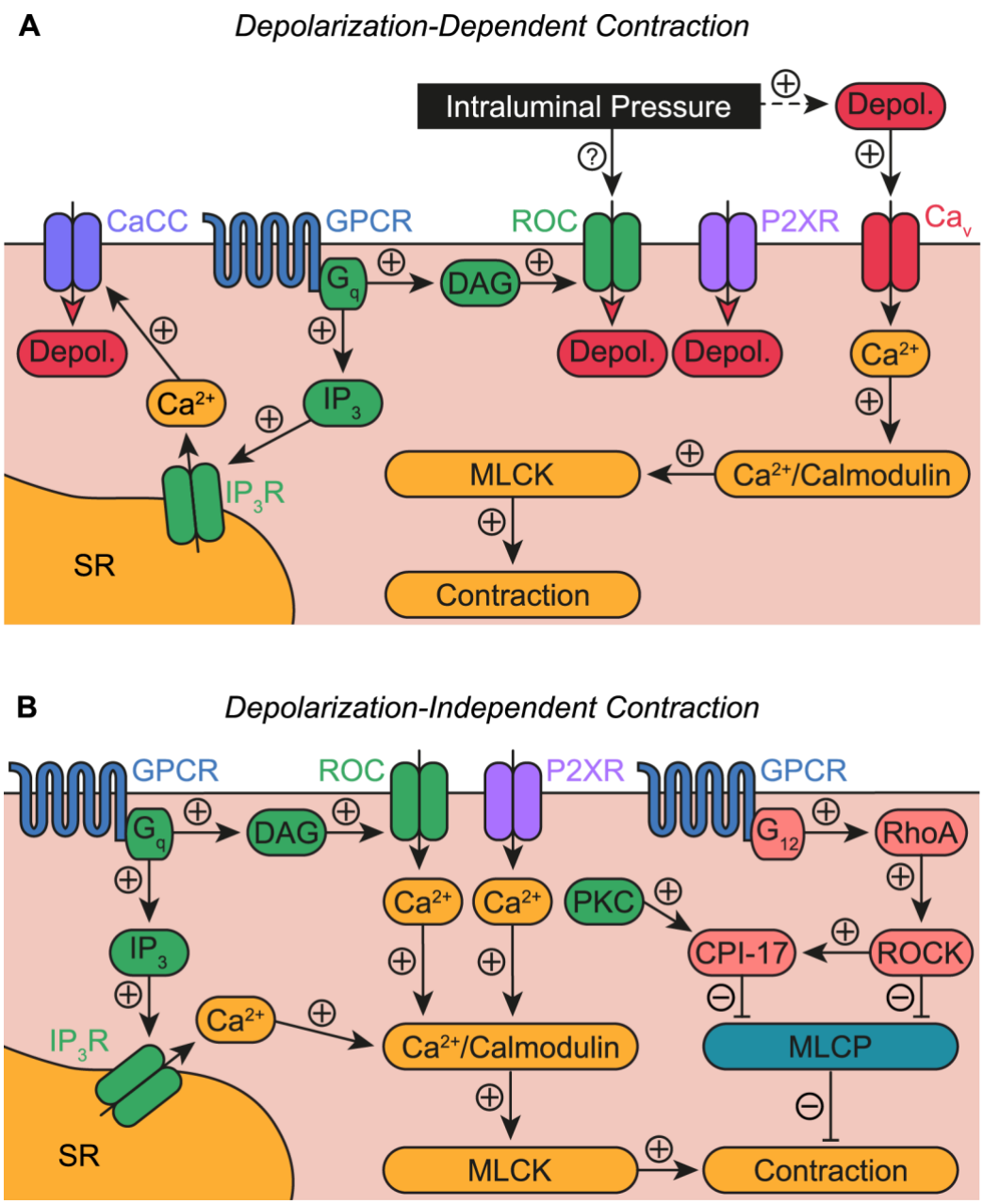


Figure 1.2.2 Mechanisms of depolarization-dependent (**A**) and -independent (**B**) VSM contraction in resistance arteries. Arrows with a red arrowhead indicate direction of positive current. Arrows with a dashed line represent an indirect effect.

1.2.3 Endothelium-independent relaxation

Receptors in the VSM plasmalemma and sarcolemma are also capable of mediating relaxation. Whilst noradrenaline (NAD) stimulates α_1-ARs to cause vasoconstriction, it can also bind β-ARs on VSMCs to produce relaxation. These receptors are coupled to G proteins containing the G_s α-subunit which stimulate adenylyl cyclase to cause the formation of cyclic adenosine monophosphate from ATP. Cyclic adenosine monophosphate activates protein kinase A (PKA) which phosphorylates multiple downstream targets, ultimately decreasing myosin-actin crossbridge formation. PKA encourages Ca^{2+} expulsion from the cytosol and sequestration into the SR, reducing the $[Ca^{2+}]_i$, and increases the open-state probability of K^+ channels to hyperpolarize the VSM and close Ca_Vs. Furthermore, it directly phosphorylates and inhibits MLCK, which desensitises the tissue to Ca^{2+} (Brozovich et al., 2016; Tykocki et al., 2017).

Another mechanism responsible for opposing VSM contraction involves an interaction between ryanodine receptors (RyRs) in the SR membrane and large-conductance Ca^{2+}-activated K^+ channels (BK_{Ca}s) in the plasma membrane. In VSMCs, activation of a cluster of RyRs causes a small, localised Ca^{2+} event, termed a Ca^{2+} spark, which can stimulate the opening of neighbouring BK_{Ca}s, leading to an efflux of K^+ and hyperpolarization. This is in contrast to skeletal and cardiac myocytes wherein the release of Ca^{2+} through RyRs causes myocyte contraction (Earley et al., 2005; Brozovich et al., 2016). Additionally, transient receptor potential cation channel subfamily V member 4 (TRPV4) expressed in the VSM membrane has been shown to facilitate the activation of the RyR-BK_{Ca}

axis. In denuded mouse and rat cerebral arteries, TRPV4 activation caused the recruitment of Ca^{2+} sparks and accompanying membrane hyperpolarization, leading to the hypothesis Ca^{2+} influx through TRPV4 activates RyRs and serves to limit the degree of contraction interpedently of the endothelium (Earley et al., 2005; Mercado et al., 2014).

1.3 ENDOTHELIAL MODULATION OF VASCULAR TONE

The endothelium regulates resistance artery contractility by secreting diffusible factors and generating hyperpolarization in response to vasoactive substances. The latter is facilitated by the MEPs which allow for direct electrical communication with the VSM layer. Like VSMCs, signalling within ECs is dictated by ion flux across the membrane with a particular dependence on Ca^{2+} activity. However, while a rise in VSMC $[Ca^{2+}]_i$ is associated with contraction, the opposite is true for the endothelium. Increased EC $[Ca^{2+}]_i$, as a result of receptor stimulation or activation during contraction, causes the production of agents which act in a paracrine manner on the overlaying VSM (Garland et al., 2011a).

1.3.1 Endothelium-dependent vasodilation

The obligatory role for the endothelium in vasodilation was elucidated by the Nobel Laureate Robert F. Furchgott, who demonstrated removing ECs from strips of rabbit thoracic aorta abrogated the ability for acetylcholine (ACh) to cause relaxation (Furchgott and Zawadzki, 1980). It is now well-established the endothelium can decrease vascular tone by producing several dilators including nitric oxide (NO), prostacyclin, hydrogen peroxide, epoxyeicosatrienoic acid (EET) and K^+, and through the generation of endothelium-derived hyperpolarization (EDH). The relative contribution of these factors to endothelium-dependent vasodilation varies with vessel size, vascular bed, species and mechanism of stimulation (Luksha et al., 2009; Straub et al., 2014).

Activation of GPCRs on ECs by agonists like ACh causes an increase in $[Ca^{2+}]_i$, similar to VSMCs, which binds to calmodulin and stimulates endothelial NO synthase (eNOS) to mediate the formation of NO from L-arginine and oxygen. NO diffuses into VSMCs where it activates soluble guanylyl cyclase and, in turn, kinases which promote relaxation, such protein kinase G. NO can also directly open VSM BK_{Ca}s, facilitating K^+ efflux and hyperpolarization (Garland et al., 2011a) (see Figure 1.3.2).

Whilst nitric oxide synthase (NOS) inhibition, with antagonists such as N_G-nitro-L-arginine methyl ester (L-NAME), significantly attenuates endothelium-dependent vasodilation in large vessels, it only partially inhibits the response in resistance arteries. The residual relaxation is characterised by VSM hyperpolarization and is prevented in the presence of raised $[K^+]_o$. This L-NAME-insensitive component can be attributed to the efflux of K^+ through EC ion channels, which generates EDH that spreads to the adjacent VSM through MEPs and closes Ca_Vs. Diffusible EDH factors can act in concert, examples being an increase in $[K^+]$ in the myoendothelial space leading to hyperpolarization by opening VSM inwardly-rectifying K^+ channels and activating the Na^+/K^+-ATPase, and EETs produced by the endothelium may activate the RyR-BK_{Ca} complex (Earley et al., 2005; Straub et al., 2014). Regardless of the factor responsible, endothelial small- and intermediate-conductance Ca^{2+}-activated K^+ channels (SK_{Ca}, IK_{Ca}) play a crucial role in producing the hyperpolarizing signal. Blockade of SK_{Ca} and IK_{Ca} with their respective antagonists, apamin and TRAM-34, significantly attenuates ACh-induced VSM hyperpolarization and the associated

reduction in vascular tone (Garland et al., 2011a; Lemmey et al., 2018). As well as opening in response to elevated EC $[Ca^{2+}]_i$, both channels colocalise with MEPs and have been shown to be strategically positioned close to ROCs and intracellular Ca^{2+} stores, which optimises their activation during direct EC stimulation with GPCR agonists and indirect activation during vasoconstriction (Dora et al., 2008; Ledoux et al., 2008; Bagher et al., 2012) (see Figure 1.3.2).

1.3.2 Myoendothelial feedback

Examination of EC-dependent agonist- and flow-induced vasodilation has historically been used to assess the role of the endothelium in modulating vasoreactivity, but there is also convincing evidence that the endothelium limits VSM contraction via intrinsic mechanisms that can operate in the absence of direct stimulation and flow. This phenomenon, termed myoendothelial feedback, is stimulated following vasoconstrictor-mediated rises in SMC Ca^{2+} by the diffusion of Ca^{2+} and/or IP_3 into ECs, relying on MEGJs. This trigger can be further amplified by EC Ca^{2+} influx and release to facilitate NO and/or EDH production, subsequently forming a negative feedback loop (see Figure 1.3.2). Dora et al. (1997) reported elevated $[K^+]_o$, which depolarizes the VSM and opens Ca_Vs, and the α_1-AR agonist phenylephrine (PE) caused vasoconstriction of hamster cheek arterioles and a parallel increase in EC $[Ca^{2+}]i$; a significant observation considering Ca_Vs and α_1-ARs aren't expressed in the endothelium. The increase in endothelial Ca^{2+} activity was postulated to mediate NO production, as NOS inhibition with L-NAME potentiated the contractile response. Since this pioneering discovery, myoendothelial feedback has been reported in a range of different

vascular beds (see Table 1.3.1). Crucially, the EC Ca^{2+} events responsible for the initiation of myoendothelial feedback reportedly occur at sites of MEPs and are capable of causing IK_{Ca}-dependent hyperpolarization of VSM (Nausch et al., 2012; Hong et al., 2018).

From hereon in, the use of the term ‘myoendothelial feedback’ in this thesis specifically refers to the intrinsic endothelium-dependent feedback mechanism within resistance arteries which negatively regulates contraction and relies on the transmission of a signal from VSMCs to adjacent ECs through MEGJs. This should not to be confused with the more general term ‘myoendothelial signalling’ which also encompasses endothelium-dependent vasodilation and vasoconstriction, that do not rely on the presence of MEPs or prior activation of the VSM and can occur in arteries larger than resistance vessels.

1.4 THESIS AIM AND OBJECTIVES

Myoendothelial feedback likely plays a ubiquitous role throughout the resistance vasculature, representing the primary physiological mechanism regulating NO and EDH production and, consequently, blood pressure and tissue perfusion. Furthermore, elucidating the pathways which govern the intrinsic feedback loop could lead to the development of novel therapies for vascular dysfunction. This is the rationale for the current investigation. This thesis aims to explore myoendothelial feedback in isolated rat mesenteric, cremasteric and coronary arteries, which have previously been used to probe how signalling through myoendothelial projections modulates resistance artery tone (Dora et al., 2000; Tuttle and Falcone, 2001; Garland et al., 2017; Wei et al., 2018). More specifically, the objectives of the enclosed chapters were to characterise the influence of myoendothelial feedback on neurogenic vasoconstriction (see Chapter 3.0), to compare the ability for the endothelium to modulate contraction in arteries under isobaric and isometric conditions (see Chapter 4.0), and probe the potential involvement of TRPV4 in the intrinsic feedback mechanism (see Chapter 5.0).

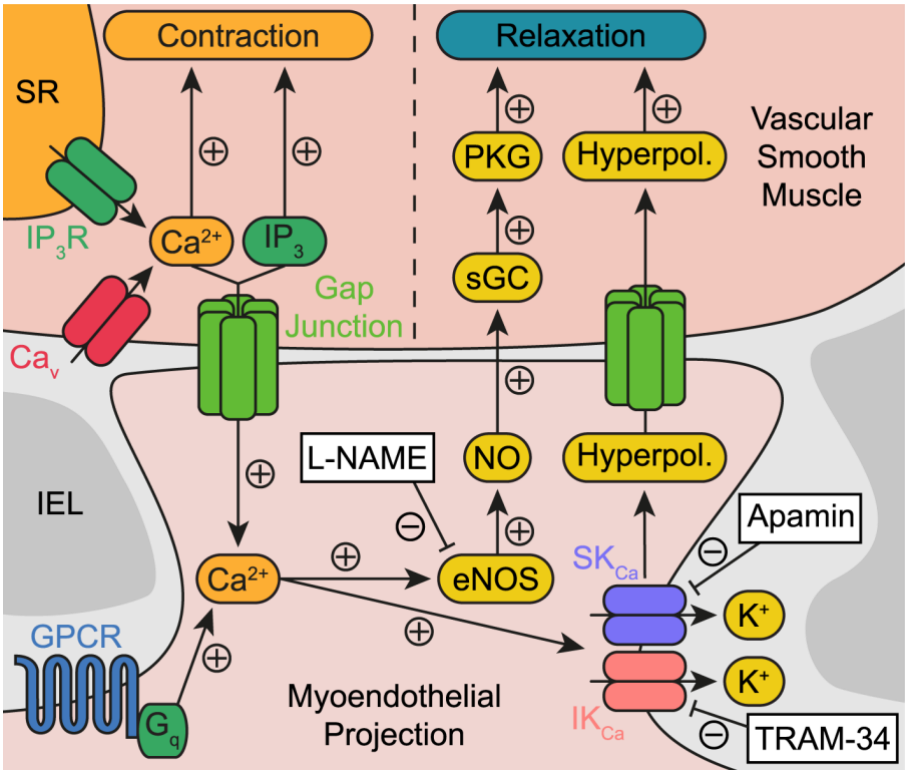


Figure 1.3.2 Mechanisms of endothelium-dependent relaxation and myoendothelial feedback in resistance arteries. Boxes with curved edges represent intracellular signalling components. Boxes with sharp edges represent antagonists.

Table 1.3.1 Chronological summary of published studies into myoendothelial feedback in isolated resistance arteries. * denotes studies which utilised pressure myography; # denotes studies which utilised wire myography.

			Reported Mechanism of…	
	Vascular Bed	**VSM Agonist**	**EC Activation**	**Relaxation**
Dora et al. (1997)	Hamster Cheek Pouch*	PE, Elevated $[K^+]_o$	Ca^{2+}	NO
Dora et al. (2000)	Rat Mesentery #	PE		NO, EDH
Yashiro and Duling (2000)	Hamster Cremaster Muscle *	PE	Ca^{2+}	EDH
Tuttle and Falcone, (2001)	Rat Cremaster Muscle *	NAD		NO
Nausch et al. (2012)	Mouse Mesentery *	EFS	IP_3	EDH
Tran et al. (2012)	Hamster Retractor Muscle *	PE	IP_3	EDH
Garland et al. (2017)	Rat Cremaster Muscle *	PE, Elevated $[K^+]_o$, BayK 8644	Ca^{2+}	EDH
Wei et al. (2018)	Rat Mesentery #	NAD, U 46619, EFS	IP_3	NO, EDH
Hong et al. (2018)	Mouse Mesentery *	PE	IP_3	NO, EDH

2.0 MATERIALS AND METHODS

2.1 ANIMALS AND TISSUE PREPARATION

All animal procedures were conducted in accordance with the University of Oxford local ethical guidelines, the ARRIVE guidelines and the UK Home Office Animal (Scientific Procedures) Act, 1986.

Male Wistar rats (7-8 weeks old, 200-250 g; Charles River, UK) were used in the present investigations. Animals were housed in individually ventilated cages under a 12:12 h light/dark cycle and at 20–22°C. Standard chow and water were available *ad libitum*. Rats were killed in accordance with schedule 1 of the Animals (Scientific Procedures) Act, 1986, by rising CO_2 and confirmed with cervical dislocation. The mesentery, cremaster muscle and heart were excised and collected in ice-cold MOPS-buffered solution (see Section 2.5).

The isolated tissue was pinned down in a Sylgard-coated dissection dish containing ice-cold MOPS-buffered solution (see Figures 2.2.2 to 2.2.4). Arteries to be studied were then carefully isolated from adhering connective tissue, adipocytes, cardiomyocytes and skeletal muscle.

2.2 PRESSURE MYOGRAPHY

The *in vitro* study of pressurised small artery structure and function, known as pressure myography, was established by Duling et al. (1981) who adapted a system originally designed for the study of isolated renal tubules. In brief, an artery or arteriole is excised from its tissue bed, submerged in an organ bath chamber and cannulated at both ends to perfuse the lumen and introduce intraluminal pressure. Changes in diameter can then be monitored during stimulation with vasoactive agents and altered intravascular pressure. Arteries studied in this manner are under isobaric conditions, meaning the pressure within the artery remains constant whilst the diameter is free to change during smooth muscle contraction and relaxation. Pressure myography can be used in combination with other techniques, such as fluorescence microscopy and immunohistochemistry, which would be otherwise difficult to conduct in arteries *in vivo*.

2.2.1 Artery cannulation and pressurization

Mesenteric, cremasteric and interventricular septal (referred to as coronary from here on in) arteries were cut into ~2 mm segments. Shorter cremasteric and coronary segments were sometimes used due to the presence of side-branches. Artery segments were then transferred to a 2 mL temperature-regulated confocal imaging chamber (RC-27, Warner Instruments, USA) containing MOPS-buffered solution (see Section 2.5). The chamber was secured to the stage of an inverted microscope (FluoView300, Olympus, Japan) with a heating platform (PH-6, Warner Instruments, USA) which was connected to a temperature controller (TC-

324C, Warner Instruments, USA). Arteries were visualised using a 10×/0.3NA objective (Olympus, Japan) and images recorded at 1 Hz. Changes in artery diameter were recorded using FluoView software (v5.0, Olympus, Japan).

Both sides of the artery were cannulated onto glass micropipettes (inner diameter, ~70 µm; outer diameter, ~140 µm) and secured with Ethilon nylon sutures (Ethicon, USA). One pipette was attached to a pressure head which could be adjusted to modulate the intraluminal pressure of the artery. The preparation was superfused with MOPS-buffered solution at a flow rate of 2 $mL.min^{-1}$ (see Section 2.5). The solution in the chamber was heated to ~37°C for mesenteric and coronary arteries, and ~34°C for cremasteric arteries. Care was taken to ensure the temperature of the solution would remain constant when the superfusion was switched on and off. Following a 15 min equilibration period, arteries were gradually pressurised and longitudinally stretched to avoid lateral bowing of the vessel. A leak test was also performed to ensure there were no side-branches in the artery segment and the sutures adequately secured the artery to the pipettes.

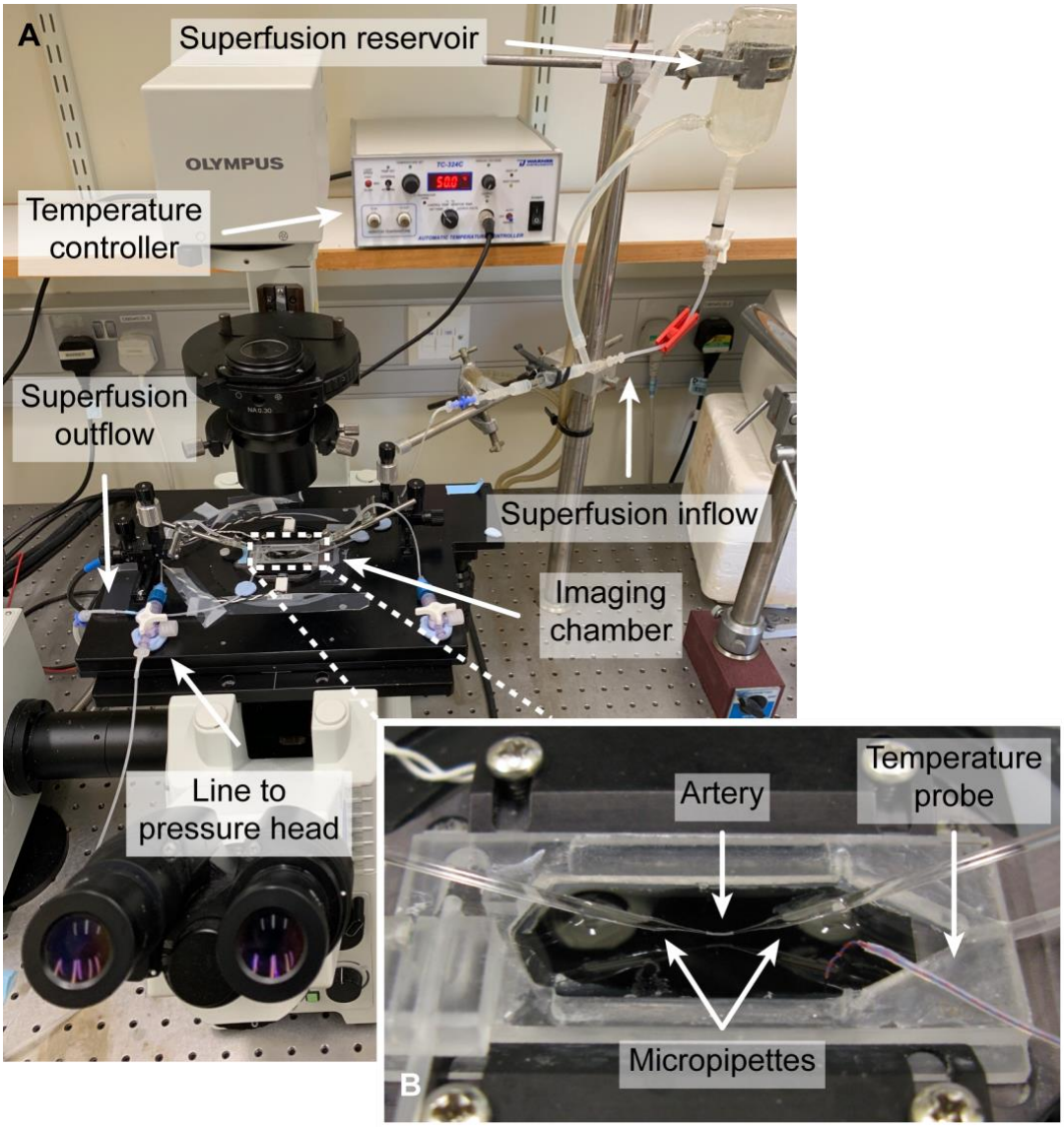


Figure 2.2.1 Pressure myography apparatus. (**A**) Image of confocal microscope used for pressure myography experiments. (**B**) Image of imaging chamber with mounted artery

2.2.2 Studying mesenteric arteries under isobaric conditions

Mesenteric arteries were pressurised to 70 mmHg and vessel health assessed with PE and ACh (ACh), a muscarinic ACh receptor (mAChR) agonist, to stimulate endothelium-dependent vasodilation. Only arteries which exhibited robust and maintained vasoconstriction to 1 µM PE and maximal vasodilation to 1 µM ACh were considered viable for experimentation. For experiments examining vasodilation, arteries were first preconstricted with a submaximal concentration of PE to stimulate ~70% vasoconstriction. At the end of every experiment with mesenteric arteries, maximum vasoconstriction was stimulated by exposure to 1 µM U 46619, a thromboxane receptor agonist, and 10 µM PE to obtain maximum vasoconstriction and the minimum diameter of the vessel. For each individual pressure myography experiment with mesenteric arteries, vasoreactivity to various agonists was assessed in the absence and presence of an antagonist or blocker. Arteries were only incubated with multiple inhibitors where indicated, and inhibitors were not washed out after their addition to eliminate the possibility of irreversible/carry-over effects of drugs between treatments.

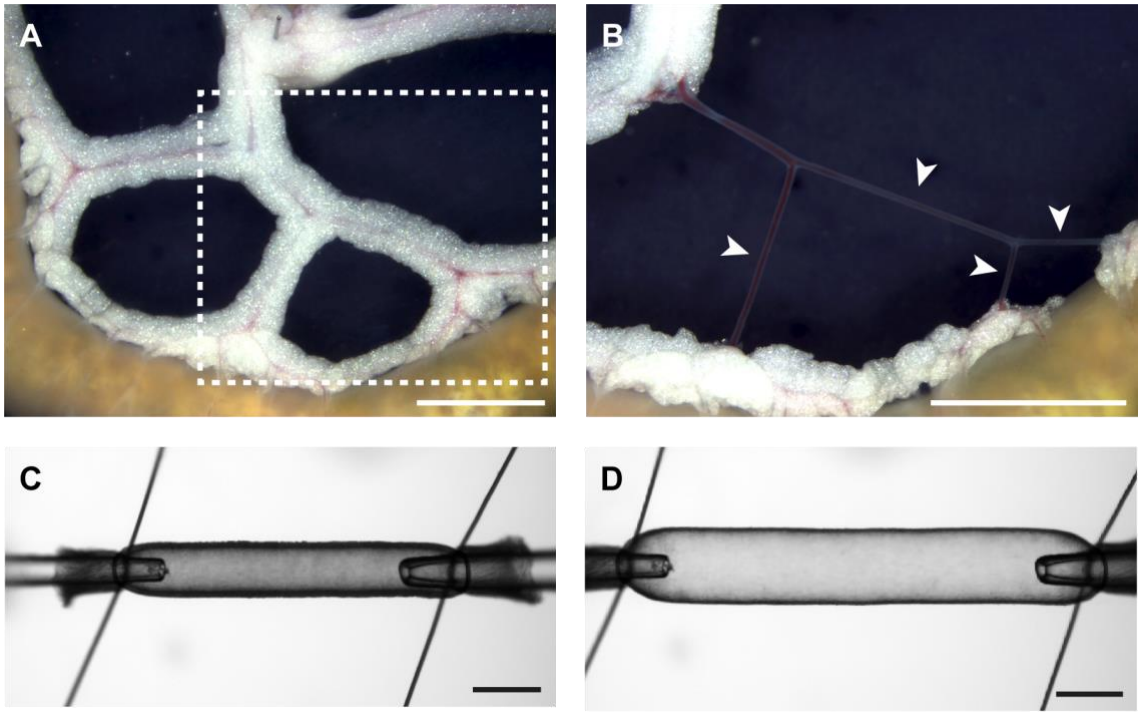


Figure 2.2.1 Excised mesentery and pressurised mesenteric artery. (**A** and **B**) Images of a section of pinned mesenteric arcade before (A) and after (B) the removal of the surrounding perivascular fat and parallel mesenteric vein. The dashed box (A) represents the region of magnification (B) and the arrowheads indicate the third- and fourth-order arteries to be studied; scale bars, 5 mm. (**C** and **D**) Bright-field images of a cannulated third-order mesenteric artery pressurised to 10 (C) and 70 mmHg (D); scale bars, 300 µm. The distance between the pipettes is increased after pressurization to 70 mmHg (D) to stretch the artery and prevent bowing.

2.2.3 Studying cremasteric and coronary arteries under isobaric conditions

Cremasteric and coronary arteries were pressurised to 80 mmHg and spontaneous myogenic tone was allowed to develop over a 20-60 min equilibration period. Cremasteric arteries consistently developed ~50% myogenic tone whereas coronary artery myogenic tone was more variable, ranging from ~20-50%. After a stable level of tone developed, endothelial health was assessed with ACh. Only arteries which exhibited a maintained level of myogenic tone in response to raised intraluminal pressure and maximal vasodilation to 1 µM ACh were considered viable for experimentation. Unlike during experiments with mesenteric arteries, cremasteric and coronary arteries were not preconstricted with PE prior to exposure to a vasodilator. At the end of every experiment with cremasteric and coronary arteries, 1 µM nifedipine was added to the superfusion to obtain the passive diameter of the vessel. As with mesenteric arteries, coronary artery reactivity to various agonists was assessed in the absence and presence of an antagonist, and inhibitors were not washed out after their addition to eliminate the possibility of irreversible/carry-over effects of drugs between treatments. Cremasteric arteries were only studied under control conditions.

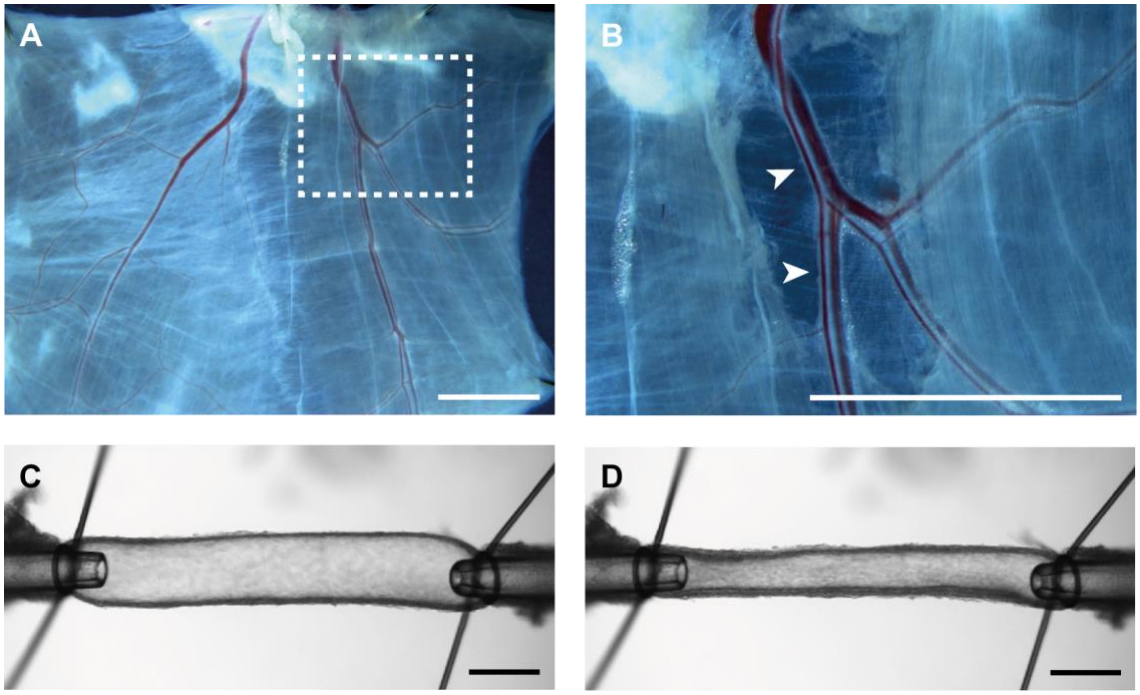


Figure 2.2.3 Excised cremaster muscle and pressurised cremasteric artery. (**A** and **B**) Images of a section of pinned cremaster muscle before (A) and after (B) the partial removal of the surrounding skeletal muscle and perivascular fat. The dashed box (A) represents the region of magnification (B) and the arrowheads indicate the arteries to be studied; scale bars, 5 mm. The larger, parallel cremasteric vein has not been removed in these images. (**C** and **D**) Bright-field images of a cannulated cremasteric artery immediately (C) and ~20 min (D) following pressurization to 80 mmHg wherein 47.0% pressure-induced myogenic tone developed; scale bars, 100 µm.

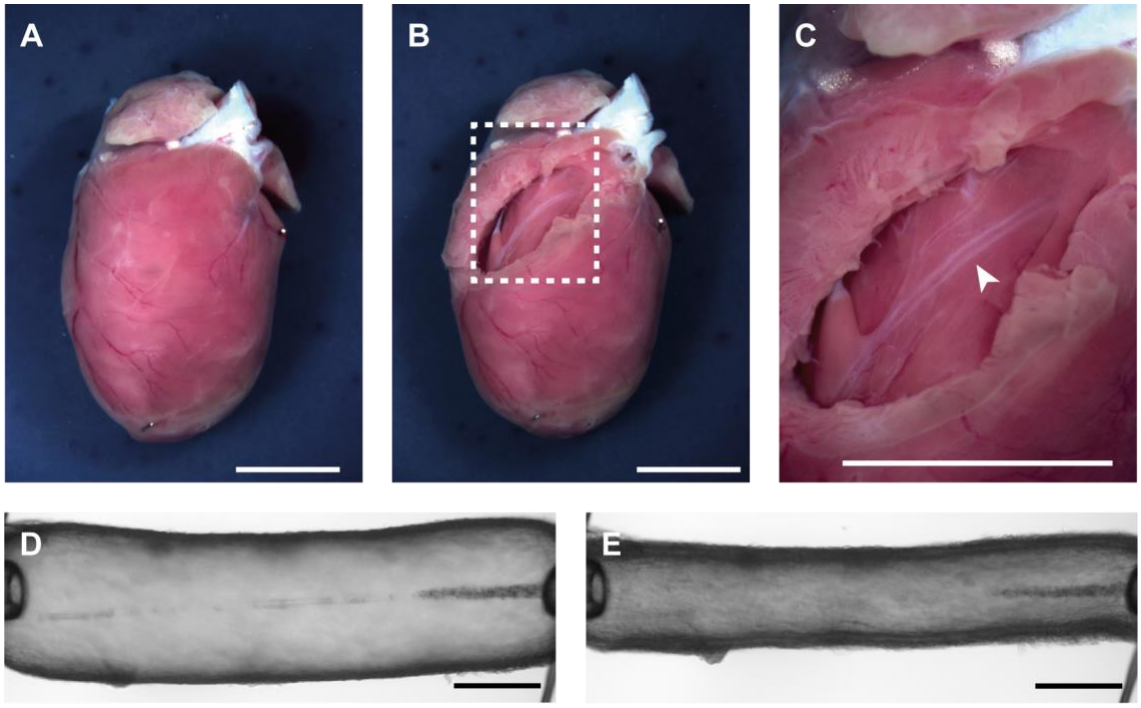


Figure 2.2.4 Excised heart and pressurised coronary artery. (**A** and **B**) Images of a pinned heart before (A) and after (B and C) the partial removal of the wall of the right atrium. The dashed box (B) represents the region of magnification (C) and the arrowheads indicate the artery to be studied; scale bars, 5 mm. (**C** and **D**) Bright-field images of a cannulated coronary artery immediately (C) and ~20 min (D) following pressurization to 80 mmHg wherein 46.0% pressure-induced myogenic tone developed; scale bars, 200 µm.

2.2.4 EFS of pressurised arteries

For electrical field stimulation (EFS), arteries were prepared as previously described (see Section 2.2.1) except arteries were mounted in an imaging chamber fitted with electrodes on either side of the artery (RC-27NE2, Warner Instruments, USA). The electrodes were connected to a custom-made stimulator and voltmeter, and oscilloscope (TDS 1002, Tektronix, USA) (see Figure 3.2.1). Trains of monophasic square pulses of varying frequencies, pulse width and pulse number were used to activate perivascular nerves (see Section 3.2.2).

2.2.5 Analysis of mesenteric artery diameter recordings

For mesenteric arteries, the outer diameter was tracked using MetaMorph software (v7.7.4.0, Molecular Devices, USA; see Figure 2.2.5). Each data point represents the mean diameter over 15 s except for transient responses to EFS and ATP which are presented as the diameter in a single frame.

Vasoconstriction is expressed as a percentage of the minimum outer diameter obtained at the end of each experiment:

$$Vasoconstriction\ (\%) = 100-(\frac{Diameter\ at\ Peak\ Response\ -\ Minimum\ Diameter}{Passive\ Diameter\ -\ Minimum\ Diameter} \times 100)$$

Vasodilation is expressed as a percentage of the passive diameter from the diameter during preconstriction with PE:

$$Vasodilation\ (\%) = \frac{Peak\ Response\ -\ Preconstriction\ Diameter}{Passive\ Diameter\ -\ Preconstriction\ Diameter} \times 100$$

2.2.6 Analysis of cremasteric and coronary artery diameter recordings

For cremasteric and coronary arteries, the inner diameter was measured using VasoTracker software (v1.1.0, VasoTracker, UK) (Lawton et al., 2019). Outer diameter was not recorded because residual skeletal muscle or cardiomyocytes on the outside of the artery interfered with detection of the outer wall. Each data point represents the mean diameter over 15 s except for transient responses to EFS and ATP which are presented as the diameter in a single frame.

Myogenic tone is expressed as a percentage of decrease from the passive diameter (without myogenic tone):

$$Myogenic\ Tone\ (\%) = \frac{Passive\ Diameter - Diameter\ with\ Myogenic\ Tone}{Passive\ Diameter} \times 100$$

Vasoconstriction is expressed as a percentage of decrease from the initial diameter (with myogenic tone):

$$Vasoconstriction\ (\%) = \frac{Initial\ Diameter - Diameter\ at\ Peak\ Response}{Initial\ Diameter} \times 100$$

Vasodilation is expressed as a percentage of the passive diameter from the initial diameter (with myogenic tone):

$$Vasodilation\ (\%) = \frac{Diameter\ at\ Peak\ Response - Initial\ Diameter}{Passive\ Diameter - Initial\ Diameter} \times 100$$

2.3 WIRE MYOGRAPHY

The study of isolated arteries under isometric conditions, wherein the length of the VSM remains constant during contraction and relaxation, was first described by Bohr and Goulet (1961). Bevan and Osher (1972) refined the technique by introducing the use of two platinum wires inserted into the vessel lumen, which were then secured to two metal plates connected to either a strain gauge or micrometer. Mulvany and Halpern (1977) advanced the experimental approach further with the design of the Mulvany-Halpern myograph consisting of two mounting jaws rather than metal plates. Once mounted, the vessel is normalised by laterally stretching it in known µm increments whilst measuring tension simultaneously. An exponential length-tension curve is constructed from the recorded points to determine the optimal resting tension to place the artery under which won't mask changes in active wall tension.

2.3.1 Mounting of mesenteric arteries in a wire myograph

2 mm segments of mesenteric arteries were mounted in a 4-channel Mulvany-Halpern myograph (700MO, Danish Myo Technology, Denmark) with 25 µm gold-plated tungsten wires in room temperature Krebs solution (see Section 2.5). The solution was then warmed to ~37°C and the arteries allowed to equilibrate for 30 min. Changes in VSM tension were recorded at 10 Hz using a PowerLab/4SP data acquisition system (ADInstruments, New Zealand) and LabChart software (v7.2.5 , ADInstruments, New Zealand). Arteries were normalised to a resting tension equivalent to that generated at 90% of the inner diameter of the vessel at 70 mmHg.

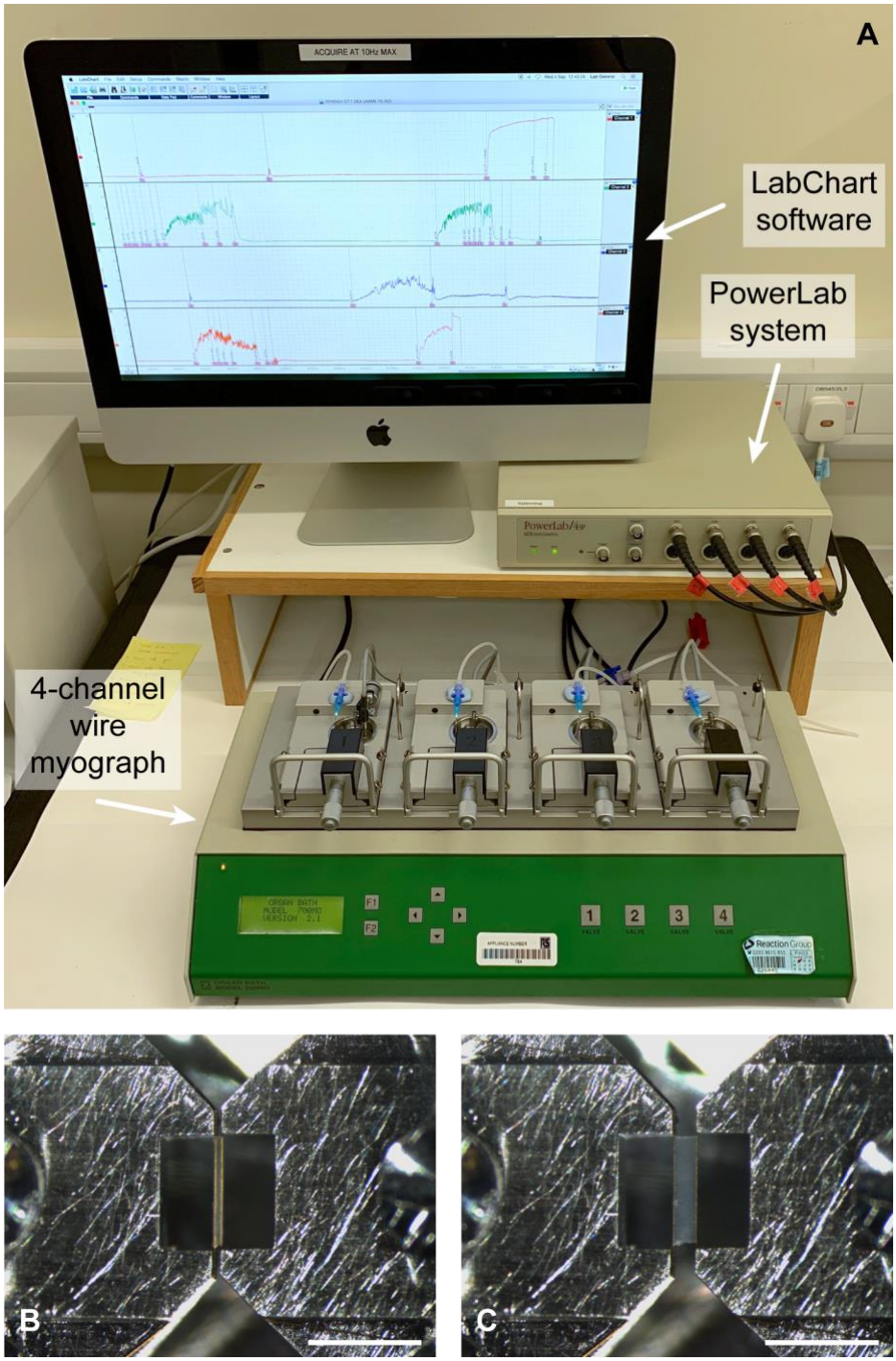


Figure 2.3.1 Wire myograph apparatus. (**A**) Image of equipment used for the assessment of VSM contraction under isometric conditions. (**B** and **C**) Images of a mesenteric artery mounted in a wire myograph with (B) and without (C) applied normalized tension. Scale bars, 2 mm.

2.3.2 Studying mesenteric arteries under isometric conditions

Following a 30 min equilibration period, vessel contractility was assessed by increasing $[K^+]_o$ to 45 mM to depolarize the VSM. Endothelial health was assessed using ACh following preconstriction with PE. Only arteries which exhibited robust and maintained contraction to elevated $[K^+]_o$ and maximal relaxation to 1 µM ACh were considered viable for further experimentation. For experiments examining relaxation, arteries were first precontracted with a submaximal concentration of PE to stimulate ~70% contraction. At the end of each experiment, the artery was stimulated with 10 µM U 46619 and 10 µM PE to obtain the maximum contractile response. For each individual wire myography experiment, vasoreactivity to various agonists was assessed in the absence and presence of an antagonist or blocker. Arteries were only incubated with multiple inhibitors where indicated, and inhibitors were not washed out after their addition to eliminate the possibility of irreversible/carry-over effects of drugs between treatments.

2.3.3 Analysis of isometric tension recordings

Each data point represents the mean tension over a 15 s period except for transient responses to ATP which are presented as the tension in a single scan.

Contraction is expressed as a percentage of the maximum contraction obtained at the end of each experiment:

$$Contraction\ (\%) = \frac{Tension\ at\ Peak\ Response - Baseline\ Tension}{Maximum\ Tension - Baseline\ Tension} \times 100$$

Relaxation is expressed as a percentage of the baseline tension from the tension during preconstriction with PE:

$$Relaxation\ (\%) = \frac{Tension\ at\ Peak\ Response - Preconstriction\ Tension}{Baseline\ Tension - Preconstriction\ Tension} \times 100$$

2.4 IMMUNOHISTOCHEMISTRY

2.4.1 Immunostaining of pressurised arteries

In a subset of experiments, arteries were fixed and stained for proteins of interest. Following functional pressure myography experiments (see Section 2.2), vessels were fixed in 2% paraformaldehyde aqueous solution (PBS; 157-2, Electron Microscopy Sciences) for 30 min at room temperature and then washed with 0.01 M phosphate-buffered saline (P3813, Sigma). Arteries were then incubated in blocking buffer containing 1% bovine serum albumin (A3059, Sigma), 0.05% Tween20 (Sigma, P2287) and 0.5% Triton X-100 (T8532, Sigma) diluted in PBS for 2 hours. They were then incubated overnight at 4°C with the primary antibody diluted in blocking buffer. The following day, arteries were washed with PBS and incubated for up to two hours with the secondary antibody diluted in blocking buffer. The secondary antibody was removed from the chamber once clear staining was observed. 5 µM propidium iodide (81845, Sigma) was also added to the chamber to visualise nuclei.

2.4.2 Imaging immunohistochemistry preparations

Arteries were excited at 488 nm and 543 nm with the emitted fluorescence acquired though a water immersion objective (40×/1.15NA objective; WD, 0.25 mm; Olympus, Japan) using a confocal line-scanning microscope (FV1000MPE, Olympus, Japan). Arteries were imaged at 1.5× and 2.5× digital zoom. z-stacks through the artery wall were obtained at 0.3 µm increments with FluoView 1000 software (FV10-ASW v4.1, Olympus, Japan) and reconstructed in Imaris software (v7.7.1, Bitplane, USA).

2.5 SOLUTIONS AND DRUGS

During tissue collection, dissection and pressure myography experiments, MOPS-buffered solution was used containing (in mM): 145.0 NaCl, 4.7 KCl, 2.0 $CaCl_2$, 1.17 $MgSO_4$, 2.0 3-(N-morpholino)propanesulfonic acid (MOPS), 1.2 NaH_2PO_4, 5.0 glucose, 2.0 pyruvate, 0.02 EDTA, and 2.75 NaOH. The pH was adjusted to 7.40 ±0.02 at 37°C. The pH was always readjusted following the addition of L-NAME.

During all wire myography experiments Krebs solution was used containing (in mM): 118.0 NaCl, 3.6 KCl, 2.5 $CaCl_2$, 1.2 $MgSO_4$, 25.0 $NaHCO_3$, 1.2 KH_2PO_4, and 11.0 glucose and gassed with 21% O_2, 5% CO_2, with N_2.

The reason two different solutions are used for pressure and wire myography stems from the need to gas Krebs solution to maintain the pH. The movement of the solution due to the bubbling causes focal drift which is incompatible with diameter measurements using confocal microscopy. Thus, a solution containing MOPS, a buffer which does not require the addition of CO_2, was used. It is essential to note when pressure myography experiments are performed with Krebs solution, there is no difference in vasoreactivity, even though bicarbonate is the central component of the pH buffering system in the blood.

Arteries were always allowed at least 15 minutes between experiments to recover. Drug and compound stock solutions were diluted into MOPS-buffered solution or Krebs solution before being added to the bath with the exception of

GSK 1016790A, RN 1734 and TRAM-34 which were diluted into DMSO. Vehicle controls were performed with DMSO and confirmed no effect of the solvent on artery function. All antagonists and blockers were incubated with the tissue for 30 min prior to experimentation with the exception of apamin and RN 1734 which were allowed 1 hour. For pressure myography experiments, agonists were added directly to the static bath whilst all antagonists were added to the superfusion.

Table 2.5.1 List of drugs and compounds used in the current investigations.

Drug/Compound	Supplier (Product Code)	[Stock] (mM)	Solvent	[Bath] (µM)
Acetylcholine	Sigma (A6625)	100.0	Milli-Q	0.001 – 1.0
ATP	Sigma (A3377)	10.0	Milli-Q	0.01 – 10.0
Apamin	Latoxan (L8407)	0.1	Milli-Q	0.1
DEA/NO	Sigma (D184)	50.0	Milli-Q	0.1 – 30.0
Glycl-H1152	Tocris (2485)	10.0	Milli-Q	1.0
GSK 1016790A	Sigma (G0798)	10.0	DMSO	0.01 – 1.0
L-NAME	Sigma (N5751)	100.0	Milli-Q	100.0
NF 449	Tocris (1391)	10.0	Milli-Q	1.0
Nifedipine	Sigma (N7634)	10.0	Ethanol	1.0
Phenylephrine	Sigma (P6126)	10.0	Milli-Q	0.001 – 10
Prazosin	Sigma (P7791)	1.0	Milli-Q	1.0
Propranolol	Sigma (P8688)	10.0	Milli-Q	1.0
RN 1734	Tocris (3746)	100.0	DMSO	30.0
Ryanodine	Calbiochem (559276)	5.0	Milli-Q	1.0
SNOG	Tocris (0603)	100.0	Milli-Q	0.1 – 100.0
Tetrodotoxin	Latoxan (L8503)	5.0	Milli-Q	1.0
TRAM-34	Sigma (T6700)	10.0	DMSO	1.0
U 46619	Calbiochem (538944)	100	DMSO	1.0

2.6 STATISTICAL ANALYSES

All pressure and wire myography data were analysed identically with a method determined prior to data collection, thus data randomization and blinding were not necessary in the current investigations. All data analysis was completed post-hoc with Microsoft Excel (v16, Microsoft Corporation, USA) and GraphPad Prism software (v8.2.1, Molecular Devices, USA). Results are presented as means ± SEM and sample size (n) is indicative of the number of animals used. Statistical analysis was only performed on datasets with sample sizes greater than or equal to 5, where normality could be accurately assessed. Due to time constraints and the technical nature of pressure and wire myography experiments, several datasets have sample sizes smaller than 5. However, these data are still included to allow for a discussion of the trends in the absence of statistical analysis. All datasets are unpaired (non-repeated measures between treatments) unless stated otherwise. Normality was assessed using a Shapiro-Wilk test. For normally distributed data, statistical comparisons were made using a two-tailed t-test, or one- or two-way ANOVA, where appropriate. If statistically significant differences were detected by an ANOVA, a Sidak's or Tukey's multiple comparisons post-test was used to compare means between two treatments, or three or more treatments, respectively. Datasets which didn't pass the normality test were analysed using a nonparametric two-tailed Mann-Whitney or Wilcoxon test, or a Kruskal-Wallis test followed by a Dunn's multiple comparisons post-test. $P < 0.05$ is considered statistically significant.

3.0 INFLUENCE OF THE ENDOTHELIUM ON NEUROGENIC VASOCONSTRICTION IN PRESSURISED RESISTANCE ARTERIES

3.1 INTRODUCTION

Neurotransmitter release from perivascular nerves modulates vascular tone in resistance arteries alongside circulating factors, intrinsic regulatory mechanisms such as myogenic tone, and endothelium-derived signals including NO and EDH (Westcott and Segal, 2013). Perivascular innervation, including sympathetic, parasympathetic and sensory nerves, is highly variable between vascular beds and species, and the effect of its activation is dependent on the expression of postjunctional receptors in the VSM. In peripheral arteries, the effects of NAD and ATP release from sympathetic varicosities has been studied extensively, and is generally accepted to cause vasoconstriction (von Kügelgen and Starke, 1985; Dunn et al., 1999; Mauban et al., 2001; Nausch et al., 2012).

Recent investigations have elucidated a role for the endothelium in opposing vasoconstriction, namely following activation of adrenergic signalling pathways (Dora et al., 1997; Tuttle and Falcone, 2001; Jackson et al., 2009; Hong et al., 2018) (see Section 1.3.2). Dora, Doyle and Duling (1997) illustrated for the first time that the α_1-AR-selective agonist PE stimulated vasoconstriction in hamster cheek arterioles which was accompanied by a Ca^{2+} response in the neighbouring endothelium and potentiated during NOS inhibition. The lack of α_1-AR expression in the endothelium led to the hypothesis that a signal originating in VSMCs can activate adjacent ECs to cause NO production and limit vasoconstriction. Furthermore, Ca^{2+}-activated K^+ channel (K_{Ca}) opening has also been shown to facilitate myoendothelial feedback in small arteries where the endothelium and smooth muscle are closely electrically-coupled and EDH is the central mediator

of endothelium-dependent vasodilation (Dora et al., 2000; Yashiro and Duling, 2000; Nausch et al., 2012; Kerr et al., 2015). Most recently, our group demonstrated Ca^{2+} entry through Ca_Vs in the VSM of rat cremasteric arteries can evoke EC Ca^{2+} events and IK_{Ca}-dependent hyperpolarization independently of adrenergic stimulation (Garland et al., 2017).

The majority of investigations into endothelial activation during vasoconstriction have been conducted with exogenously administered neurotransmitters or selective agonists of their receptors (see Table 1.3.1). Considering myoendothelial feedback may represent an important intrinsic regulator of vasoconstriction, and subsequently blood pressure and tissue perfusion, further exploration with a more physiologically representative stimulus is required. A small number of investigations into the ability of the endothelium to limit nerve-dependent vasoconstriction caused by EFS have yielded conflicting results which provides the rationale for the current study (Martínez et al., 1995; Aldasoro et al., 1996; Nausch et al., 2012; Wei et al., 2018).

3.1.1 Aims and hypotheses

The aim of the current investigation was to examine the influence of the endothelium on neurogenic vasoconstriction in pressurised resistance arteries.

It was hypothesised blockade of endothelium-dependent vasodilation would potentiate vasoconstriction during sympathetic perivascular nerve activation in pressurised mesenteric and cremasteric arteries.

3.2 MATERIALS AND METHODS

3.2.1 Pressure myography

Mesenteric and cremasteric arteries were prepared for pressure myography experiments in an imaging chamber fitted with electrodes, as previously described (see Figure 3.2.1 and Section 2.2).

3.2.2 EFS parameters

The parameters used for all EFS experiment were 10 V, with a pulse train interval of 1 min and train duration of 7s. The number of pulses per train depended on the pulse frequency. To determine the optimal pulse frequency a pulse frequency-response curve (3-20 Hz) was generated. 7 Hz was chosen because it elicited a submaximal vasoconstriction (see Figure 3.2.2A). For all other experiments a pulse-width-response curve was generated (0.5-1 ms; see Figure 3.2.2B). Pulse-width-curves could be repeated up to four times in a row without causing desensitization.

3.2.3 Inhibitors

The following drugs were used in this chapter to block their respective targets, at concentrations which have previously been shown to be effective: 1.0 µM TTX to block voltage-gated Na^+ channels (Na_Vs) (Nausch et al., 2012), 1.0 µM nifedipine to block Ca_Vs (Bagher et al., 2012), 1.0 µM prazosin to antagonise α_1-ARs (Garland et al., 2011b),10.0 µM NF 449 to block $P2X_1$Rs (Søndergaard et al., 2019), 100.0 µM L-NAME to antagonise NOS

(Garland et al., 2017), and 1.0 µM TRAM-34 and 0.1 µM apamin to block IK_{Ca} and SK_{Ca}, respectively (Lemmey et al., 2018).

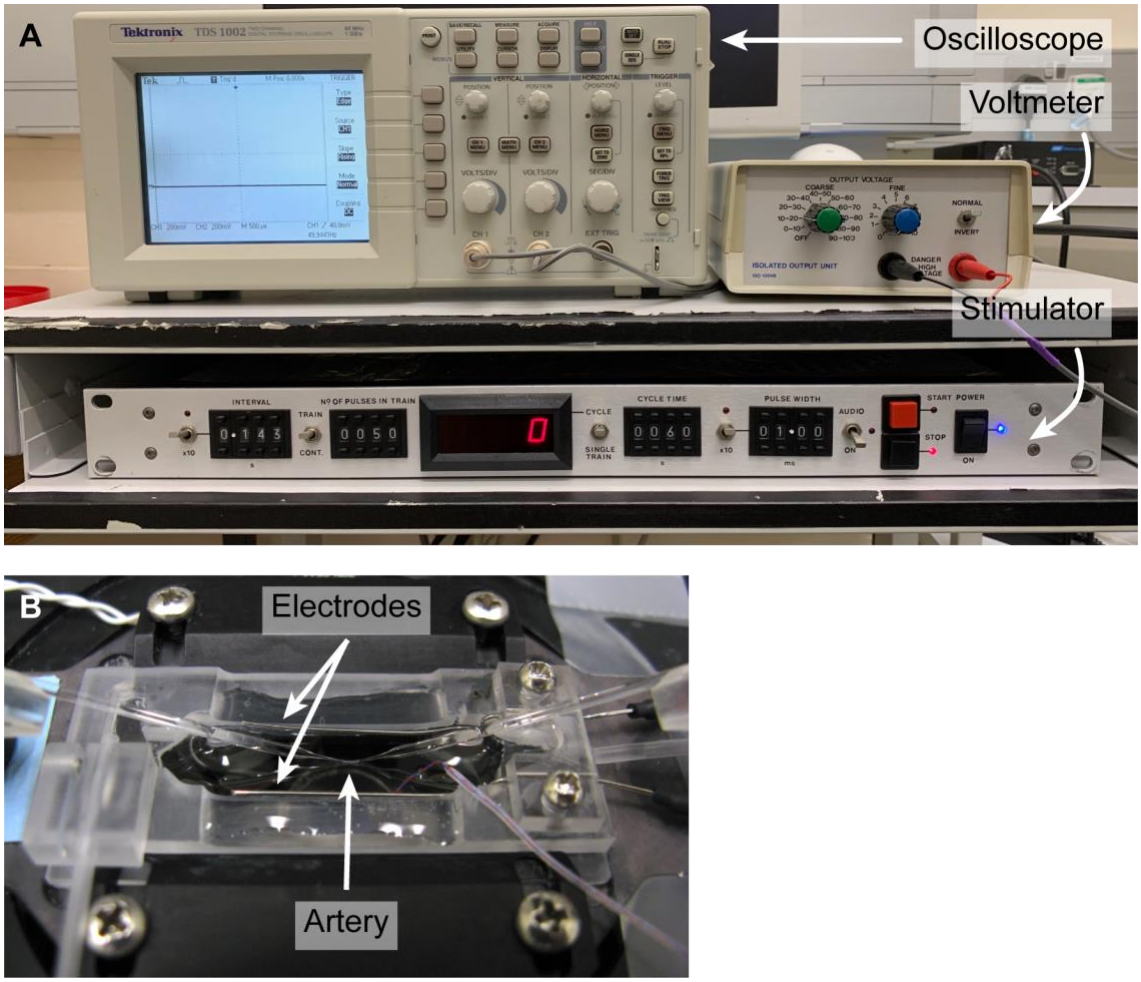


Figure 3.2.1 EFS apparatus. (**A**) Image of equipment used for EFS. (**B**) Image of imaging chamber with mounted artery and parallel stimulating electrodes.

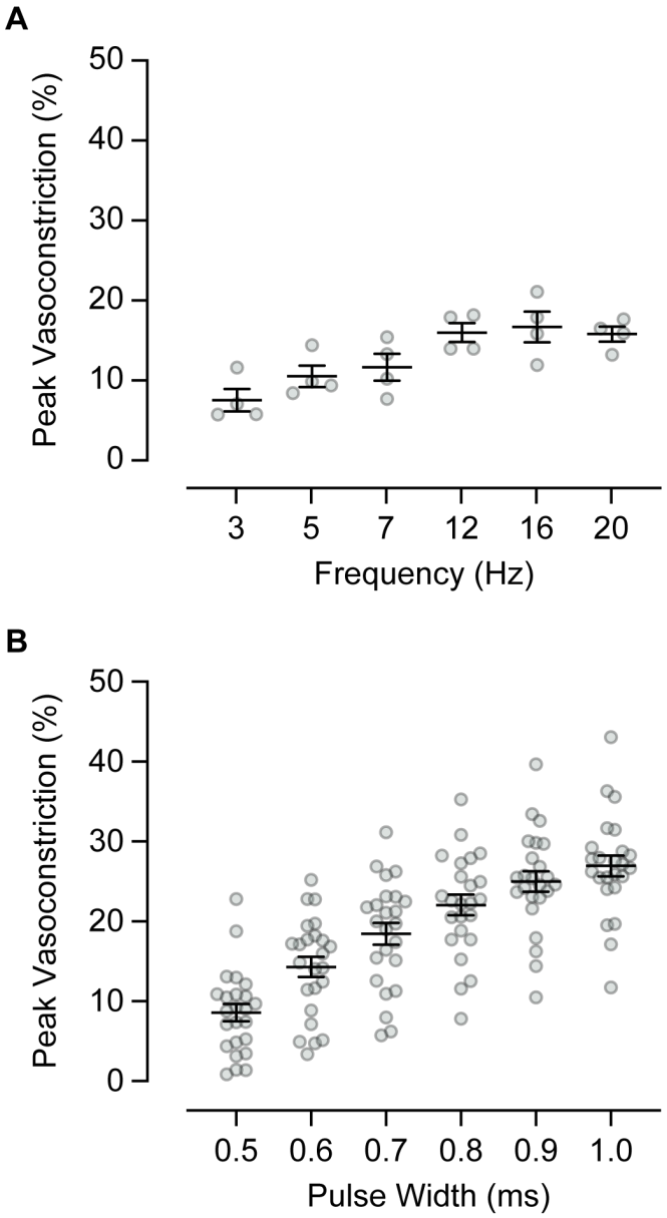


Figure 3.2.2 EFS-induced vasoconstriction in pressurised mesenteric arteries. (**A**) Scatter plot summarizing vasoconstriction during EFS with increasing pulse frequency (0.5 ms pulse-width); n=4. (**B**) Scatter plot summarizing vasoconstriction during EFS with increasing pulse width (7 Hz, 50 pulses); n = 24. Data presented as means ± SEM.

3.2.4 Immunohistochemistry

Mesenteric and cremasteric arteries were prepared for immunohistochemistry as previously described (see Section 2.4). A polyclonal anti-rat tyrosine hydroxylase antibody raised in rabbit (0.3 µg.ml^{-1}, 1:500; NB300-109, Novus) was used as a marker of catecholamine-producing nerve varicosities. The secondary antibody was a polyclonal anti-rabbit IgG antibody raised in goat and conjugated to Alexa Fluor 488 (2 µg.mL^{-1}, 1:1000; A11034, Invitrogen; excitation, 488; emission, < 519). Perivascular nerves were clearly stained within 15 minutes of the secondary antibody being added to the bath. Perfusing the lumen of the artery with the antibodies, as well as adding it to the bath, did not affect the staining.

3.3 RESULTS

3.3.1 EFS-induced vasoconstriction is attenuated during Ca_V and Na_V blockade

Under control conditions, EFS caused graded vasoconstriction with increasing pulse width in pressurised mesenteric arteries (1 ms: 26.9 ± 1.3%; n = 24). The contractile response was attenuated by the addition of the Na_V blocker tetrodotoxin (TTX) (1 ms: 6.6 ± 0.6%, n = 6) confirming a role for neurotransmitter release in mediating EFS-induced vasoconstriction. The Ca_V blocker nifedipine also attenuated the response (1 ms: 11.0 ± 2.8%, n = 8) and almost completely abolished it when used in combination with TTX (1.1 ± 0.7%, n = 3) (see Figures 3.3.1 and 3.3.3). These data indicate EFS causes the release of neurotransmitters which stimulate vasoconstriction through Ca_V-dependent and -independent processes. However, the residual EFS-induced vasoconstriction in the presence of TTX was blocked by nifedipine suggesting a direct effect at Ca_Vs on perivascular nerves or VSM, or the presence of tetrodotoxin-resistant Na_V isoforms. This effect was observed even at the lowest pulse-width tested (0.5 ms: control, 8.6 ± 1.1%, n=24; TTX, 1.8 ± 0.4%, n = 6; nifedipine + TTX, 0.3 ± 0.1%, n = 3).

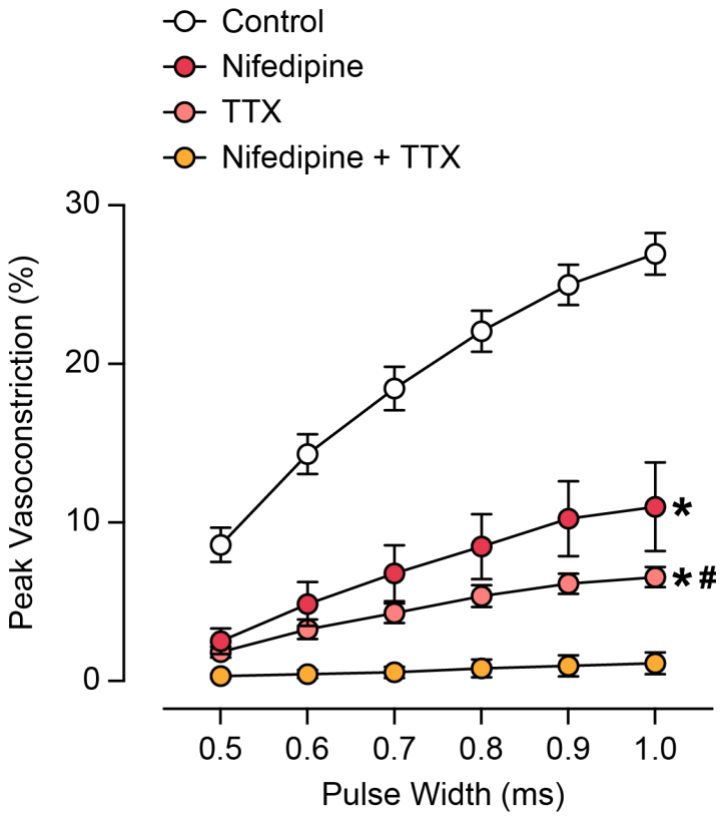


Figure 3.3.1 Effect of Ca_v and Na_v blockers on EFS-induced vasoconstriction in pressurised mesenteric arteries. Scatter plot summarizing vasoconstriction during EFS in the presence of 1 µM nifedipine, 1 µM TTX or nifedipine + TTX. Data are means ± SEM; n = 3-24. *P < 0.05 compared to control; #P < 0.05 compared to Nifedipine.

3.3.2 EFS-induced vasoconstriction is attenuated during α_1-AR and $P2X_1R$ antagonism

In a subset of paired experiments, EFS was used on mesenteric arteries incubated with the same combination of antagonists, and in the same order, allowing for repeated measures analysis. The non-selective β-AR antagonist propranolol did not affect the response to EFS (1 ms: control, 24.4 ± 2.0%; + propranolol, 22.0 ± 2.9%; n = 5). Prazosin, a selective α_1-AR antagonist, slightly attenuated the vasoconstriction (1 ms: 19.6 ± 1.8%; n = 5), compared with the addition of NF 449, a selective $P2X_1R$ antagonist, which greatly diminished the response (1 ms: 11.0 ± 1.3%; n = 5) (see Figure 3.3.2A). These data indicate a role for both NAD and ATP released from sympathetic varicosities in causing vasoconstriction during EFS. The lack of effect of propranolol suggests β-ARs are not activated by the released NAD or the downstream effect of its activation is not evident during vasoconstriction.

The reduced response in the additional presence of NF 449 suggests ATP is the main neurotransmitter responsible for EFS-induced vasoconstriction. However, NF 449 did not have the same degree of effect when used alone (1 ms: control, 25.7 ± 3.5%; + NF 449, 19.8 ± 4.3; n = 3). The addition of prazosin after NF 449 attenuated the response to match that of the previous experiment (1 ms: 10.3 ± 1.2%; n=3) (see Figure 3.3.2B). Overall, these data indicate NAD and ATP can both cause significant vasoconstriction during EFS with these parameters and neither operates as a primary neurotransmitter or cotransmitter.

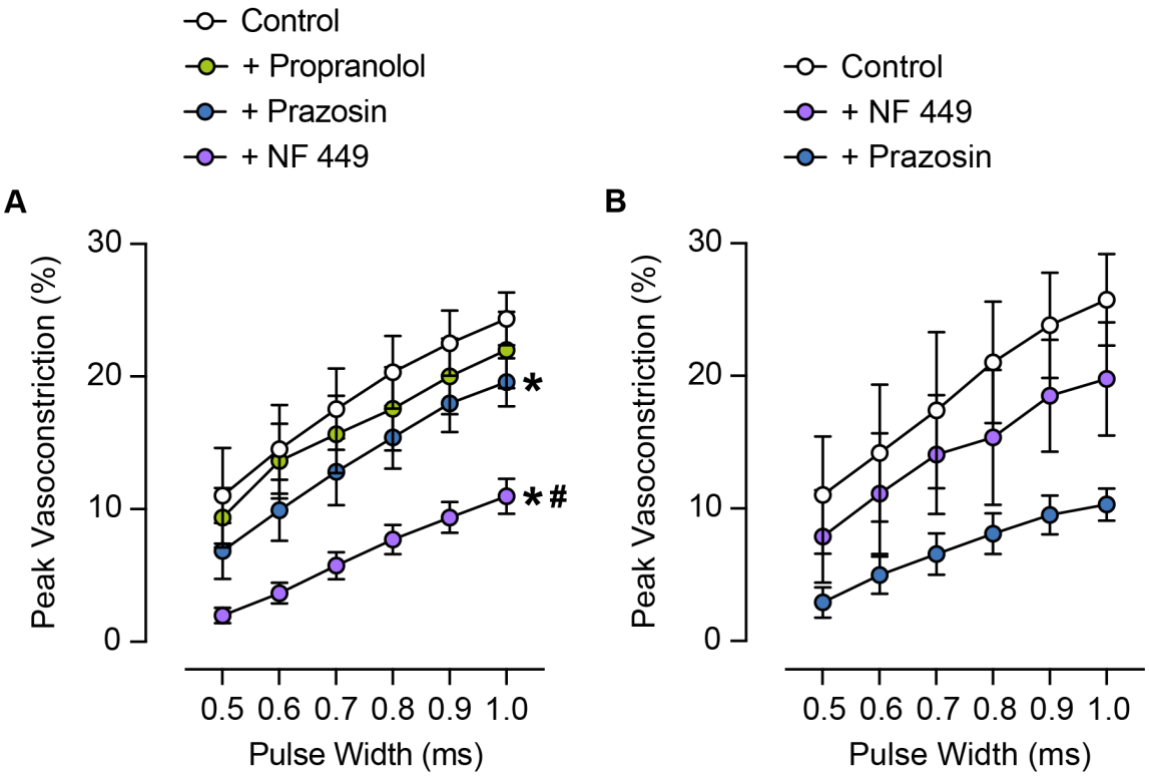


Figure 3.3.2 Effect of α_1-AR and $P2X_1R$ antagonism on EFS-induced vasoconstriction in pressurised mesenteric arteries. (**A**) Scatter plot summarizing vasoconstriction during EFS in the absence and presence of 1 µM propranolol and the additional presence of 1 µM prazosin and 10 µM NF 449. (**B**) Scatter plot summarizing vasoconstriction during EFS in the absence and presence of NF 449 and the additional presence of prazosin. These data represent paired experiments. Data are means ± SEM; n = 3-5. $^{*}P < 0.05$ compared to control; $^{\#}P < 0.05$ compared to + Prazosin.

During nifedipine treatment, prazosin and NF 449 decreased the response to EFS further (1 ms: nifedipine, 11.7 ± 3.4%, n = 6; nifedipine + prazosin, 3.3 ± 0.7%, n = 4; nifedipine + prazosin + NF 449, 0.6 ± 0.1%, n = 6) (see Figure 3.3.3). This effect is further evidence for the involvement of Ca_V-independent pathways following α_1-AR and $P2X_1R$ activation. However, this observation does not eliminate the possibility other neurotransmitters are released from the same synaptic terminals. Such molecules may mediate their effect through Ca_V activation or act as cotransmitters by sensitizing the contractile machinery to Ca^{2+} and amplifying the response to NAD and ATP.

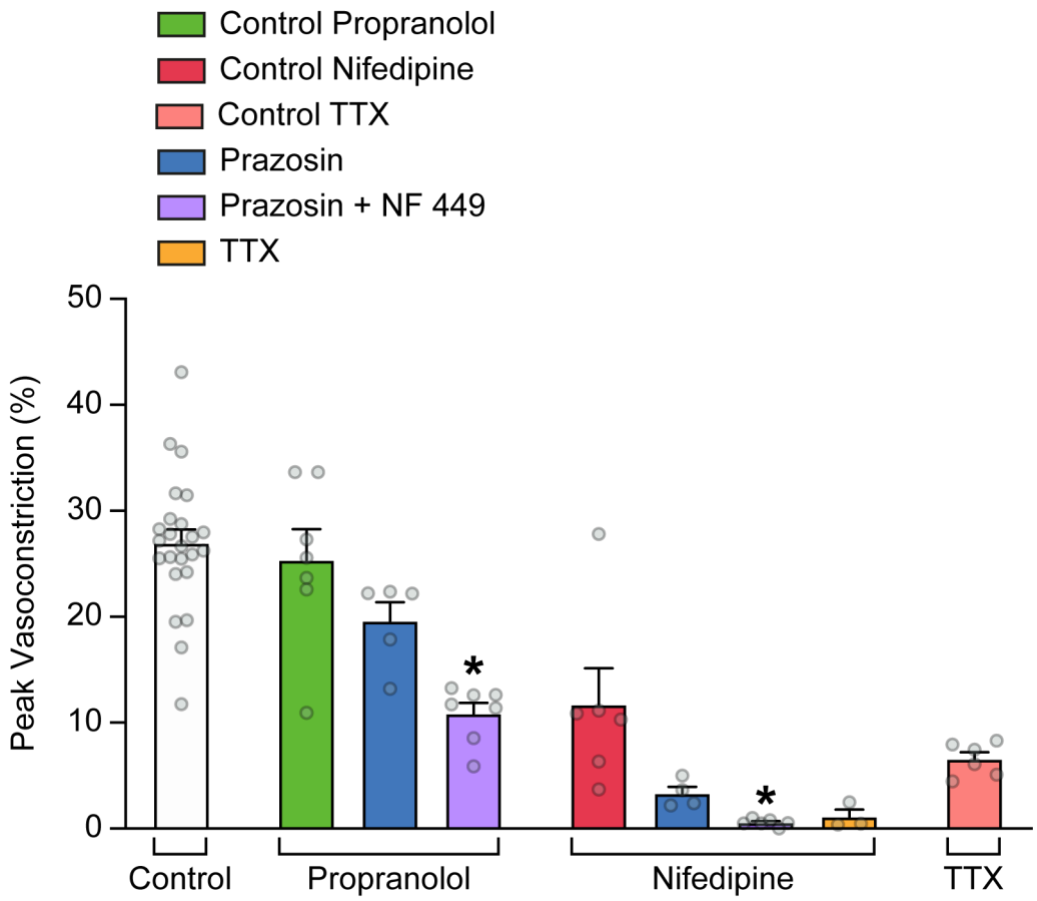


Figure 3.3.3 Summary of the effect of antagonists on EFS-induced vasoconstriction in pressurised mesenteric arteries. Bar graphs summarizing vasoconstriction to EFS with 1 ms pulse-width under control conditions; and with 1 µM propranolol, 1 µM nifedipine, or 1 µM TTX; and the additional presence of 1 µM prazosin, prazosin + 10 µM NF 449 or TTX. Data are means ± SEM; n = 3-24. *$P < 0.05$ compared to the corresponding control.

3.3.3 Blockade of endothelium-dependent vasodilation does not modulate EFS-induced vasoconstriction

In a set of paired experiments, EFS was performed on mesenteric arteries before and after the addition of L-NAME, TRAM-34 and apamin to antagonise NOS, IK_{Ca} and SK_{Ca}, respectively. Blockade of NO and EDH production in the endothelium had no effect on EFS-induced vasoconstriction (1ms; control, 24.3 ± 6.9%; + L-NAME, TRAM-34 & apamin, 19.7 ± 4.0%; n = 3) (see Figure 3.3.4). This lack of effect suggests EFS does not cause an increase in Ca^{2+} activity in the endothelium or the vasoconstriction is not attenuated by endothelium-dependent vasodilation under these conditions.

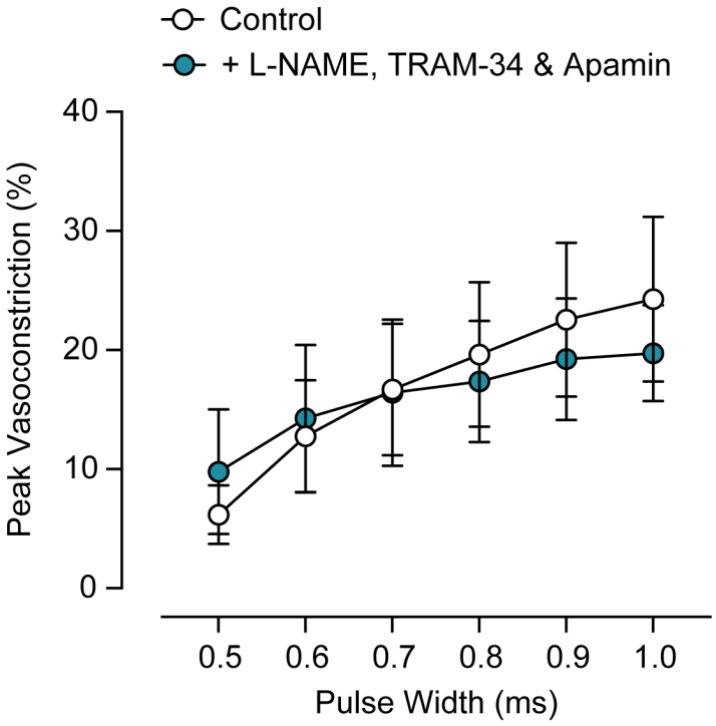


Figure 3.3.4 Effect of inhibition of NO and EDH production on EFS-induced vasoconstriction. Scatter plot summarizing vasoconstriction during EFS under control conditions and in the presence of 100 µM L-NAME, 1 µM TRAM-34 and 0.1 µM apamin. These data represent paired experiments. Data are means ± SEM; n = 3.

3.3.4 EFS does not cause vasoconstriction of pressurised cremasteric arteries

The same EFS parameters which caused a robust reduction in diameter in mesenteric arteries were tested on pressurised cremasteric arteries and, interestingly, failed to evoke any response (1 ms: mesenteric, 46.1 ± 2.4 µm, n = 24; cremasteric, 1.6 ± 0.9 µm, n = 5) (see Figure 3.3.5). This observation was unexpected as it suggests the receptors for the sympathetic neurotransmitters aren't expressed in the VSMCs, or EFS does not cause enough neurotransmitter release from perivascular nerve varicosities of cremasteric arteries to elicit an effect. Furthermore, the lack of response in this preparation indicates EFS also had no direct effect at Ca_Vs, as it may do in mesenteric arteries. This finding made it challenging to investigate myoendothelial feedback during EFS in pressurised cremasteric arteries.

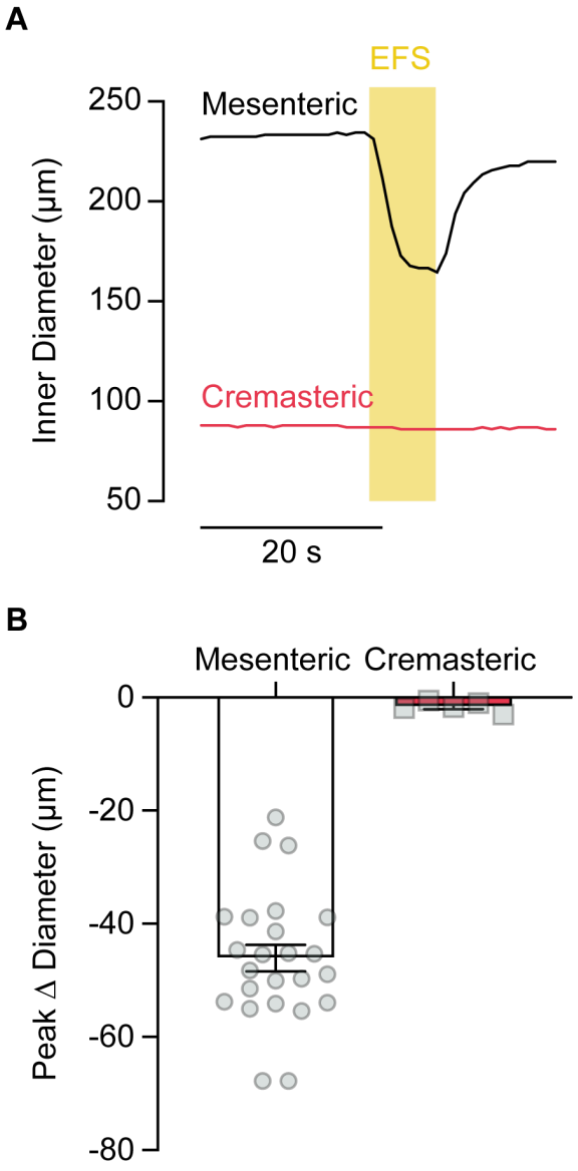


Figure 3.3.5 Effect of EFS in pressurised cremasteric arteries. (**A**) Representative traces of inner diameter of pressurised mesenteric and cremasteric arteries during EFS with 1 ms pulse-width. (**B**) Bar graph summarizing the change in outer diameter in mesenteric and inner diameter in cremasteric arteries during EFS with 1 ms pulse-width. Data are means ± SEM; n = 5-24.

3.3.5 Pressurised cremasteric arteries exhibit vasoconstriction to exogenously added PE and ATP

To assess the sensitivity of pressurised cremasteric arteries to neurotransmitters originating from sympathetic varicosities, arteries were exposed to exogenously added PE and ATP (see Figure 3.3.6). Both PE and ATP stimulated concentration-dependent vasoconstriction confirming the functional expression of α_1-ARs and $P2X_1$Rs in VSMCs.

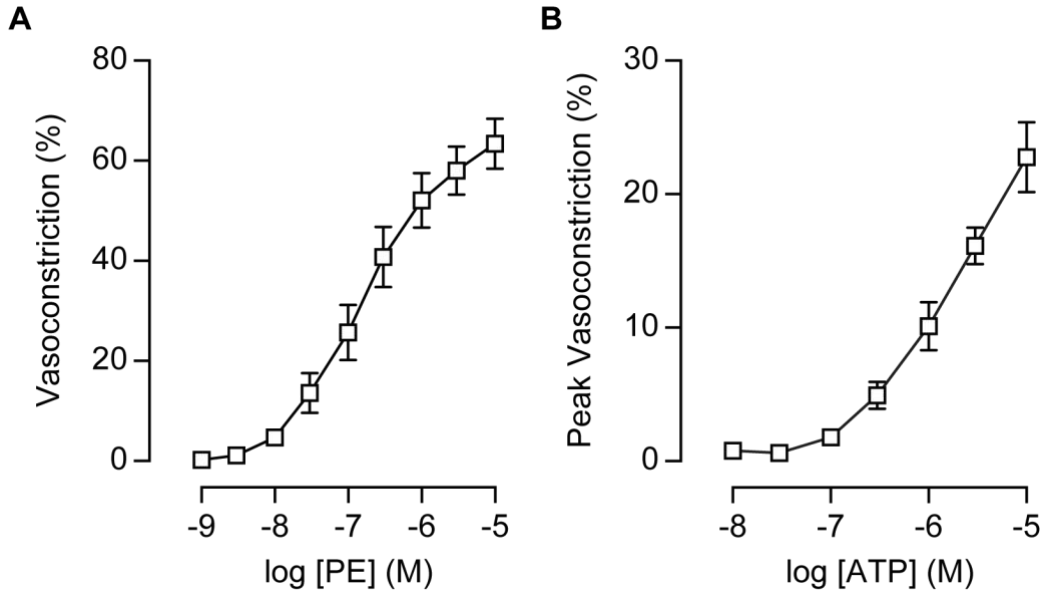


Figure 3.3.6 PE- and ATP-induced vasoconstriction in pressurised cremasteric arteries. (**A** and **B**) Cumulative concentration-response curves summarizing vasoconstriction to PE and ATP. Data are means ± SEM; n = 5.

3.3.6 Mesenteric arteries are more densely innervated with sympathetic nerve varicosities than cremasteric arteries

To compare the sympathetic nerve innervation of mesenteric and cremasteric arteries, immunohistochemistry was performed with an antibody against tyrosine hydroxylase, a key enzyme involved in catecholamine biosynthesis and commonly used marker for adrenergic nerve fibres. Clear and punctate staining of nerve varicosities was observed throughout the adventitia of mesenteric arteries (see Figure 3.3.7). In contrast, cremasteric artery innervation was considerably less dense (see Figure 3.3.8). This observation may reflect a difference in the physiological role sympathetic nerves play between arteries from different tissue beds.

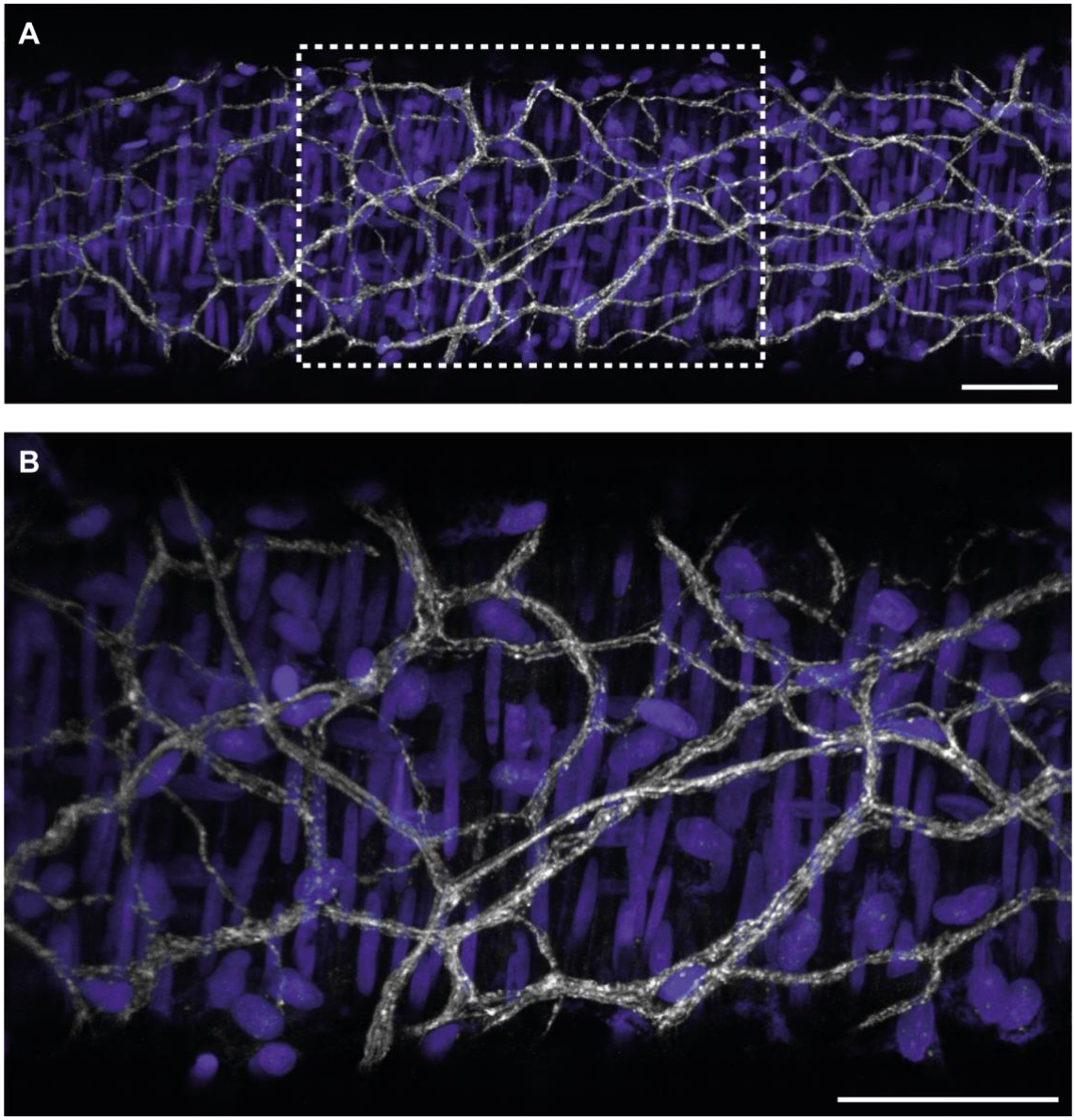


Figure 3.3.7 Tyrosine hydroxylase staining in mesenteric arteries. (**A** and **B**) Confocal fluorescence images of the adventitia of a pressurised artery stained with an antibody against tyrosine hydroxylase (white). Nuclei are counterstained with propidium iodide (purple). The dashed box (A) represents the region of magnification (B). Images are representative of 3 separate experiments. Scale bars, 50 µm.

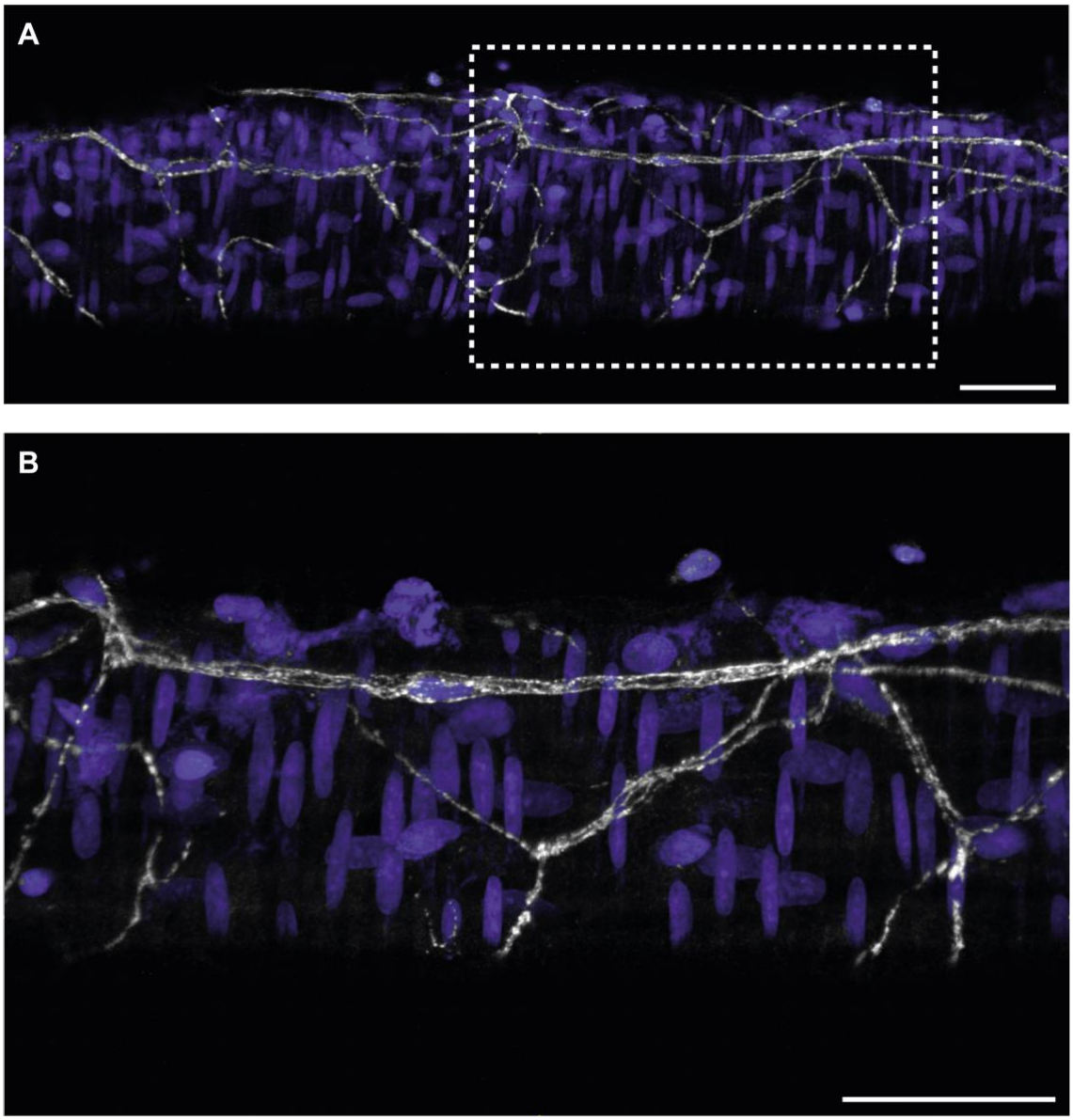


Figure 3.3.8 Tyrosine hydroxylase staining in cremasteric arteries. (**A** and **B**) Confocal fluorescence images of the adventitia of a pressurised artery stained with an antibody against tyrosine hydroxylase (white). Nuclei are counterstained with propidium iodide (purple). The dashed box (A) represents the region of magnification (B). Images are representative of 3 separate experiments. Scale bars, 50 µm.

3.4 DISCUSSION

The current investigation utilised EFS to activate perivascular nerves in pressurised rat mesenteric arteries and evaluate the role of the endothelium in modulating the resulting contraction.

EFS-induced vasoconstriction was sensitive to TTX, prazosin and NF 449, confirming NAD and ATP were released from sympathetic varicosities and activated α_1-ARs and $P2X_1$Rs, respectively. It is widely accepted NAD and ATP are stored together in synaptic vesicle in the sympathetic nerve terminal and upon their release mobilise Ca^{2+} in VSMCs to cause vasoconstriction (von Kügelgen and Starke, 1985; Dunn et al., 1999; Lamont et al., 2006; Nausch et al., 2012; Goonetilleke et al., 2013) (see Section 1.2). However, studies with EFS in isolated arteries have produced contradictory results with some concluding NAD alone mediates EFS-induced vasoconstriction (Van Riper and Bevan, 1991; Martínez et al., 1995; Aldasoro et al., 1996; Wei et al., 2018). In contrast, the current investigation identified a role for both noradrenergic and purinergic signalling mechanisms as the EFS response was attenuated in the combined presence of prazosin and NF 449 to a greater degree than with either antagonist alone. Interestingly, the lack of a $P2X_1$R-dependent component reported in the previously published works may be due to the differences in experimental approach used.

Rummery et al. (2007) studied vasoconstriction during EFS of rat mesenteric arteries pressurised to 30 and 90 mmHg. They reported the response to EFS was

greater at higher pressures due to an increase in the suramin-sensitive ATP-mediated component. This observation is in contrast to the aforementioned investigations into EFS-induced contraction in arteries under isometric conditions that identified NAD as the sole mediator of the response, suggesting pressurizing the artery may unmask the purinergic vasoconstriction, a possibility that warrants further investigation. Using another approach, the perfused mesenteric vascular bed, the purinergic component of the EFS response is reportedly larger following preconstriction with U 46619 or endothelin-1 compared to basal tone (Pakdeechote et al., 2007). Furthermore, in mesenteric arteries isolated from spontaneously hypertensive rats, which sustain chronically elevated intraluminal pressure, microelectrode impalements of VSMCs revealed the amplitude of ATP-mediated excitatory junction potentials in VSMCs was higher compared to recordings from normotensive rats (Brock and Van Helden, 1995; Goonetilleke et al., 2013). Subsequently, EFS-induced vasoconstriction in pressurised mesenteric arteries from hypertensive rats was also larger compared to arteries from their normotensive littermates (Goonetilleke et al., 2013). Altogether, these data lend support to the hypothesis that the effect of neuronally-derived ATP is pressure- and tone-dependent and may be more easily detected in pressurised arteries than arteries studied with wire myography.

Limited published works have compared responses between arteries under isometric and isobaric conditions, but Rummery and colleagues (2007) postulated arteries mounted in a pressure myograph are more depolarized than arteries mounted in a wire myograph, leading to an increase in Ca_V activation and

a greater sensitivity to purinergic transmission. This avenue of research could provide explanations for some of the discrepancies reported in the study of neurogenic responses in isolated arteries and the field of vascular physiology overall.

As well as stimulating vasoconstriction through α_1-ARs, NAD can act on VSM β_1-ARs to cause vasodilation through cyclic adenosine monophosphate production, signalling to inhibit myosin light chain kinase and activate ATP-sensitive K_+ channel (Briones et al., 2005; Garland et al., 2011b; Yarova et al., 2013). A recent investigation into the role of β-ARs during perivascular nerve stimulation in rat mesenteric arteries reported an increase in EFS- and NAD-induced vasoconstriction in the presence of the selective β_1-AR antagonist atenolol (Søndergaard et al., 2019). In our hands, propranolol did not increase the response to EFS suggesting β-AR stimulation by neuronally-derived NAD does not limit vasoconstriction. The study conducted by Søndergaard et al. (2019) was performed *in vivo* using intravital microscopy which could explain the difference in effect compared with the *in vitro* experiments reported here. It seems unlikely, however, that studying isolated arteries in a pressure myograph would interfere with β-AR signalling considering previously published research from our group has investigated β_1-AR-dependent vasodilation to exogenous NAD in isolated rat mesenteric arteries (Garland et al., 2011b).

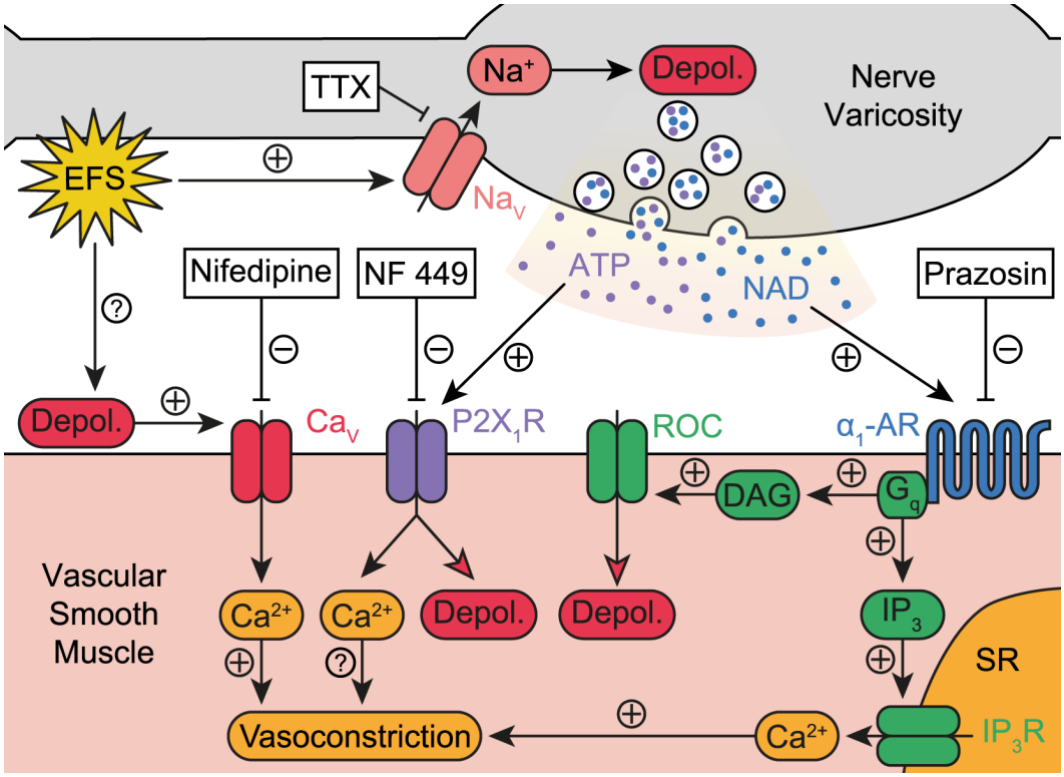


Figure 3.4.1 Proposed mechanism of EFS-induced vasoconstriction in the current investigation. Boxes with curved edges represent intracellular signalling components. Boxes with sharp edges represent antagonists. Arrows with a red arrowhead indicate direction of positive current.

The EFS parameters used in the current study caused TTX-sensitive and -insensitive vasoconstriction, with the latter not accounted for. The current literature on TTX-resistant vasoconstriction during EFS in isolated arteries is limited, but TTX-resistant EFS-induced vasodilation has been observed in mesenteric (Jensen, 1995), coronary (Feletou and Vanhoutte, 1989; Yasuda et al., 1994), tail (Anschütz and Schubert, 2005) and cerebral (Hardebo et al., 1989) arteries from various mammalian species. Several explanations have been provided for the lack of effect of TTX, but Feletou and Vanhoutte (1989) reported the response in canine coronary arteries was blocked by dopaminergic inhibitors and in the absence of extracellular Ca^{2+}, implicating the presence of TTX-resistant Na_V isoforms in dopaminergic neurons. The expression of such channels in rat perivascular sympathetic varicosities may explain the contraction observed in the presence of TTX. However, the residual response was completely attenuated by nifedipine lending support to the alternative view that it represents a direct effect at Ca_Vs in the VSM membrane. Nevertheless, myoendothelial feedback would still expect to be stimulated as we have previously demonstrated Ca^{2+} influx through Ca_Vs can activate myoendothelial feedback alongside adrenergic signalling (Garland et al., 2017).

EFS of pressurised cremasteric arteries was performed to investigate endothelial influence on neurogenic contraction during intrinsic myogenic activity in skeletal muscle arterioles. However, the EFS parameters used to activate perivascular nerves on mesenteric arteries unexpectedly caused no response, yet contraction was observed to exogenously administered NAD and ATP. The lack of response

to EFS may reflect a smaller role for neuronally-derived factors in skeletal muscle arterioles where vasoconstriction during exercise-associated sympathetic activity is undesired. Alternatively, during activation of the sympathetic nervous system the tissue may be more responsive to agents which cause vasodilation such as circulating ATP and elevated interstitial K^+ and adenosine (Dora, 2017). Interestingly, direct comparison of the tyrosine hydroxylase-positive staining in the two artery types suggests cremasteric arteries have a much lower density of catecholaminergic axons. This may indicate fewer sympathetic varicosities and, consequently, less NAD and ATP release. Previous exploration of sympathetic innervation in rat cremasteric arteries has reported vasoconstriction *in vivo* during electrical stimulation of the sympathetic trunk or posterior hypothalamus (Fleming et al., 1987). However, the authors used a pulse train duration of > 45 s and only arterioles of < 40 µm exhibited rapid responses within 10 s. Furthermore, Tarasova et al. (2003) observed EFS-induced vasoconstriction of the isolated external sural artery, the large artery supplying the gastrocnemius muscle, which was entirely inhibited during α-AR blockade despite sensitivity to exogenous ATP. These data imply the onset of contraction is slower in skeletal muscle arteries, perhaps due to the absence of an ATP-mediated component, and the EFS parameters used in the current study may not have been sufficient to cause vasoconstriction. Further investigation is warranted to establish the amount of neurotransmitter released during EFS in cremasteric arteries and how the profile of neurogenic vasoconstriction compares to that of other peripheral resistance arteries.

The key finding of the research presented here is that neurogenic vasoconstriction was not potentiated during inhibition of NO and EDH production. A role for the endothelium in limiting vasoconstriction during EFS was first reported by Martínez et al. (1995) and Aldasoro et al. (1996) who studied the ability of NO to reduce neurogenic contraction in isolated human pulmonary and cerebral arteries, respectively. Under isometric conditions, responses to EFS were potentiated in arteries denuded of an endothelium and in the presence of L-NAME. However, NOS inhibition also completely blocked ACh-mediated vasodilation in these arteries, which is in contrast to small resistance arteries where EDH is considered the main mechanism of endothelium-dependent vasodilation. Thus, the different effects of L-NAME on EFS-mediated vasoconstriction may be explained by the functional and structural characteristics of the arteries studied.

Nausch et al. (2012) provided the first evidence for activation of EDH-dependent myoendothelial feedback during EFS. In mouse mesenteric arteries, trains of electrical pulses stimulated vasoconstriction in pressurised vessels and an increase in EC Ca^{2+} pulsar frequency in *en face* preparations. In their hands, prazosin partially blocked the EFS-induced vasoconstriction and prevented the recruitment of Ca^{2+} pulsars whilst IK_{Ca} blockade potentiated neurogenic vasoconstriction. The current study established no such effect during inhibition of EDH production in similar calibre arteries, albeit from rat. Furthermore, Nausch and colleagues also reported a significant degree of myogenic tone under control conditions, which was increased following block of IK_{Ca}, whereas no basal

vasoconstriction was observed in rat mesenteric arteries. Considering this, the opposing conclusions drawn may represent differences in the species studied and highlights the importance of considering the experimental model when interpreting results.

Additional support for a role for myoendothelial feedback during EFS was provided by Wei et al. (2018) who demonstrated an increase in contraction to EFS during NOS and IK_{Ca} inhibition in rat mesenteric arteries under isometric tension. Although more closely aligned with the current investigation in terms of the vascular bed studied, the conclusions drawn are again contradictory. Compellingly, they also reported contraction to U 46619 was sensitive to L-NAME yet unaffected by inhibition of IK_{Ca}. This led to the conclusion that the vasoconstrictor stimulus and mechanism of contraction determine the functional contribution of the endothelium. Thus, if contractile mechanisms differ between arteries under isobaric and isometric conditions, it may follow that the ability for myoendothelial feedback to occur also differs depending on the experimental approach.

3.5 CONCLUSIONS

The aim of the current investigation was to evaluate a role for the endothelium in modulating neurogenic vasoconstriction in pressurised mesenteric and cremasteric arteries. It was anticipated EFS causes the release of sympathetic neurotransmitters from perivascular nerves, mediating vasoconstriction that is negatively regulated by myoendothelial feedback. The current study identified a role for both noradrenergic and purinergic signalling during the EFS response in mesenteric arteries, which is in contrast to research conducted in vessels under isometric conditions that only reported a role for NAD. However, the key finding that EFS-induced vasoconstriction is unchanged during blockade of NO and EDH production did not support the hypothesis. This is in disagreement with previous investigations into myoendothelial feedback during neurogenic contraction which concluded EFS indirectly activates the endothelium to limit the degree of vasoconstriction (Martínez et al., 1995; Aldasoro et al., 1996; Nausch et al., 2012; Wei et al., 2018). This discrepancy may be explained by differences in the tissue beds studied or the experimental approaches employed, with the latter forming the focus of the next chapter.

4.0 MYOENDOTHELIAL FEEDBACK IN RESISTANCE ARTERIES UNDER ISOBARIC AND ISOMETRIC CONDITIONS

4.1 INTRODUCTION

Resistance artery vasoreactivity is most routinely studied in vessels under isobaric or isometric conditions in a pressure or wire myograph, respectively. Interestingly, differences in artery sensitivity to external stimuli between the two experimental approaches have been reported, but investigations into the reasons for these differences are scarce and the discrepancies remain largely unexplained.

Only three studies have directly compared contractility between wire and pressure myography, but all reported pressurised mesenteric arteries were 5- to 10-fold more sensitive to NAD and PE than arteries under isometric conditions (Buus et al., 1994; Dunn et al., 1994; Falloon et al., 1995). Buus et al. (1994) were the first to provide an explanation for the disparate responses. Blocking neuronal amine uptake with cocaine, or *in vitro* denervation with 6-hydroxydopamine, potentiated contraction during adrenergic stimulation in both assays and ameliorated the difference between isobaric and isometric conditions. The same effect of cocaine was observed by Dunn et al. (1994) and Falloon et al. (1995). This led to the conclusion that uptake of monoamines is less prevalent in pressurised arteries, resulting in a higher effective concentration of α-AR agonists in the bath of the wire myograph. However, this has not been developed further and does not appear to be the full explanation as pressurised arteries exhibited a larger contractile response to non-monoamines including vasopressin, histamine and angiotensin II (AngII) (Dunn et al., 1994; Falloon et al., 1995). As an aside, it should also be noted the focus of these studies has

been on responses to metabotropic receptor agonists, and none have considered contraction to activators of ionotropic receptors, such as ATP, which may also differ between isobaric and isometric conditions. Furthermore, in their hands, pressurised rat and rabbit mesenteric arteries exhibited a basal level of nerve-independent intrinsic vasoconstriction, which didn't develop in arteries studied isometrically (Buus et al., 1994; Dunn et al., 1994). The presence of myogenic tone and increased responsiveness to non-monoamines in pressurised arteries was not reconciled by the authors as they could not be explained by differences in amine uptake.

Interestingly, microelectrode recordings of VSMCs in rabbit mesenteric arteries studied isometrically revealed the resting membrane potential to be ~-54 mV, which is relatively hyperpolarized compared to the resting membrane potential range of -40 to -50 mV previously reported for arteries pressurised to 60 mmHg (Dunn et al., 1994). Furthermore, when arteries mounted in the wire myograph were slightly depolarized to ~-47 mV by increasing $[K^+]_o$ to 20 mM, the sensitivity to NAD, histamine and AngII increased dramatically. These findings suggest the VSM of vessels is more depolarized during isobaric conditions than isometric and, as a result, more likely to contract. Contrary to this, Ca_V blockade attenuated NAD-induced contraction in arteries under isometric tension but had little effect in pressurised arteries (Dunn et al., 1994). Furthermore, the ability for elevated $[K^+]_o$ to cause contraction was similar between the experimental assays suggesting VSM Ca_V reactivity did not differ between arteries mounted in pressure and wire myographs (Buus et al., 1994). Thus, there is evidence for and

against the proposition that the differences between pressure and wire myography are a result of an elevated VSM resting membrane potential under isobaric conditions. Alternatively, the difference in reactivity may be due to activation of ROCK signalling, which has previously been shown to play a predominant role in pressure-induced depolarization and myogenic tone in various tissue beds (Ito et al., 2007; Li and Brayden, 2017; Björling et al., 2018) (see Section 1.2.2). Compellingly, investigations with rat mesenteric arteries studied isometrically have reported no effect of ROCK inhibition on PE-induced contraction (Rao et al., 2013; Zhong et al., 2019).

With regard to comparisons of endothelium-dependent responses in the experimental setups, Falloon et al. (1995) reported the ability for ACh to cause relaxation was similar between rat mesenteric arteries under isometric and isobaric conditions, but did not probe the relative contributions of NO and K_{Ca}-mediated EDH. In contrast, Boettcher and de Wit (2011) studied feed arteries within the mouse gracilis muscle and, despite a similar EC_{50} for ACh under control circumstances, demonstrated NOS inhibition attenuated ACh-induced relaxation in arteries under isometric conditions whilst having no effect in isolated pressurised arteries or arteries studied *in vivo*. Thus, the mechanism by which endothelium-dependent vasodilation occurs may also be dependent on the experimental approach.

Previously, inhibition of NOS and K_{Ca}s has been shown to increase artery sensitivity to vasoconstrictors in isobaric and isometric conditions, but the

conclusions drawn have been inconsistent (see Section 1.3.2). Some investigations have reported NO is stimulated during contraction to limit the response (Dora et al., 1997, 2000; Tuttle and Falcone, 2001), whilst others conclude NOS inhibition with L-NAME has no effect on contraction (Yashiro and Duling, 2000; Shaw et al., 2009), or EDH is the main mediator of the negative feedback loop (Nausch et al., 2012; Tran et al., 2012) (see Table 1.3.1). Furthermore, no investigations have directly compared the ability for the endothelium to modulate contraction during pressure and wire myography.

The reports of differences in sensitivity to vasoconstrictors and mechanisms of endothelium-dependent relaxation between experimental setups could influence the ability to initiate myoendothelial feedback and for any generated dilators to then evoke feedback. Establishing the determinants of this process will allow experiments regarding myoendothelial feedback to proceed within the defined framework.

4.1.1 Aims and hypotheses

The aim of the current investigation was to systematically compare contraction, endothelium-dependent relaxation and myoendothelial feedback in isolated resistance arteries under isobaric and isometric conditions.

It was anticipated pressurised arteries would exhibit greater sensitivity to vasoconstrictor agonists and reduced sensitivity to stimulators of endothelium-dependent vasodilation than arteries mounted in the wire myograph.

4.2 MATERIALS AND METHODS

4.2.1 Pressure myography

Mesenteric arteries were prepared for pressure myography experiments, as previously described (see Section 2.2). In all pressure myography experiments, intraluminal pressure was set to 70 mmHg.

4.2.2 Wire myography

Mesenteric arteries were prepared for wire myography experiments, as previously described (see Section 2.3). In all wire myography experiments, arteries were normalised to a resting tension equivalent to that generated at 90% of the diameter of the vessel at 70 mmHg.

4.2.3 Inhibitors

The following drugs were used in this chapter to block their respective targets, at concentrations which have previously been shown to be effective: 1.0 µM glycyl-H1152 to antagonise ROCK (Li and Brayden, 2017), 1.0 µM nifedipine to block Ca_Vs (Bagher et al., 2012), 100.0 µM L-NAME to antagonise NOS (Garland et al., 2017), and 1.0 µM TRAM-34 and 0.1 µM apamin to block IK_{Ca} and SK_{Ca}, respectively (Lemmey et al., 2018).

4.3 RESULTS

4.3.1 PE-mediated contraction is limited by the endothelium to a greater degree in arteries under isometric conditions than isobaric

Contraction to PE was studied in the absence and presence of inhibitors of NO and EDH production to assess myoendothelial feedback during α_1-AR activation in mesenteric arteries under isobaric and isometric conditions. PE caused dose-dependent contraction with pressurised vessels exhibiting greater contraction at small concentrations (1.0 µM: isobaric control, 83.5 ± 1.3%, n = 14; isometric control, 45.0 ± 5.2%, n = 24). L-NAME alone and in combination with TRAM-34 and apamin slightly potentiated vasoconstriction to maximal concentrations of PE in arteries under isobaric conditions (1.0 µM: L-NAME, 90.0 ± 1.2%, n = 3; L-NAME + TR + Ap, 93.7 ± 1.2%, n = 6) (see Figures 4.3.1A and 4.3.1C). This observation suggests NO and EDH play a small role in limiting vasoconstriction in pressurised mesenteric arteries.

In arteries studied in the wire myograph, the combination of L-NAME, TRAM-34 and apamin potentiated contraction to submaximal PE concentrations which caused very little response in control circumstances (0.3 µM: control, 6.9 ± 3.6%, n = 24; L-NAME + TR + Ap, 54.3 ± 5.3%, n = 14). At higher PE concentrations, L-NAME alone increased the response (1.0 µM: L-NAME, 74.8 ± 3.2, n = 5) (see Figures 4.3.1B and 4.3.1D). These data confirm the endothelium negatively modulates the contractile response to PE through NO and EDH production in mesenteric arteries under isometric conditions.

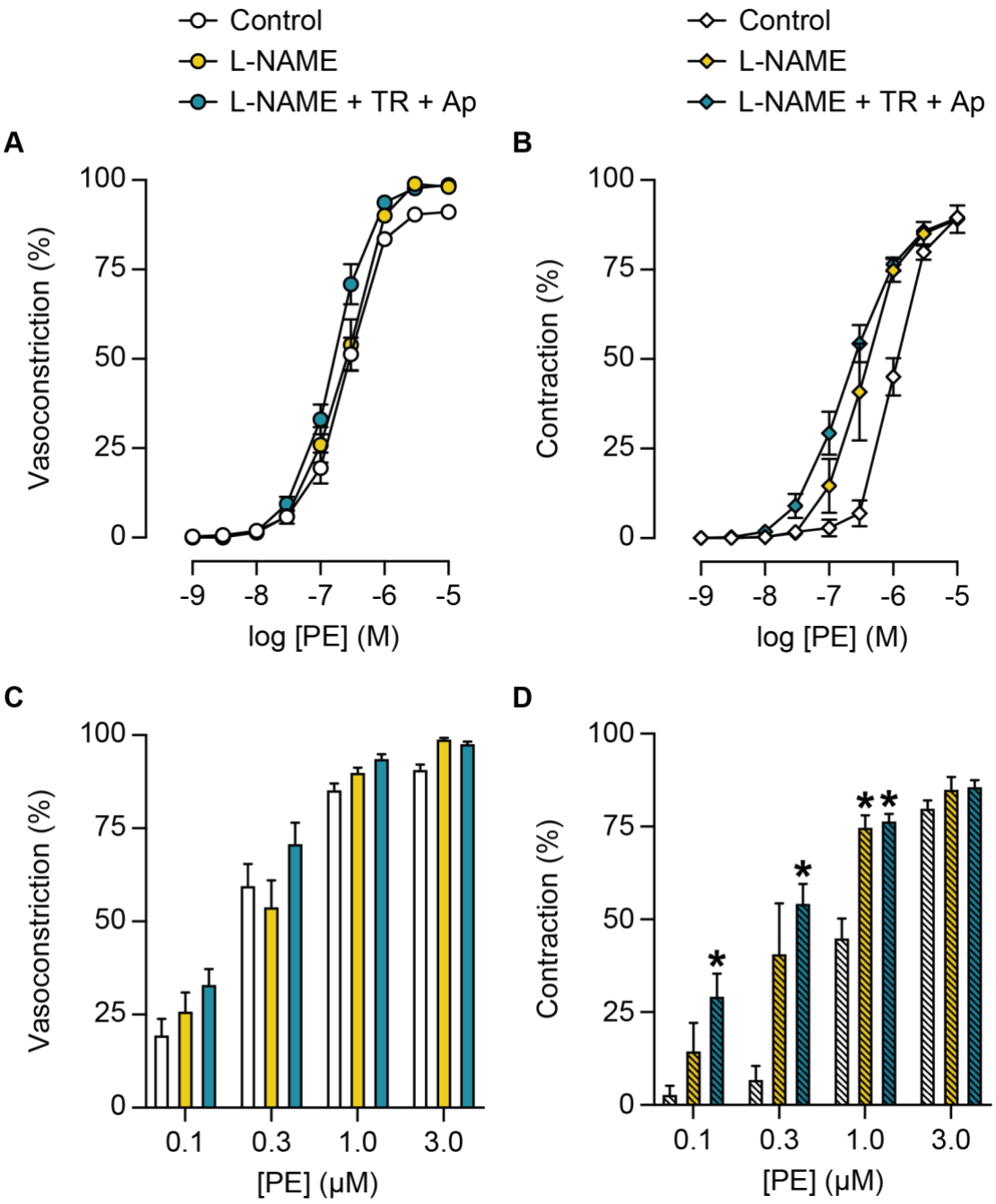

A
Control
L-NAME
L-NAME + TR + Ap
Vasoconstriction (%)
100
75
50
25
0
-9
-8
-7
-6
-5
log [PE] (M)
B
Control
L-NAME
L-NAME + TR + Ap
Contraction (%)
100
75
50
25
0
-9
-8
-7
-6
-5
log [PE] (M)
C
Vasoconstriction (%)
100
75
50
25
0
0.1
0.3
1.0
3.0
[PE] (μM)
D
Contraction (%)
100
75
50
25
0
*
*
**
0.1
0.3
1.0
3.0
[PE] (μM)

Figure 4.3.1 Effect of blockade of NO and EDH production on PE-induced contraction in mesenteric arteries under isobaric and isometric conditions. (**A** and **C**) Cumulative concentration-response curves and bar graph summarizing vasoconstriction in arteries under isobaric conditions to PE in the absence and presence of 100 µM L-NAME alone or L-NAME, 1 µM TRAM-34 (TR) and 0.1 µM apamin (Ap). (**B** and **D**) Cumulative concentration-response curves and bar graph summarizing contraction in arteries under isometric conditions to PE in the absence and presence of L-NAME or L-NAME, TR and Ap. Data are means ± SEM; n = 3-24. *P < 0.05 compared to control at the same concentration.

4.3.2 NO and EDH limit contraction to ATP in arteries mounted in the wire myograph, but not pressure myograph

A role for myoendothelial feedback during $P2X_1R$ activation was investigated by studying the effect of NOS and K_{Ca} blockade on ATP-induced contraction in mesenteric arteries under isobaric and isometric conditions. ATP caused dose-dependent contraction with pressurised vessels exhibiting greater contraction at small concentrations (10.0 µM: isobaric control, 25.5 ± 3.7%, n =6; isometric control, 4.4 ± 0.7%, n = 11). In both pressure and wire myography experiments, contraction to ATP was blocked by 10 µM NF 449 (data not shown). In pressurised arteries, the response was not potentiated by inhibitors of NO and EDH production (10.0 µM: L-NAME, 23.1 ± 2.4%, n = 4; L-NAME + TR + Ap, 22.3 ± 4.6%, n = 4) suggesting the endothelium is not stimulated during vasoconstriction to ATP (see Figures 4.3.2A and 4.3.2C).

In comparison, under isometric conditions, the contractile response to ATP was increased by L-NAME (10.0 µM: 10.9 ± 2.6%, n = 8) and further potentiated in the additional presence of TRAM-34 and apamin(10.0 µM: 25.8 ± 4.2%, n = 12) (see Figures 4.3.2B and 4.3.2D). These data indicate a role for both NO and EDH in limiting the degree of contraction to ATP under isometric conditions.

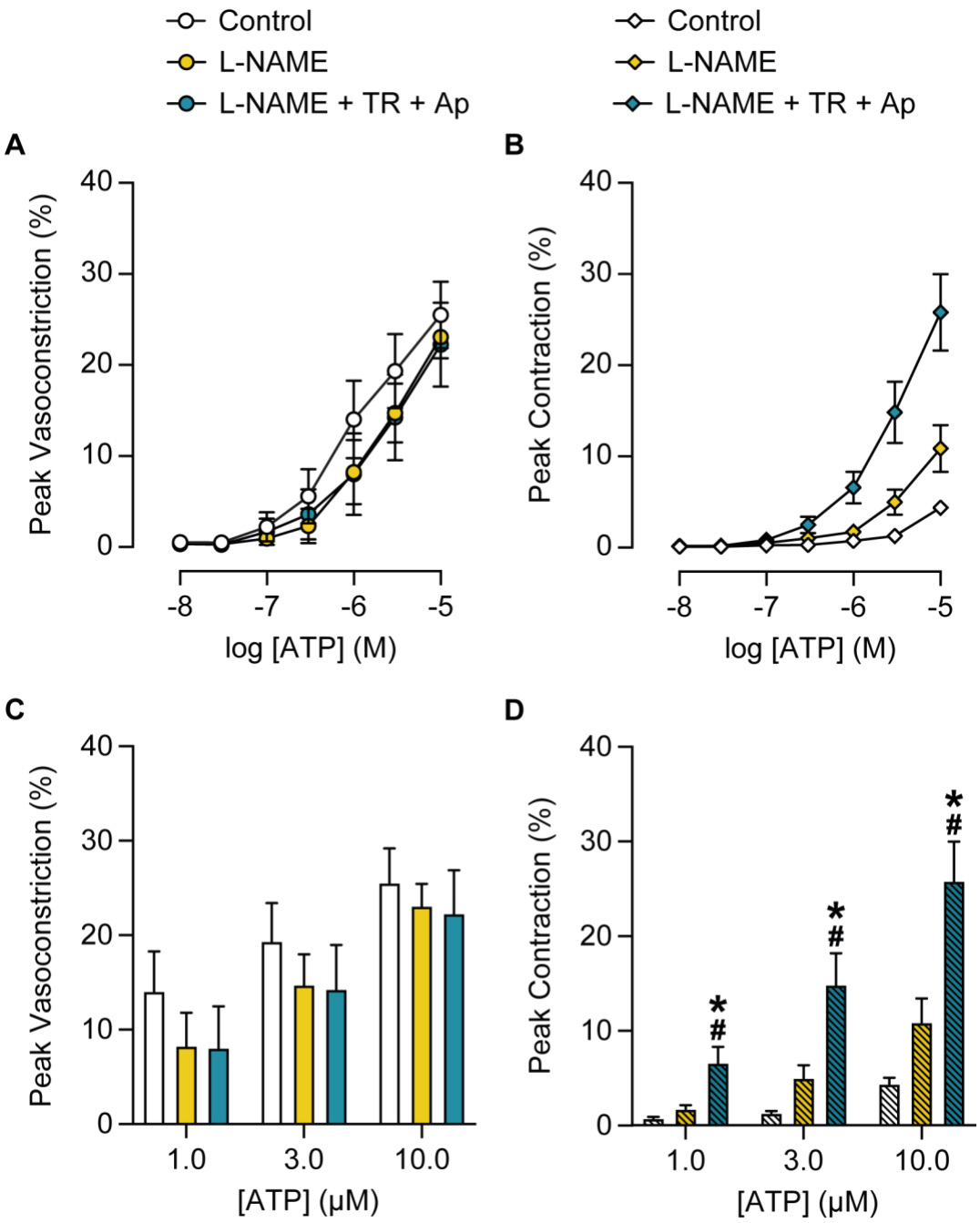

Control
L-NAME
L-NAME + TR + Ap
A
Peak Vasoconstriction (%)
log [ATP] (M)
B
Peak Contraction (%)
log [ATP] (M)
C
Peak Vasoconstriction (%)
[ATP] (μM)
D
Peak Contraction (%)
[ATP] (μM)

Figure 4.3.2 Effect of blockade of NO and EDH production on ATP-induced contraction in mesenteric arteries under isobaric and isometric conditions. (**A** and **C**) Cumulative concentration-response curves and bar graph summarizing vasoconstriction in arteries under isobaric conditions to ATP in the absence and presence of 100 µM L-NAME alone or L-NAME, 1 µM TRAM-34 (TR) and 0.1 µM apamin (Ap). (**B** and **D**) Cumulative concentration-response curves and bar graph summarizing contraction in arteries under isometric conditions to ATP in the absence and presence of L-NAME alone or L-NAME, TR and Ap. Data are means ± SEM; n = 4-12. $^{*}P < 0.05$ compared to control at the same concentration; $^{\#}P < 0.05$ compared to L-NAME at the same concentration.

4.3.3 The mechanism of ACh-mediated vasodilation differs between arteries under isobaric and isometric conditions

To evaluate the contribution of NO and EDH production to endothelium-dependent vasodilation in mesenteric arteries under isometric and isobaric conditions, ACh-induced relaxation was studied before and after treatment with L-NAME, TRAM-34 and apamin. The combination of L-NAME, TRAM-34 and apamin did not cause the development of basal tone in pressurised vessels or arteries studied isometrically (data not shown). ACh stimulated dose-dependent relaxation with vessels mounted in the wire myograph exhibiting greater relaxation at small concentrations (0.1 µM: isobaric control, 81.3 ± 5.8%, n = 14; isometric control, 96.4 ± 1.0%, n = 15). Under isobaric conditions the response was unaffected by the addition of L-NAME but was partially attenuated in the additional presence of TRAM-34 and apamin (0.1 µM: L-NAME, 79.2 ± 7.0%, n = 4; L-NAME + TR + Ap, 0.6 ± 0.3%, n = 9) (see Figures 4.3.3A and 4.3.3C). Addition of L-NAME, TRAM-34 and apamin to the perfused luminal solution as well as the superfusion during pressure myography experiments had no further effect on their ability to inhibit vasodilation (data not shown). These data suggest ACh-induced vasodilation is mediated by K_{Ca} activation but not NO production.

In contrast, the response in arteries under isometric conditions was reduced in the presence of L-NAME and completely blocked with the addition of TRAM-34 and apamin (0.1 µM: L-NAME, 68.6 ± 7.0%, n = 15; L-NAME + TR + Ap, -0.1 ± 0.4%, n = 13) (see Figures 4.3.3B and 4.3.3D). These effects indicate a role for

both NO and EDH production in ACh-induced relaxation in mesenteric arteries mounted in the wire myograph.

Interestingly the ACh response in pressurised arteries did not involve NO and a K_{Ca}-independent vasodilator mechanism was seen, which was absent under isometric conditions.

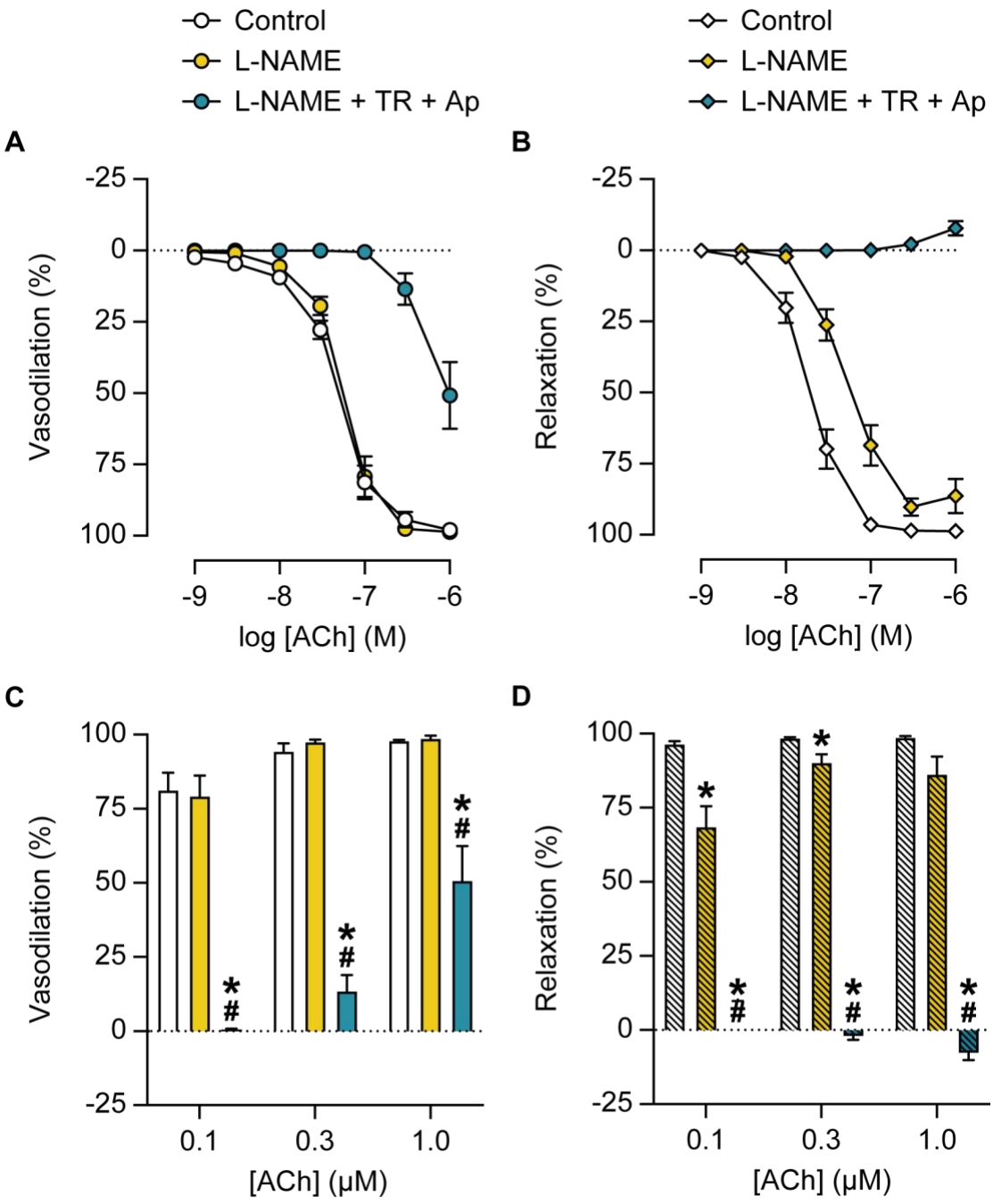

A
Control
L-NAME
L-NAME + TR + Ap
Vasodilation (%)
-25
0
25
50
75
100
-9
-8
-7
-6
log [ACh] (M)
B
Control
L-NAME
L-NAME + TR + Ap
Relaxation (%)
-25
0
25
50
75
100
-9
-8
-7
-6
log [ACh] (M)
C
Vasodilation (%)
100
75
50
25
0
-25
*
#
0.1
0.3
1.0
[ACh] (μM)
D
Relaxation (%)
100
75
50
25
0
-25
*
#
0.1
0.3
1.0
[ACh] (μM)

Figure 4.3.3 Effect of inhibition of NO and EDH production on ACh-induced relaxation in mesenteric arteries under isobaric and isometric conditions. (**A** and **C**) Cumulative concentration-response curves and bar graph summarizing vasodilation in arteries under isobaric conditions to ACh in the absence and presence of 100 µM L-NAME alone or L-NAME, 1 µM TRAM-34 (TR) and 0.1 µM apamin (Ap). (**B** and **D**) Cumulative concentration-response curves and bar graph summarizing relaxation in arteries under isometric conditions to ACh in the absence and presence of L-NAME alone or L-NAME, TR and Ap. Data are means ± SEM; n = 4-15. $^{*}P < 0.05$ compared to control at the same concentration; $^{\#}P < 0.05$ compared to L-NAME at the same concentration.

4.3.4 Arteries mounted in the wire myograph are more responsive to NO donors than pressurised arteries

To compare the relaxation of mesenteric arteries under isobaric and isometric conditions to NO, responses to the NO donors diethylamine NONOate (DEA/NO) and S-Nitrosoglutathione (SNOG) were evaluated. DEA/NO stimulated dose-dependent relaxation with arteries mounted in the wire myograph exhibiting greater relaxation (30 µM: isobaric control, 43.2 ± 5.0%, n = 7; isometric control, 98.5 ± 0.7%, n = 4) (see Figure 4.3.4A). A similar trend was also observed for SNOG-induced relaxation (10 µM: isobaric control, 16.8 ± 3.3%, n = 4; isometric control, 96.8 ± 1.2%, n = 2) (see Figure 4.3.4B). Together, these observations suggest artery pressurization confers reduced sensitivity to NO, which may contribute to the lack of effect of L-NAME on ACh-induced vasodilation.

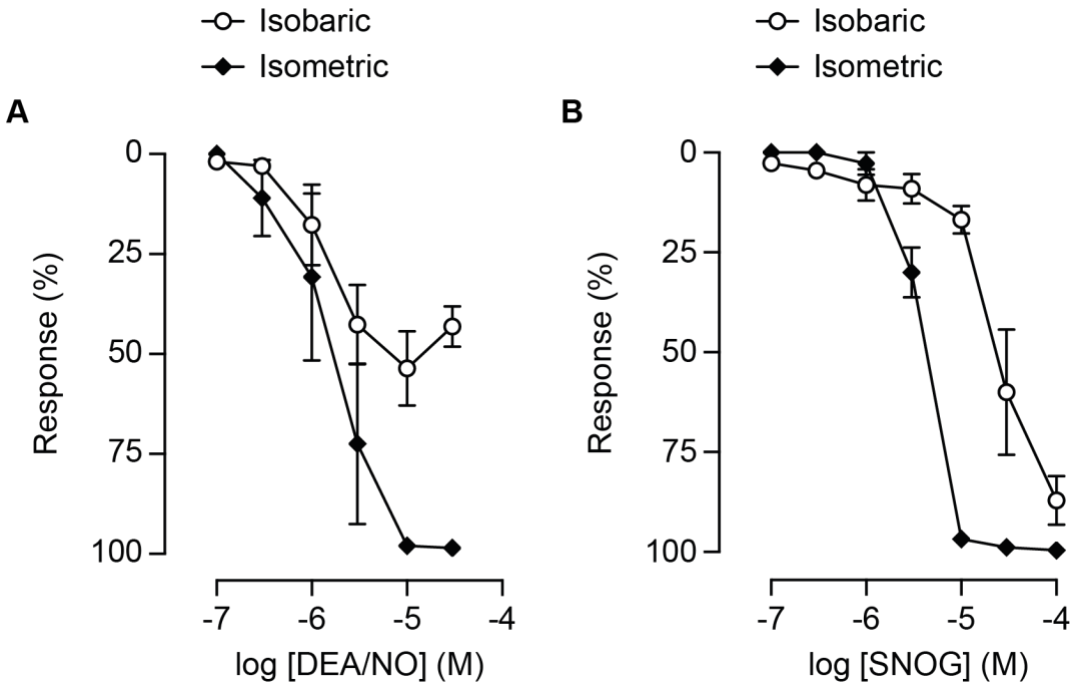


Figure 4.3.4 DEA/NO- and SNOG-induced relaxation in mesenteric arteries under isobaric and isometric conditions. (**A** and **B**) Cumulative concentration-response curves summarizing relaxation in arteries under isobaric and isometric conditions to DEA/NO and SNOG. Data are means ± SEM; n = 2-6.

4.3.5 PE-mediated vasoconstriction is sensitive to Ca_V blockade in arteries under isometric and isobaric conditions

In a set of paired experiments, Ca_V activation during PE-induced contraction in mesenteric arteries under isobaric and isometric conditions was assessed with the Cav blocker nifedipine. In the presence of nifedipine, vasoconstriction to submaximal concentrations of PE was right-shifted (1.0 µM: control, 85.5 ± 2.9%; + Nifedipine, 48.4 ± 11.8%; n = 3) (see Figures 4.3.5A and 4.3.5C). Comparably, contraction to PE in vessels under isometric conditions was also right-shifted (3 µM: control, 80.9 ± 10.5%; + Nifedipine, 27.3 ± 2.9%; n = 4) (see Figures 4.3.5B and 4.3.5D). The magnitude of effect of nifedipine appears to be similar between arteries under isobaric and isometric conditions, suggesting the involvement of Ca^{2+} influx through Ca_Vs during PE-induced contraction is similar between the two experimental approaches.

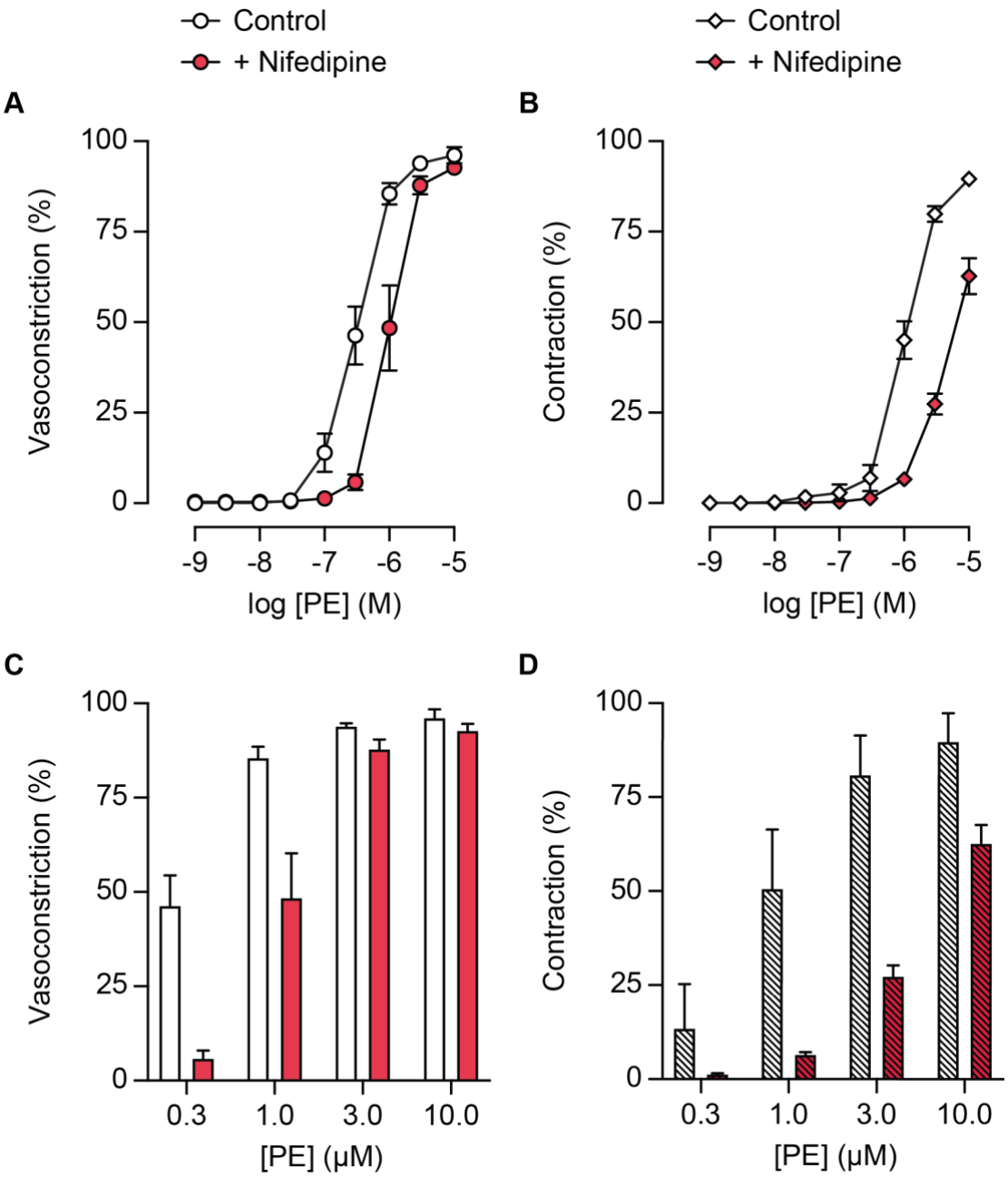

A
Control
+ Nifedipine
Vasoconstriction (%)
100
75
50
25
0
-9
-8
-7
-6
-5
log [PE] (M)
B
Control
+ Nifedipine
Contraction (%)
100
75
50
25
0
-9
-8
-7
-6
-5
log [PE] (M)
C
Vasoconstriction (%)
100
75
50
25
0
0.3
1.0
3.0
10.0
[PE] (μM)
D
Contraction (%)
100
75
50
25
0
0.3
1.0
3.0
10.0
[PE] (μM)

Figure 4.3.5 Effect of Ca_V blockade on PE-induced contraction in mesenteric arteries under isobaric and isometric conditions. (**A** and **C**) Cumulative concentration-response curves and bar graph summarizing vasoconstriction in arteries under isobaric conditions to PE in the absence and presence of 1 μM nifedipine. (**B** and **D**) Cumulative concentration-response curves and bar graph summarizing contraction in arteries under isometric conditions to PE in the absence and presence of nifedipine. These data represent paired experiments. Data are means ± SEM; n = 3-4.

4.3.6 ROCKII inhibition in pressurised arteries decreases contraction to PE and increases relaxation to ACh and exogenously-added NO

To assess the role of ROCKII in mediating mesenteric artery reactivity during pressurization, pressure myography experiments were conducted in the presence of the selective ROCKII inhibitor glycyl-H 1152. ROCKII inhibition right-shifted the vasoconstriction to PE (0.3 µM: control, 51.3 ± 4.6%, n = 14; Glycyl-H 1152, 0.7 ± 0.4%, n = 3) (see Figures 4.3.6A and 4.3.6B). In addition, Glycyl-H 1152 increased the relaxation of pressurised arteries to the NO donor DEA/NO (30 µM: control, 43.2 ± 5.0%, n = 7; Glycyl-H 1152, 96.9 ± 0.8%, n = 3) (see Figure 4.3.7A). Interestingly, 0.1 µM glycyl-H 1152 had no effect on DEA/NO-induced vasodilation (data not shown). Furthermore, ACh-induced vasodilation was left-shifted in the presence of glycl-H 1152 (0.03 µM: control, 27.8 ± 3.1%, n = 14; Glycyl-H 1152, 65.7 ± 12.1%, n = 3) (see Figure 4.3.7B). These data suggest blockade of ROCKII increase the sensitivity of the VSM to NO and endothelium-dependent vasodilation and may represent an unmasking of the effect of myoendothelial feedback.

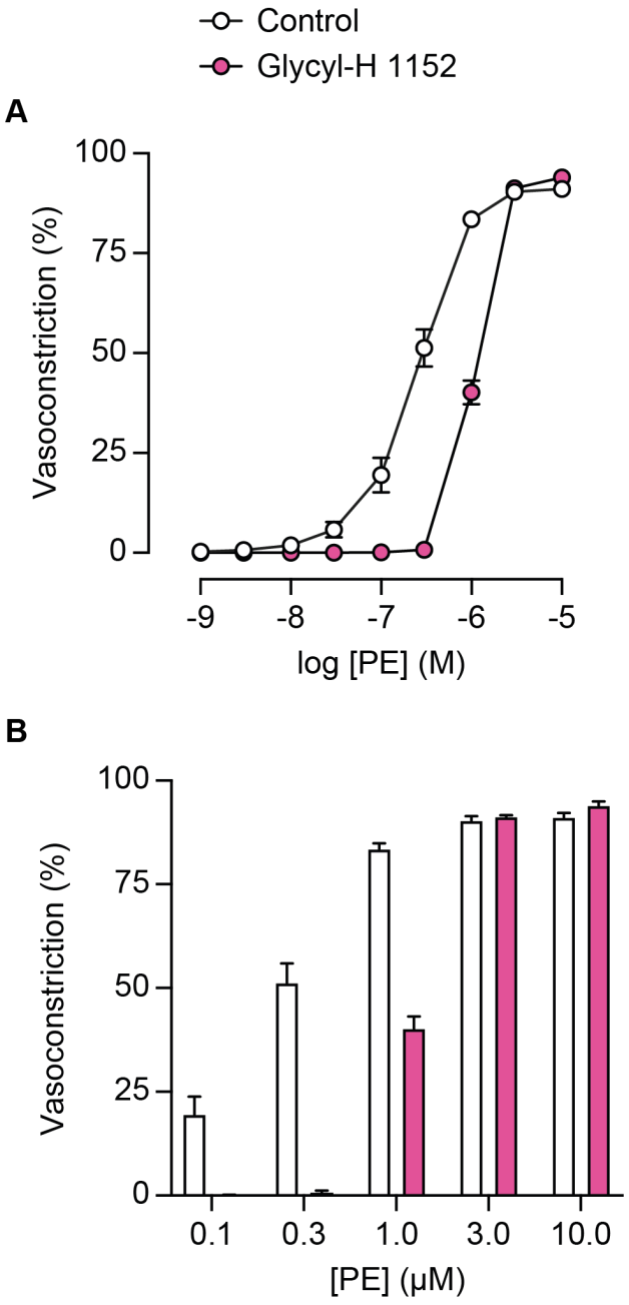


Figure 4.3.6 Effect of ROCKII inhibition on PE-induced vasoconstriction in pressurised mesenteric arteries. (**A** and **B**) Cumulative concentration-response curves and bar graph summarizing vasoconstriction in arteries under isobaric conditions to PE in the absence and presence of 1 μM glycyl-H 1152. Data are means ± SEM; n = 3-14.

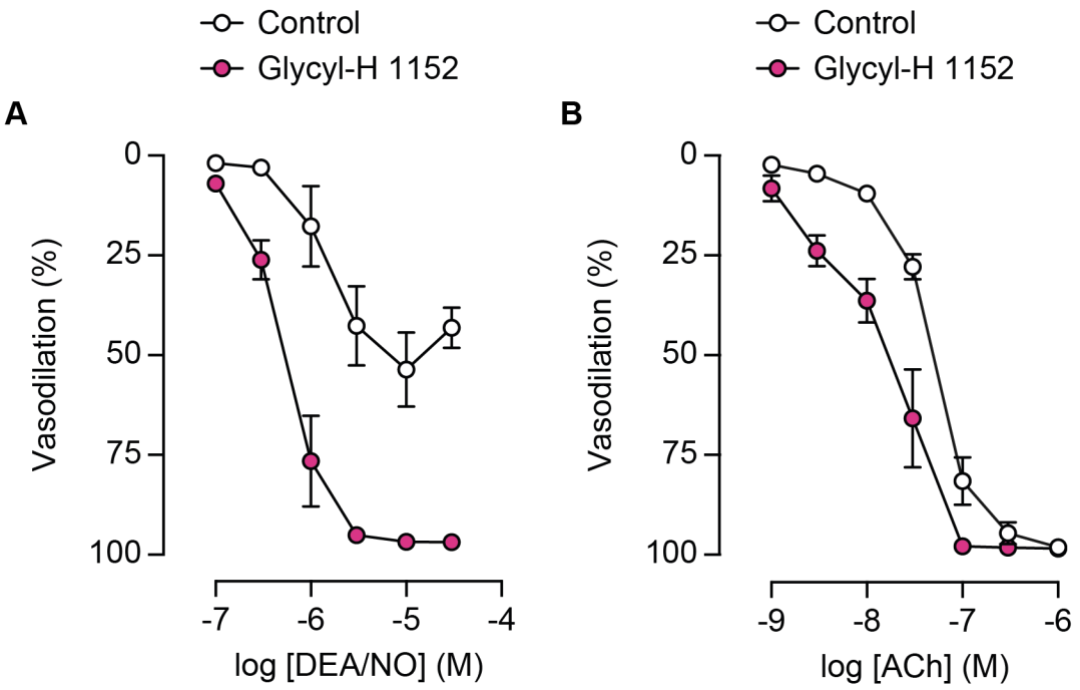


Figure 4.3.7 Effect of ROCKII inhibition on DEA/NO- and ACh-induced vasodilation in pressurised mesenteric arteries. (**A**) Cumulative concentration-response curves summarizing vasodilation in arteries under isobaric to DEA/NO in the absence and presence of 1 μM glycyl-H 1152. (**B**) Cumulative concentration-response curves summarizing vasodilation in arteries under isobaric to ACh in the absence and presence of glycyl-H 1152. Data are means ± SEM; n = 3-14.

4.4 DISCUSSION

The current study investigated differences in vasoreactivity between mesenteric arteries under isobaric and isometric conditions with pressure and wire myography, respectively. The findings supported the hypothesis as pressurised arteries were more responsive to smaller concentrations of vasoconstrictors than arteries studied isometrically. This difference in vasoreactivity may reflect an altered responsiveness to endothelium-dependent vasodilation and myoendothelial feedback, and activation of ROCK signalling.

Arteries studied isometrically exhibited greater relaxation to mediators of endothelium-dependent and -independent vasodilation. Additionally, NOS inhibition attenuated ACh-induced relaxation in arteries mounted in the wire myograph, whilst eliciting no effect in pressurised arteries. Similar observations have been made in mouse gracilis feed arteries, wherein L-NAME and indomethacin, a nonselective cyclooxygenase inhibitor, reduced ACh-induced relaxation in the wire myograph but had no effect on the response in arteries under isobaric conditions or *in vivo* (Boettcher and de Wit, 2011). This suggests either the ability for ACh to stimulate eNOS is compromised, EDH can compensate for the loss of NO production or the VSM is insensitive to NO. The diminished response to the NO donors DEA/NO and SNOG in the pressure myograph lends support to the latter. Compellingly, a previous investigation into pressurised rat mesenteric artery vasoreactivity reported an inverse relationship between intraluminal pressure and sensitivity to ACh and the NO donor sodium

nitroprusside (Gündüz et al., 2008), however the mechanism behind the phenomenon has not been determined.

Another striking difference observed between the two experimental approaches was that the combination of L-NAME, TRAM-34 and apamin did not completely attenuate ACh-induced vasodilation in the pressure myograph as it did in arteries under isometric conditions. This result demonstrates a role for an eNOS- and K_{Ca}-independent vasodilatory mechanism which is unmasked by pressurization. Such an effect was also observed by Boettcher and de Wit (2011) in pressurised mouse gracilis arteries from connexin 40 deficient-mice. They illustrated connexin 40, a MEGJ protein, is essential for EDH-mediated relaxation in arteries under isometric conditions, but its knockdown had no effect on vasodilation in arteries in the pressure myograph. Intriguingly, they still reported the response was hyperpolarization-dependent as ACh caused no relaxation in arteries preconstricted with 50 mM K^+ in both experimental assays. The reduced vasodilation of pressurised arteries to exogenous NO, and the lack of effect of NOS and K_{Ca} inhibition on the ACh response point to an unaccounted-for vasodilatory mechanism that is pressure-dependent, which certainly warrants further investigation.

Under control conditions, the threshold concentrations of PE and ATP which stimulated contraction in pressurised arteries were lower than in arteries studied isometrically, supporting the findings of previous investigations which concluded artery pressurization conveys greater sensitivity to contractile agonists including

NAD, histamine and AngII (Buus et al., 1994; Dunn et al., 1994; Falloon et al., 1995).

Most pertinent to the study of myoendothelial feedback, inhibition of NOS, IK_{Ca} and SK_{Ca} left-shifted the response to PE and ATP in arteries under isometric conditions, whilst the same treatment only affected PE-induced vasoconstriction in isobaric conditions, and only at concentrations which stimulated a maximum response. Previously, simultaneous measurement of diameter and EC Ca^{2+} concentration demonstrated a concomitant increase in EC Ca^{2+} activity alongside PE-induced vasoconstriction in pressurised arteries isolated from hamster check pouch (Dora et al., 1997), hamster cremaster muscle (Jackson et al., 2009) and rat mesentery (Schuster et al., 2001; Lamboley et al., 2005). This parallel increase in EC $[Ca^{2+}]_i$ is theorised to prevent Ca_V opening probability, thus left-shifting the response to PE. However, the pressure myography experiments conducted in the current investigation do not support this hypothesis and indicate NO and EDH are activated to limit over-constriction of the vessel rather than increase the threshold concentration of PE. This conclusion is more in-line with a recent study from our research group into vasoconstriction in rat cremasteric arterioles, in which myoendothelial feedback was only observed following the peak response to PE and elevated extracellular K^+ (Garland et al., 2017).

Evidence for myoendothelial feedback during adrenergic stimulation was observed in both wire and pressure myography experiments, but the profile of its influence was different between experimental approaches. Interestingly, Wei et

al. (2018) reported EFS-induced contraction of arteries mounted in the wire myograph was limited by IK_{Ca} activation, whereas the neurogenic response was attenuated by SK_{Ca} activation in the perfused mesenteric vascular bed approach. This led to the proposition that the functional contribution of myoendothelial feedback is determined by the contractile stimulus, a notion which may also be applicable to the findings reported here.

The current study also investigated the role of the endothelium in modulating purinergic contraction. Although previous reports have suggested ATP-induced vasoconstriction is pressure- and tone-dependent (Pakdeechote et al., 2007; Rummery et al., 2007), this is the first investigation to directly compare ATP responses between arteries under isometric and isobaric conditions. Inhibition of NO and EDH production greatly increased the contractile response to ATP in arteries mounted in the wire myograph but had no effect on ATP-induced vasoconstriction in the pressure myograph, similar to the observations made with PE. However, responses to ATP need to be interpreted carefully as, unlike α_1-ARs, $P2X_1$Rs and ATP- gated purinoceptors, subclass Y (P2YRs) are reportedly expressed in ECs as well as VSMCs (Harrington and Mitchell, 2004; Winter and Dora, 2007; Dora, 2017). Thus, ATP may stimulate both cell types simultaneously in isometrically studied arteries and the effect of L-NAME, TRAM-34 and apamin represents inhibition of the EC-mediated component, which allows the contractile response to predominate.

It is nonetheless interesting to note the potentiating effect of NOS and K_{Ca} inhibition was not observed in pressurised vessels. Winter and Dora, (2007) demonstrated luminal application of ATP in pressurised mesenteric arteries stimulated P2YR-dependent vasodilation which was attenuated by blocking NO and EDH production. Consequently, the trends observed in the pressure myograph may reflect an inability for ATP to penetrate the vessel wall and reach the underlying endothelium. However, abluminal ACh causes mobilization of EC Ca^{2+} and vasodilation by activating mAChRs which, like P2YRs, are coupled to G proteins containing the G_q α-subunit. Alternatively, the difference in effect of L-NAME, TRAM-34 and apamin on ATP-induced contraction may reiterate the altered influence of the endothelium observed during ACh and PE stimulation.

The difference in vasoreactivity reported between pressure and wire myography experiments has been postulated to be due to pressure-induced depolarization of the VSM and subsequent increased likelihood of Ca_V opening (Dunn et al., 1994). The resting membrane potential of isometrically studied rabbit mesenteric arteries was slightly hyperpolarized compared to pressurised vessels, and Ca_V-dependent myogenic tone was reported to only occur in control circumstances under isobaric conditions (Buus et al., 1994; Dunn et al., 1994; Wei et al., 2018). The higher Ca_V opening probability could also provide an explanation for the reported effects of pressure and tone on ATP-induced vasoconstriction, which is highly dependent on voltage-dependent Ca^{2+} influx (Pakdeechote et al., 2007; Rummery et al., 2007; Goonetilleke et al., 2013). If this were the case, Ca_V blockade would attenuate PE-induced contraction to a higher degree in arteries

under isobaric conditions than isometric. However, the current study did not observe such an outcome. Ca_V blockade with nifedipine right-shifted the response to PE in both experimental approaches, suggesting voltage-dependent Ca^{2+} influx contributed equally to the contraction in pressurised arteries and arteries studied isometrically. This observation reiterates the previous finding that direct depolarization of the VSM with elevated $[K^+]_o$ was comparable between wire and pressure myography experiments (Buus et al., 1994). Although this result does not eliminate the possibility that the VSM resting membrane potential is pressure-sensitive, it provides evidence against the notion the discrepancies between wire and pressure myography experiments are due to differential Ca_V opening dynamics.

Agonist- and pressure-induced activation of ROCK signalling has recently been implicated in vascular tone regulation and as a potential target for the treatment of hypertension (Chitaley and Webb, 2002; Brozovich et al., 2016; Li and Brayden, 2017; Björling et al., 2018). In the pressure myography experiments presented here, the effect of the ROCKII-selective inhibitor glycyl-H 1152 was two-fold; it decreased contraction to PE and amplified the vasodilatory response to ACh and DEA/NO. The former suggests a role for RhoA activation during vasoconstriction, which may be directly upregulated following α_1-AR stimulation or a consequence of pressurization itself (see Figure 4.4.1). In a recent investigation in pressurised rat parenchymal arteries, blockade of ROCKII with H 1152 attenuated intracellular Ca^{2+} elevation, depolarization and vasoconstriction during pressurization and P2Y-receptor stimulation (Li and

Brayden, 2017). Thus, ROCK signalling may govern mechanotransduction and Ca^{2+} mobilization in the pressure myograph, in addition to Ca^{2+} sensitization. This proposition is supported by our findings in rat mesenteric arteries and from other studies with different vascular beds (Gokina et al., 2005; Björling et al., 2018). An evaluation of the influence of RhoA in arteries studied isometrically is pivotal to determining if ROCK signalling is enhanced under isobaric conditions, and potentially provide a much-needed explanation for the discrepancies between pressure and wire myography. Compellingly, previous investigations with rat mesenteric arteries under isometric conditions have already reported ROCK inhibition with Y-27632 had no effect on PE-induced contraction (Rao et al., 2013; Zhong et al., 2019).

The effect of glycyl-H 1152 on ACh- and DEA/NO-induced vasodilation also implicates RhoA as a possible determinant of VSM sensitivity to NO. A similar effect was reported by Chitaley and Webb, (2002) who demonstrated ROCK inhibition with Y-27632 increased the sensitivity of rat aortic rings to the NO donor sodium nitroprusside. They theorised NO can inhibit RhoA signalling to cause VSM relaxation and the absence of ROCK allows for a larger effect of endothelium-dependent vasodilation. It then follows that amplified RhoA signalling may also limit the influence of myoendothelial feedback (see Figure 4.4.1).

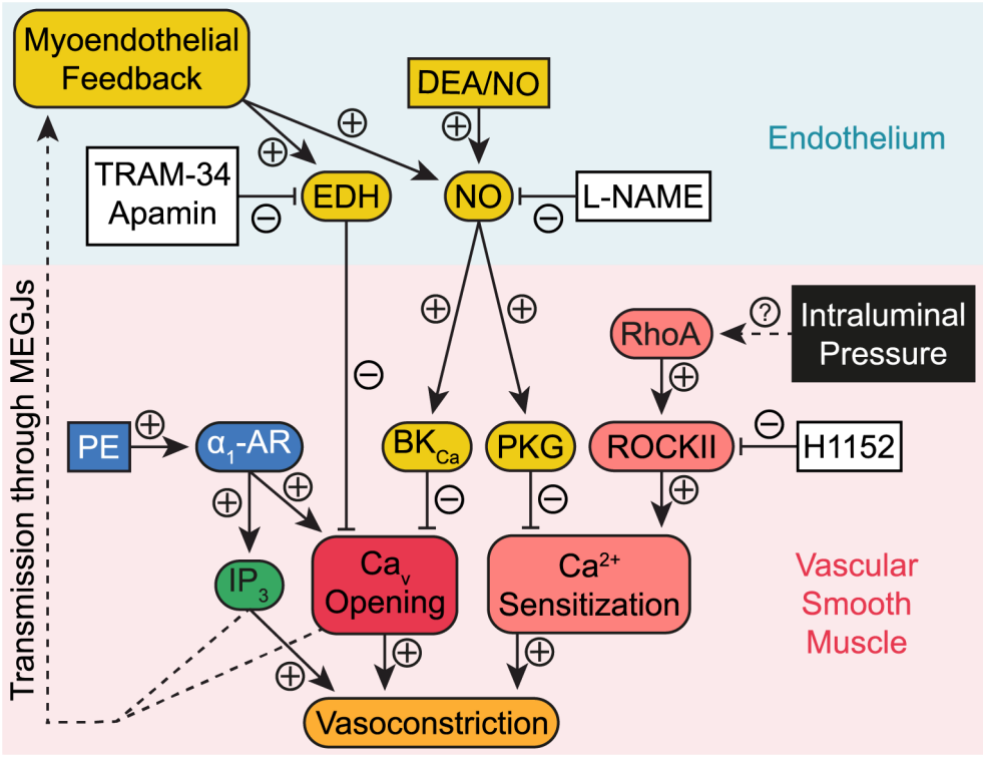


Figure 4.4.1 Proposed mechanism of pressure-induced ROCKII activation in current investigation. Boxes with curved edges represent intracellular signalling components. Boxes with sharp edges represent agonists or antagonists. Arrows with a dashed line represent an indirect effect.

It is also important to consider here the potential limitations of the current investigation with regards to the technical differences between the two experimental approaches. It is a possibility that exogenously administered drugs have limited access to the endothelium of pressurized arteries, compared to arteries mounted in the wire myograph, as the solution inside the vessel is kept separate to the superfused solution. This, for example, may explain why the relaxation to ACh and NO donors is greater under isometric conditions. However, as mentioned previously, including L-NAME, TRAM-34 and apamin in the perfused solution, as well as the superfusion, did not alter their effectiveness at blocking ACh-induced vasodilation (see Section 4.3.3). This suggests these drugs are able to 'reach' the EC layer from the outside of the vessel. Alternatively, limited access to ECs in the pressure myograph would indicate ACh is causing vasodilation through an endothelium-independent process (see Section 4.3.3). Such a process may involve the activation of nAChRs on sensory nerves to stimulate the release of dilatory neurotransmitters like calcitonin gene-related peptide and substance P. Once again, however, there is evidence against this notion as this mechanism was not observed in arteries under isometric conditions. Moving forward, a simple method of accounting for this possibility is to measure the vasoreactivity of denuded arteries mounted in the pressure and wire myographs. If denudation ameliorated the difference where the blockade of NOS and EDH production could not, it would confirm access of drugs to the EC layer is a confounding variable in this investigation.

An additional consideration to make is the fact that the mesenteric arteries used in the current study did not develop myogenic tone. This is in contrast with previous investigations which have reported mesenteric arteries can develop ~20-30% tone under control conditions when pressurised to 60 mmHg (Dunn et al., 1994; Mathewson and Dunn, 2014; Björling et al., 2018). It is puzzling why a basal level of vasoconstriction was not observed, as the vessel diameters (200-300 µm) and branching order (third- and fourth-order) were similar to those studied previously. Nonetheless, if the mesenteric arteries did exhibit myogenic tone, it may confer a basal level of EC activation due to Ca^{2+} influx through VSM Ca_Vs. As a result, the addition of L-NAME, TRAM-34 and/or apamin would cause an even greater degree of pressure-induced vasoconstriction. However, no such effect of blockade of endothelium-dependent vasodilation was observed in myogenically-active rat coronary arteries studied in the next chapter (see Section 5.3.9) or in pressurised rat cremasteric arteries (Bagher et al., 2012). Furthermore, under both isobaric and isometric conditions myogenic tone was absent yet the combination of L-NAME, TRAM-34 and apamin was still able to potentiate the contractile responses. Thus, it seems unlikely the presence of a basal level of VSM depolarization would unmask the influence of the endothelium or account for the differences observed between the two experimental approaches.

4.5 CONCLUSIONS

The hypothesis of the current investigation was supported as pressurization had a clear effect on vascular reactivity and the ability for the endothelium to modulate vascular tone. The stark differences observed between arteries studied with pressure and wire myography highlight the importance of considering the experimental approach employed when interpreting data.

A role for NO and EDH in mediating myoendothelial feedback in pressurised rat mesenteric arteries was identified during a maximal level of vasoconstriction, suggesting their production prevents vessel occlusion and maintains the flow of blood during high levels of VSM stimulation. However, in the wire myograph the same conditions increased the contraction of the tissue to submaximal adrenergic and purinergic stimulation. Furthermore, the ability for ACh and NO donors to cause relaxation varied between the experimental approaches. These findings may be explained by pressure-induced ROCK activation, rather than a direct influence of pressurization at $Ca_V s$ or an increased uptake of amines as shown by others in the same tissue, but the possibility of a unifying mechanism requires further investigation.

The next chapter will continue to explore heterocellular signalling in resistance arteries, with a particular focus on Ca^{2+} influx through ROCs which may play a central role in facilitating EC-dependent relaxation and myoendothelial feedback.

5.0 THE ROLE OF TRPV4 DURING RELAXATION AND CONTRACTION OF RESISTANCE ARTERIES

5.1 INTRODUCTION

TRP channels are a superfamily of non-selective cation channels expressed ubiquitously throughout the body, which exhibit sensitivity to a range of external stimuli and facilitate numerous physiological processes (Earley and Brayden, 2015). Within the field of vascular physiology, recent investigations have focussed specifically on TRPV4. TRPV4 is sensitive to temperature, $[Ca^{2+}]_i$, $[IP_3]_i$, mechanical stress, osmolarity and pH, and has been identified as an important component of signalling pathways which govern resistance artery function. TRPV4 is expressed in ECs, VSMCs and perivascular sensory nerves and has been shown to play a pivotal role in endothelium-dependent and -independent vasodilation, and myoendothelial feedback in several tissue beds (Earley et al., 2005; Sukumaran et al., 2013; Mercado et al., 2014; Hong et al., 2018). Furthermore, TRPV4 dysfunction has been postulated to contribute to the vascular pathology associated with hypertension, diabetes mellitus and ageing (Earley et al., 2009; Ma et al., 2013; Nishijima et al., 2014; Sonkusare et al., 2014; Du et al., 2016; Seki et al., 2017). Therefore, identifying the pathways which modulate TRPV4 opening and the consequences of its activation are of great therapeutic interest.

A role for TRPV4 in endothelium-dependent vasodilation has been well-established. Activation of TRPV4 caused EC-dependent relaxation in human coronary arteries (Bubolz et al., 2012), rat pulmonary arteries (Sukumaran et al., 2013) and rat and mouse mesenteric arteries (Sonkusare et al., 2012; Seki et al., 2017; Heathcote et al., 2019). Moreover, TRPV4 blockade or knockdown

attenuated mAChR- and flow-mediated vasodilation, indicating it is a component of endothelial signal transduction pathways which rely on the production of NO or EDH (Zhang et al., 2009; Bubolz et al., 2012; Ma et al., 2013; Sonkusare et al., 2014; Seki et al., 2017) (see Section 1.3.2). Sonkusare et al. (2014) demonstrated activation of mAChR in mouse mesenteric arteries stimulated relatively small EC Ca^{2+} events localised to MEPs which were prevented during TRPV4 blockade. These TRPV4-dependent Ca^{2+} events, termed 'sparklets', reportedly activate endothelial K_{Ca}s to cause VSM hyperpolarization and relaxation (Bagher et al., 2012; Ma et al., 2013; Sukumaran et al., 2013; Seki et al., 2017). Sonkusare et al. (2014) also demonstrated sparklet activity was dependent on the presence of A-kinase anchoring protein 150 (AKAP150), which is hypothesised to facilitate the activation of TRPV4 by PKC during GPCR activation (Sonkusare et al., 2014; Hong et al., 2018). Furthermore, a recent investigation using mouse mesenteric arteries illustrated EC TRPV4s may be involved in myoendothelial feedback (see Section 1.3.2) as VSMC α_1-AR activation caused an increase in EC sparklet activity which subsequently limited the degree of vasoconstriction (Hong et al., 2018).

TRPV4s localised to perivascular sensory nerves and VSMCs have also previously been shown to regulate contractility by stimulating CGRP release and BK_{Ca}-mediated hyperpolarization, respectively (Earley et al., 2005; Gao and Wang, 2010; Mercado et al., 2014). Bolus intravenous injection of the TRPV4 agonist 4α-PDD had a hypotensive effect in rats which was partially antagonised following CGRP receptor blockade or sensory nerve depletion with capsaicin

(Gao and Wang, 2010). Immunohistochemical analysis confirmed colocalization of TRPV4 with CGRP in the adventitia of mesenteric arteries, suggesting cation influx through neuronal TRPV4 causes CGRP release and vasodilation. In addition, Earley et al. (2005) demonstrated the endothelium-derived arachidonic acid derivative EET caused VSM hyperpolarization and vasodilation of endothelium-denuded rat cerebral arteries by stimulating Ca^{2+} release through RyRs and, subsequently, activation of BK_{Ca}s (see Section 1.2.3). EET-induced vasodilation was inhibited following TRPV4 blockade or knockdown with antisense oligonucleotides. The authors hypothesised TRPV4 forms a Ca^{2+} signalling complex with RyRs and BK_{Ca}s in VSMCs. This notion was reinforced by Mercado et al. (2014) who reported AngII-induced contraction was potentiated in endothelium-denuded cerebral arteries from TRPV4-null mice compared to wild-type animals. Moreover, they showed AngII stimulated an increase in sparklets in isolated mouse cerebral artery myocytes, and postulated VSM TRPV4 is activated by AngII to limit contraction. Thus, the TRPV4-RyR-BK_{Ca} axis may be activated during vasoconstriction as well as vasodilation. Together, these findings demonstrate a role for TRPV4 in limiting contraction independently of endothelial activation.

Compared to investigations into the involvement of TRPV4 in vasodilation, few have examined its contribution to vasoconstriction. Some studies have concluded TRPV4 inhibition or knockdown has no direct effect on the ability for arteries to constrict (Earley et al., 2005, 2009; Bubolz et al., 2012; Zheng et al., 2013), whilst others have provided evidence to the contrary. In endothelium-denuded rat

pulmonary arteries, the TRPV4 activator GSK 1016790A caused concentration-dependent contraction (Sukumaran et al., 2013) and TRPV4 blockade antagonised hypoxia-induced increases in myogenic tone (Yang et al., 2012). Additionally, TRPV4 activation was essential for pressure-induced VSM depolarization and myogenic tone in neonatal pig renal interlobular arteries (Soni et al., 2017). Collectively, these results offer evidence against the notion TRPV4-dependent Ca^{2+} activity in VSMCs only mediates vasodilation and provide the rationale for further examination into their function.

5.1.1 Aims and hypotheses

The aim of the current investigation was to investigate a role for TRPV4 in relaxation, contraction and myoendothelial feedback in isolated resistance arteries.

It was hypothesised cation influx through TRPV4s facilitates the activation of IK_{Ca} in ECs during endothelium-dependent vasodilation and myoendothelial feedback, and the RyR-BK_{Ca} complex in VSMCs. Thus, TRPV4 blockade was anticipated to potentiate α_1-AR-mediated contraction.

5.2 MATERIALS AND METHODS

5.2.1 Pressure myography

Mesenteric and coronary arteries were prepared for pressure myography experiments, as previously described (see Section 2.2).

5.2.2 Wire myography

Mesenteric arteries were prepared for wire myography experiments, as previously described (see Section 2.3).

5.2.3 Inhibitors

The following drugs were used in this chapter to block their respective targets, at concentrations which have previously been shown to be effective: 30.0 µM RN 1734 to block TRPV4 (Bagher et al., 2012), 1.0 µM ryanodine to block RyRs (Earley et al., 2005), 1.0 µM nifedipine to block Ca_Vs (Bagher et al., 2012), 100.0 µM L-NAME to antagonise NOS (Garland et al.,2017), and 1.0 µM TRAM-34 and 0.1 µM apamin to block IK_{Ca} and SK_{Ca}, respectively (Lemmey et al., 2018).

5.3 RESULTS

5.3.1 Endothelium-dependent vasodilation is facilitated by activation of eNOS, IK_{Ca} and SK_{Ca}

Relaxation to ACh was attenuated by the NOS inhibitor L-NAME, and further reduced in the additional presence of TRAM-34 or apamin which block IK_{Ca} and SK_{Ca}, respectively (0.1 µM; Control, 96.4 ± 1.0%, n = 15; L-NAME, 68.6 ± 7.0%, n = 15; L-NAME + TR, 22.4 ± 5.5%, n = 10; L-NAME + Ap, 17.9 ± 8.6%, n = 12). In the presence of all three antagonists the relaxation was completely prevented, and higher concentrations of ACh instead caused slight contraction (0.1 µM; L-NAME + TR + Ap, -0.1 ± 0.4%, n = 13) (see Figures 5.3.1A and 5.3.1B). These data confirm ACh causes endothelium-dependent relaxation by stimulating NO and EDH production. Furthermore, efflux of K^+ through both IK_{Ca} and SK_{Ca} contribute to the transmission of hyperpolarization.

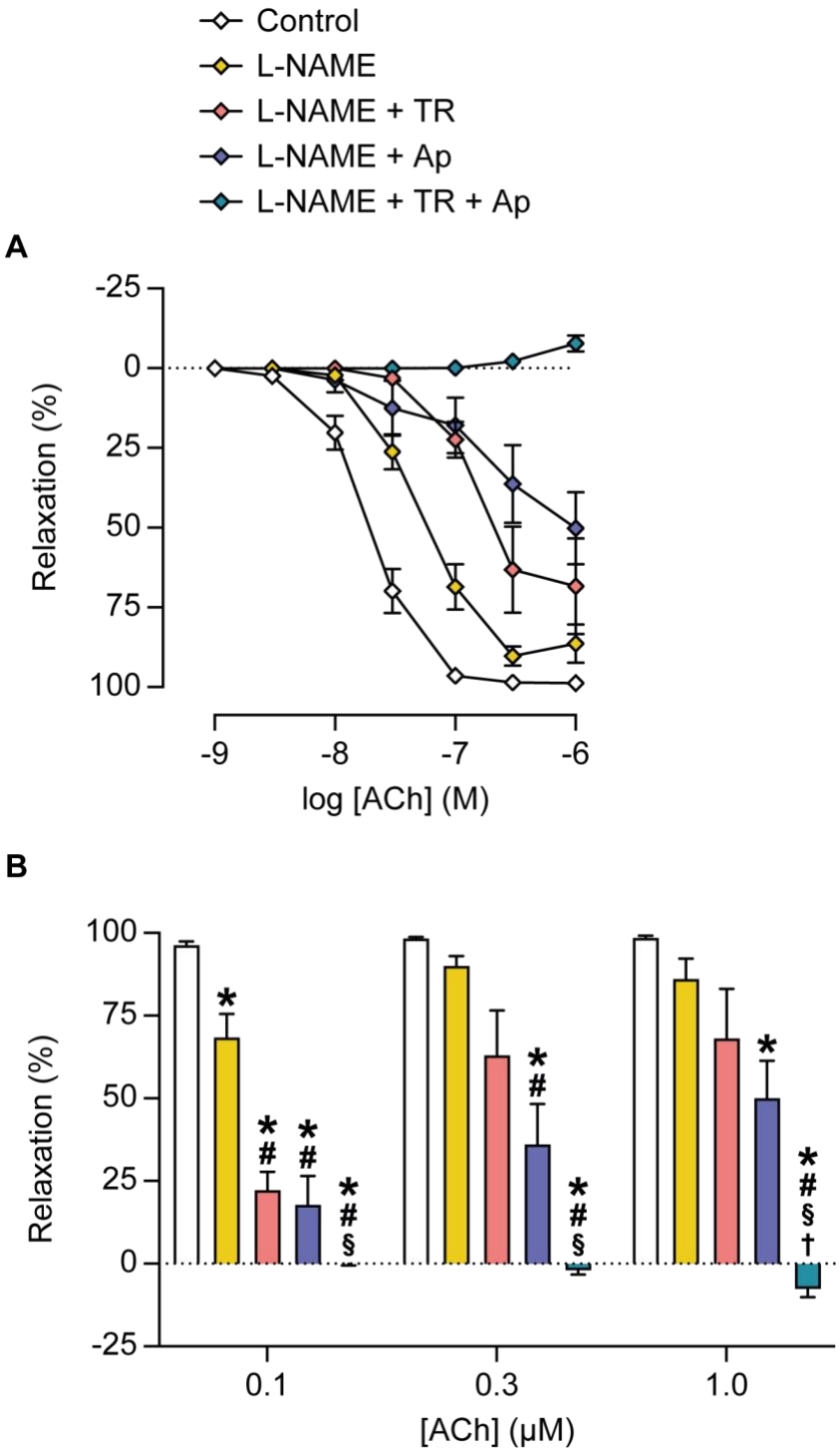

Control
L-NAME
L-NAME + TR
L-NAME + Ap
L-NAME + TR + Ap
A
Relaxation (%)
-25
0
25
50
75
100
-9
-8
-7
-6
log [ACh] (M)
B
Relaxation (%)
100
75
50
25
0
-25
0.1
0.3
1.0
[ACh] (μM)

Figure 5.3.1 Effect of NOS, IK_{Ca} and SK_{Ca} inhibition on ACh-induced relaxation in mesenteric arteries. (**A** and **B**) Cumulative-concentration response curves and bar graph summarizing relaxation to ACh in the absence and presence of 100 µM L-NAME, L-NAME + 1 µM TRAM-34 (TR), L-NAME + 0.1 µM apamin (Ap) or L-NAME + TR + Ap. Control, L-NAME, and L-NAME + TR + Ap data adapted from Figure 4.3.3. Data are means ± SEM; n = 10-15. $^{*}P < 0.05$ compared to control at the same concentration; $^{\#}P < 0.05$ compared to L-NAME at the same concentration; $^{\S}P < 0.05$ compared to L-NAME + TR at the same concentration; $^{\dagger}P <$ compared to L-NAME + Ap at the same concentration.

5.3.2 IK_{Ca}-mediated EDH is dependent on TRPV4 opening

Under control conditions, the selective TRPV4 agonist GSK 1016790A caused maximal relaxation in preconstricted arteries. Furthermore, the relaxation was blocked in the presence of RN 1734, confirming the drug's antagonistic effect at TRPV4 (0.3 µM, Control, 97.6%, n = 1; RN 1734, 0.0 ± 0.0%, n = 3).

To probe an obligatory role for TRPV4 during IK_{Ca} activation, relaxation to ACh was studied during TRPV4, NOS and SK_{Ca} blockade. In the presence of RN 1734, the response to ACh was right-shifted (0.1 µM; Control, 96.4 ± 1.0%, n = 15; 66.7 ± 4.4%, n = 4). The addition of L-NAME further attenuated the response, whilst Apamin, in combination with RN 1734 and L-NAME, completely blocked it (0.3 µM; Control, 98.5 ± 0.3%, n = 15; RN, 93.1 ± 3.8%, n = 4; RN + L-NAME, 32.5 ± 7.5%, n = 3; RN + L-NAME + Ap, -6.1 ± 3.4%, n = 4) (see Figures 5.3.2A and 5.3.2B). The effect of RN 1734 on ACh-induced relaxation during NOS and SK_{Ca} blockade was almost identical to that of TRAM-34 under the same circumstances (see Section 5.3.1). These data suggest TRPV4 activation is essential for opening of IK_{Ca} during stimulation with ACh.

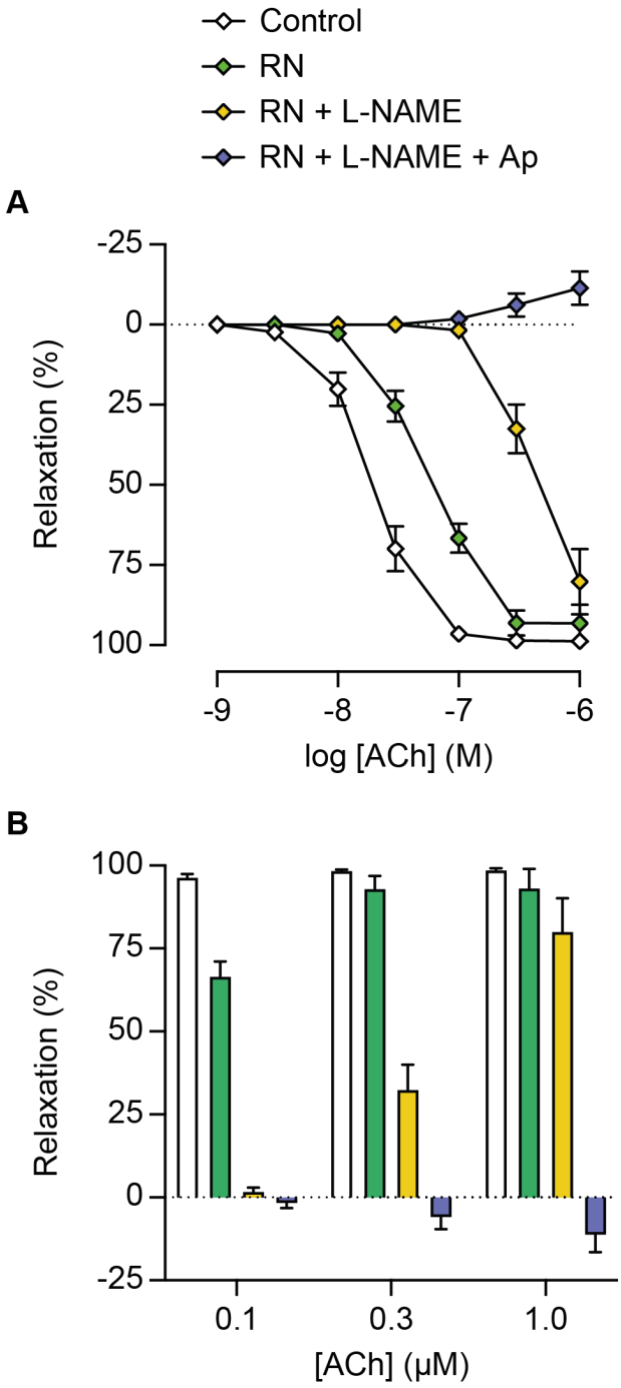

Control
RN
RN + L-NAME
RN + L-NAME + Ap
A
Relaxation (%)
-25
0
25
50
75
100
-9
-8
-7
-6
log [ACh] (M)
B
Relaxation (%)
100
75
50
25
0
-25
0.1
0.3
1.0
[ACh] (μM)

Figure 5.3.2 Effect of TRPV4, NOS and SK_{Ca} inhibition on ACh-induced relaxation in mesenteric arteries. (**A** and **B**) Cumulative-concentration response curves and bar graph summarizing relaxation to ACh in the absence and presence of 30 µM RN 1734 (RN), RN + 100 µM L-NAME, or RN + L-NAME + 0.1 µM apamin (Ap). Control data adapted from Figure 4.3.3. Data are means ± SEM; n = 3-15.

5.3.3 Ca_V and TRPV4 activation facilitate PE-induced contraction

During studies of the effect of RN 1734 on ACh-induced relaxation, a higher concentration of PE was required to stimulate the same level of precontraction as in control conditions. This was unexpected and prompted an investigation into the role of TRPV4 in mediating contraction.

PE-induced contraction was attenuated during either Ca_V or TRPV4 blockade (10.0 µM; Control, 89.5 ± 1.6%, n = 24; Nif, 62.7 ± 4.9%, n = 4; RN, 45.4 ± 5.7%, n = 7). In combination, Nifedipine and RN 1734 inhibited the response to a greater degree than with either antagonist alone (10.0 µM; Nif + RN, 21.2 ± 4.5%, n = 4) (see Figures 5.3.3A and 5.3.3B). This observation suggests TRPV4 opening contributes to contraction during α_1-AR activation, independently of Ca_V activation.

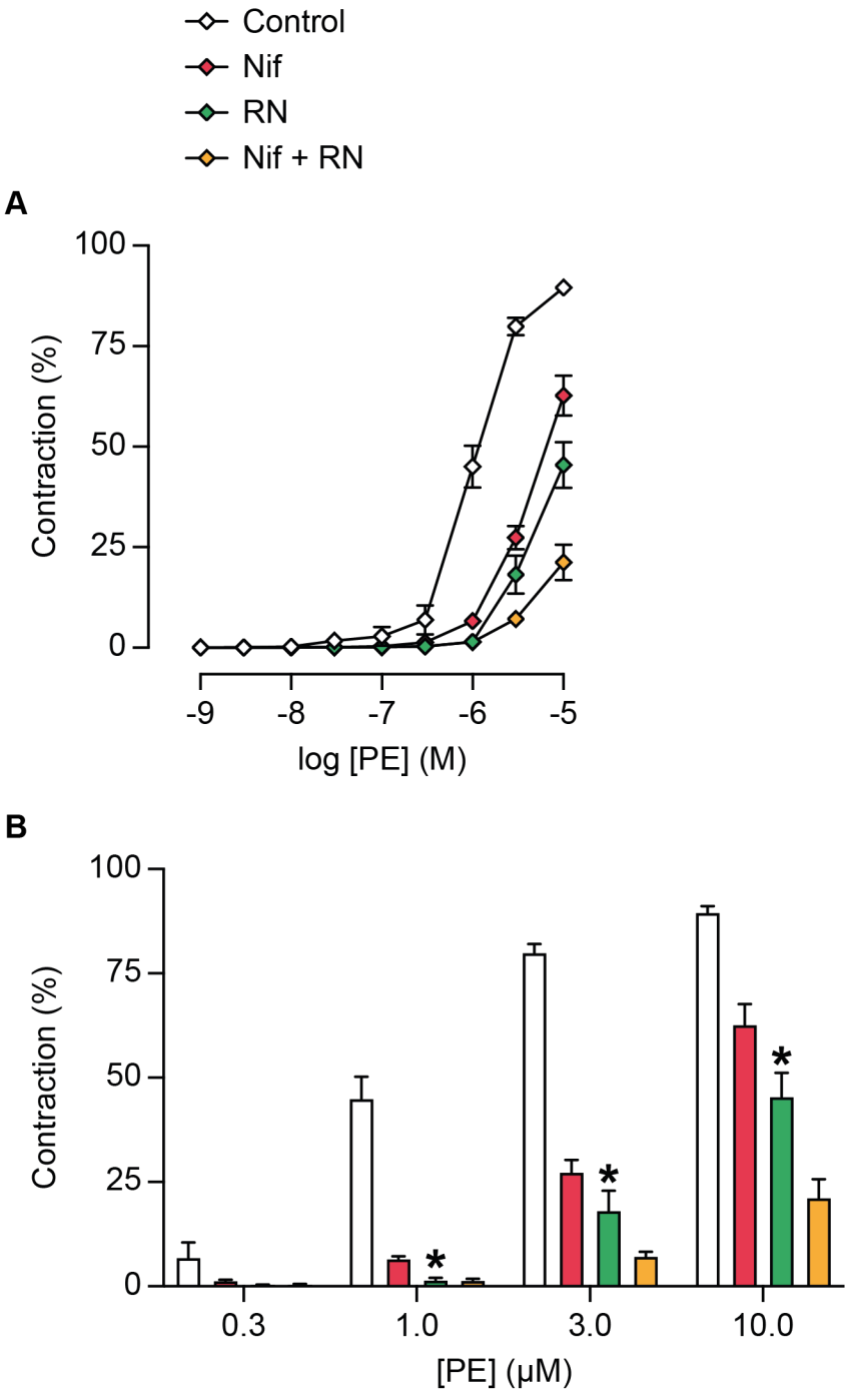

Control
Nif
RN
Nif + RN
A
100
75
50
25
0
Contraction (%)
-9
-8
-7
-6
-5
log [PE] (M)
B
100
75
50
25
0
Contraction (%)
*
*
*
0.3
1.0
3.0
10.0
[PE] (μM)

Figure 5.3.3 Effect of Ca_V and TRPV4 blockade on PE-induced contraction in mesenteric arteries. (**A** and **B**) Cumulative-concentration response curves and bar graph summarizing contraction to PE in the absence and presence of 1 μM nifedipine (Nif), 30 μM RN 1734 (RN) or Nif + RN. Control data adapted from Figure 4.3.1. Data are means ± SEM; n = 4-24. *P < 0.05 compared to control at the same concentration.

5.3.4 Myoendothelial feedback during α_1-AR stimulation is not prevented by TRPV4 blockade

The observation that TRPV4 blockade inhibits both EC-dependent relaxation and contraction made it difficult to probe the channel's involvement in myoendothelial feedback using a pharmacological approach. Nonetheless, contractile responses to PE were studied during TRPV4 blockade before and after inhibition of NOS, SK_{Ca} and IK_{Ca}. As reported previously, RN 1734 reduced contraction to PE, whilst the addition of L-NAME, apamin and TRAM-34 potentiated the response (10.0 µM; Control, 89.5 ± 1.6%, n = 24; RN, 45.4 ± 5.7%, n = 7; RN + L-NAME, 74.3 ± 6.7%, n = 4; RN + L-NAME + Ap, 76.0 ± 5.9%, n = 5; RN + L-NAME + Ap, 69.2 ± 5.2%, n = 9) (see Figures 5.3.4A and 5.3.4B). The increase in contraction was only significant following the addition of L-NAME and apamin, but L-NAME alone caused a marked augmentation in response. These data imply TRPV4 inhibition does not prevent myoendothelial feedback, as the endothelium can be activated secondary to VSM Ca^{2+} influx through Ca_Vs, activation of VSM IP_3Rs, or other mechanisms, and does not appear to rely on EC TRPV4s to amplify the Ca^{2+} in the microdomains necessary for the release of NO or activation of K_{Ca}s.

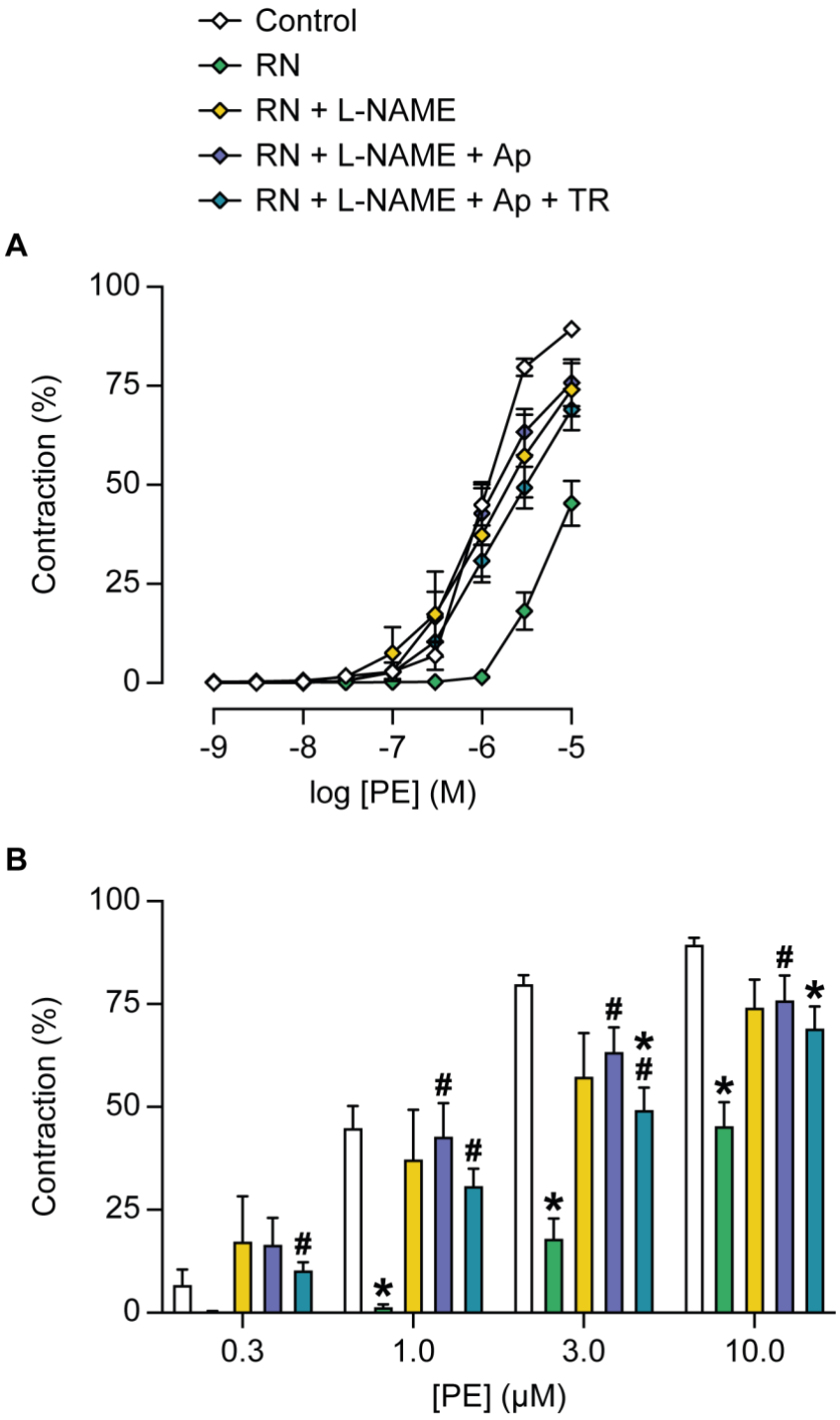

Control
RN
RN + L-NAME
RN + L-NAME + Ap
RN + L-NAME + Ap + TR
A
Contraction (%)
100
75
50
25
0
-9
-8
-7
-6
-5
log [PE] (M)
B
Contraction (%)
100
75
50
25
0
0.3
1.0
3.0
10.0
[PE] (μM)

Figure 5.3.4 Effect of TRPV4, NOS, SK_{Ca} and IK_{Ca} inhibition on PE-induced contraction in mesenteric arteries. (**A** and **B**) Cumulative-concentration response curves and bar graph summarizing contraction to PE in the absence and presence of 30 µM RN 1734 (RN), RN + 100 µM L-NAME, RN + L-NAME + 0.1 µM apamin (Ap) or L-NAME + Ap + 1 µM TRAM-34 (TR). Control data adapted from Figure 4.3.1. Data are means ± SEM; n = 4-24. $^{*}P < 0.05$ compared to control at the same concentration; $^{\#}P < 0.05$ compared to RN at the same concentration.

5.3.5 Myoendothelial feedback during α_1-AR stimulation is not prevented by Ca_V blockade

The requirement of Ca^{2+} influx through VSM Ca_Vs to generate the signal for myoendothelial feedback was assessed by evaluating the effect of nifedipine on PE-induced contraction during inhibition of endothelium-dependent vasodilation. Inhibition of NOS, IK_{Ca} and SK_{Ca} potentiated responses to PE during Ca_V blockade, albeit only significantly at a low concentration of the α_1-AR agonist (10.0 µM; Control, 89.5 ± 1.6%, n = 24; Nif, 62.7 ± 4.9%, n = 4; Nif + L-NAME + TR + Ap, 73.3 ± 5.7%, n = 4) (see Figures 5.3.5A and 5.3.5B). This observation indicates Ca^{2+} influx through Ca_Vs is not essential for myoendothelial feedback during PE stimulation, and the endothelium can be activated during depolarization-independent contractile mechanisms.

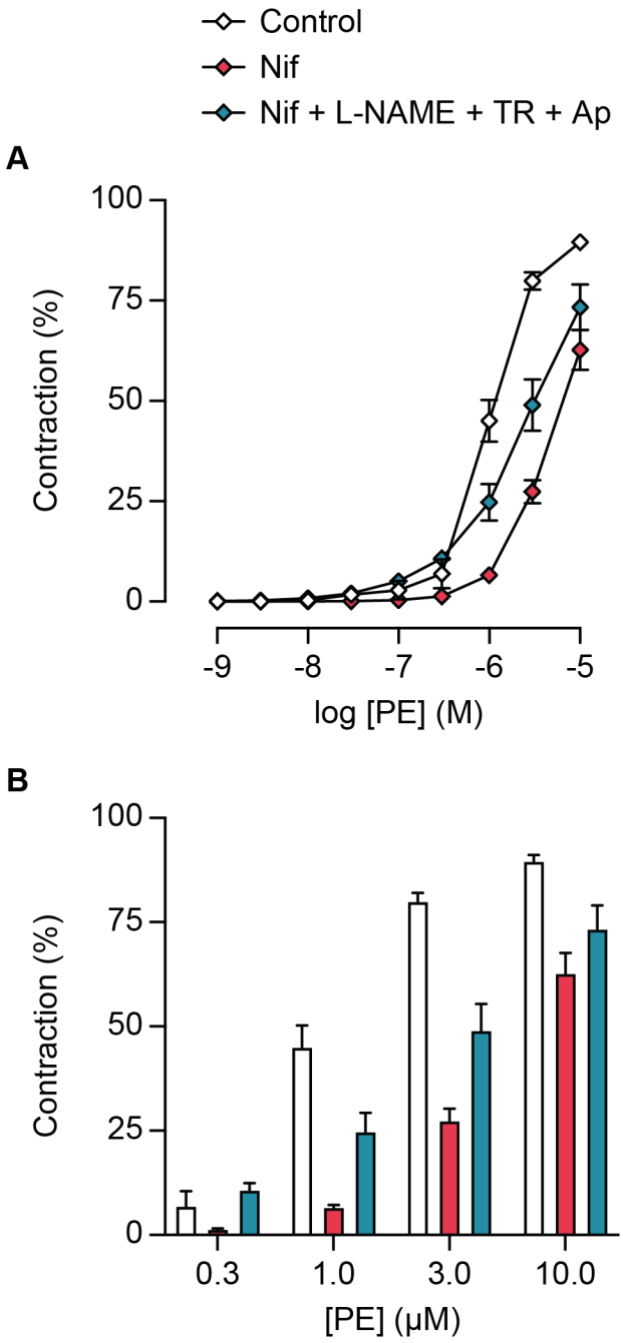

Control
Nif
Nif + L-NAME + TR + Ap
A
Contraction (%)
100
75
50
25
0
-9
-8
-7
-6
-5
log [PE] (M)
B
Contraction (%)
100
75
50
25
0
0.3
1.0
3.0
10.0
[PE] (μM)

Figure 5.3.5 Effect of Cav, NOS, IK_{Ca} and SK_{Ca} inhibition on PE-induced contraction in mesenteric arteries. (**A** and **B**) Cumulative-concentration response curves and bar graph summarizing contraction to PE in the absence and presence of 1 µM nifedipine (Nif) or Nif + 100 µM L-NAME + 1 µM TRAM-34 (TR) + 0.1 µM apamin (Ap). Control data adapted from Figure 4.3.1. Data are means ± SEM; n = 4-24.

5.3.6 RyR activation limits contraction but does not contribute to relaxation

In a set of paired experiments, artery vasoreactivity was examined following exposure to ryanodine and RN 1734 to investigate a role for a TRPV4-RyR complex in VSMCs. Blockade of RyRs with ryanodine potentiated the contractile response to PE, suggesting Ca^{2+} sparks originating from the SR may limit agonist-induced contraction (10.0 µM; Control, 91.9 ± 2.9%; + Ryanodine, 90.9 ± 1.2%; n = 5). With the addition of RN 1734, the contraction was significantly attenuated and matched the previously reported responses to PE in the presence of RN alone (10.0 µM; + RN, 43.4 ± 2.9%, n = 5) (see Figures 5.3.6A and 5.3.6C, and Section 5.3.3B).

The effect of ryanodine on endothelium-dependent relaxation was also considered. Blockade of RyRs had no effect on ACh-induced relaxation, confirming ryanodine potentiates contraction to PE by acting on RyRs in VSMCs, rather than blocking Ca^{2+} release in ECs which could attenuate myoendothelial feedback (0.03 µM; Control, 67.4 ± 11.1%; + Ryanodine, 59.1 ± 10.3%; n = 5). Together, these findings indicate a role for VSM RyRs in regulating contraction during stimulation of α_1-ARs. Due to the direct effect of RN 1734 on contraction, it is difficult to probe a possible association of TRPV4 with RyRs in this tissue. Thus, these results neither support nor dispute the notion TRPV4 is part of a signalling complex in VSMCs which regulates contraction.

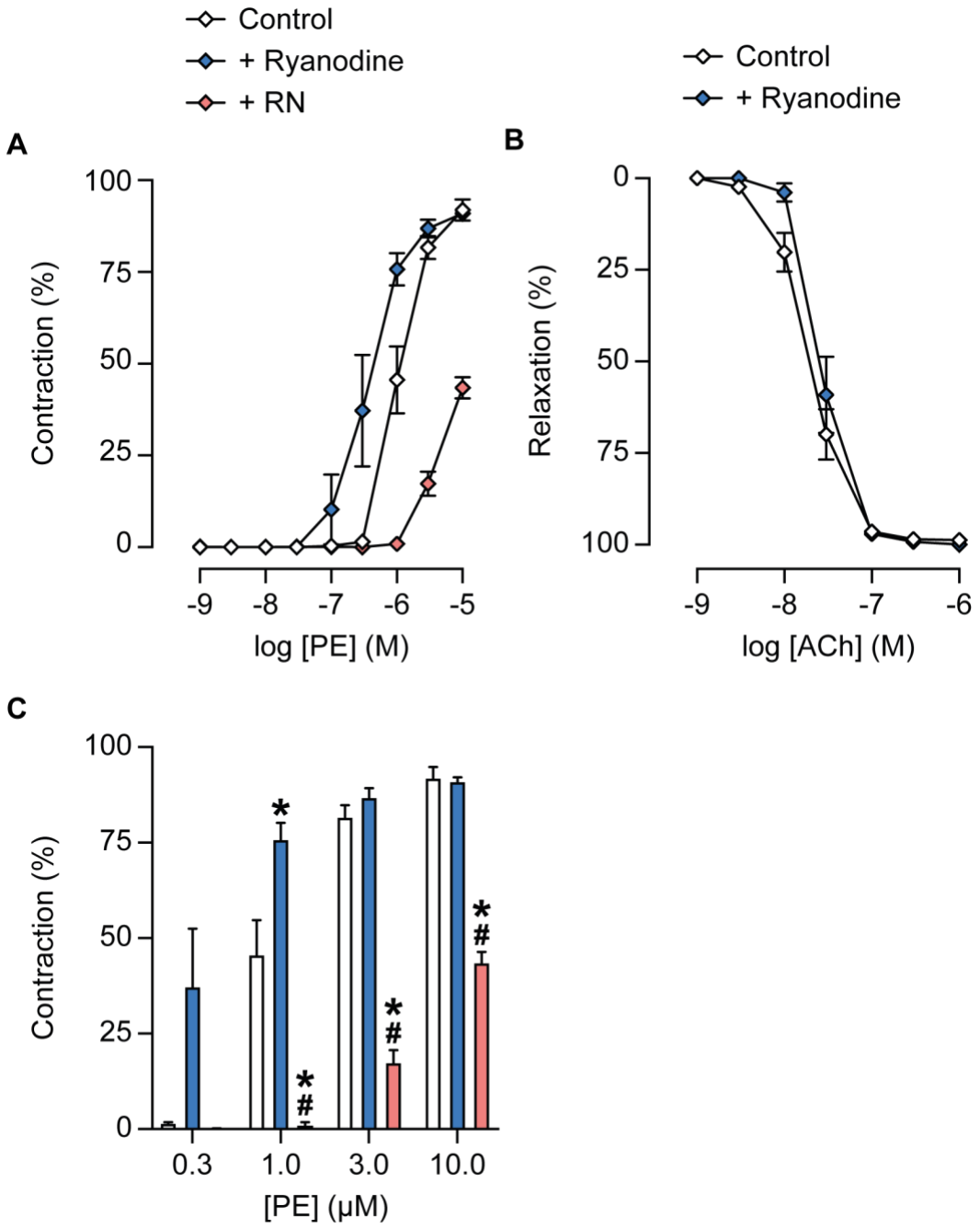

A
Control
+ Ryanodine
+ RN
Contraction (%)
100
75
50
25
0
-9
-8
-7
-6
-5
log [PE] (M)
B
Control
+ Ryanodine
Relaxation (%)
0
25
50
75
100
-9
-8
-7
-6
log [ACh] (M)
C
Contraction (%)
100
75
50
25
0
*
*#
*#
*#
0.3
1.0
3.0
10.0
[PE] (μM)

Figure 5.3.6 Effect of RyR and TRPV4 blockade on PE-induced contraction and ACh-induced relaxation in mesenteric arteries. (**A** and **C**) Cumulative concentration-response curves and bar graph summarizing contraction to PE in the absence and presence of 1 µM ryanodine and the additional presence of 30 µM RN 1734 (RN). (**B**) Concentration-response curves summarizing relaxation to ACh in the absence and presence of Ryanodine. These data represent paired experiments. Data are means ± SEM; n = 5; **P* < 0.05 compared to control at the same concentration; #*P* < 0.05 compared to Ryanodine at the same concentration.

5.3.7 TRPV4 mediates Ca_v activation during VSM depolarization

To determine if VSM TRPV4 opening is dependent on α_1-AR stimulation or a receptor-independent mechanism, contraction following direct VSM depolarization was studied. Increasing $[K^+]_o$ to 45 mM directly depolarized the VSM and opened Ca_vs, as confirmed by blockade of the resulting contraction with nifedipine (Control, 34.2 ± 5.6%, n = 5; Control Nif, 3.2 ± 0.5%, n = 4). Surprisingly, the response was also sensitive to RN 1734, suggesting TRPV4 plays a role in voltage-dependent contraction (Control RN, 10.7 ± 1.4%, n = 4). The combination of nifedipine and RN 1734 attenuated the response to a greater degree than either antagonist alone, albeit not significantly (Control Nif + RN, 0.8 ± 0.5%, n = 4) (see Figure 5.3.7). These data suggest TRPV4 facilitates voltage-dependent contraction, and its activation is not dependent on signalling via an intermediate messenger.

The contractile response to direct VSM depolarization was potentiated by inhibition of endothelium-dependent vasodilation (Control L-NAME + TR + Ap, 61.7 ± 2.9%, n = 4). In the presence of L-NAME, TRAM-34 and apamin, Ca_v and TRPV4 blockade reduced the contraction, as in in control conditions, but the contraction was significantly larger in the presence of RN 1734 than nifedipine (L-NAME + TR + Ap + Nif, 5.2 ± 0.9%, n = 3; L-NAME + TR + Ap + RN, 21.4 ± 1.8%, n = 5) (see Figure 5.3.7). These results indicate influx of Ca^{2+} through VSM Ca_vs may activate the underlying endothelium and trigger myoendothelial feedback. Furthermore, the negative feedback stimulated by direct VSM depolarization can occur independently of TRPV4 activity.

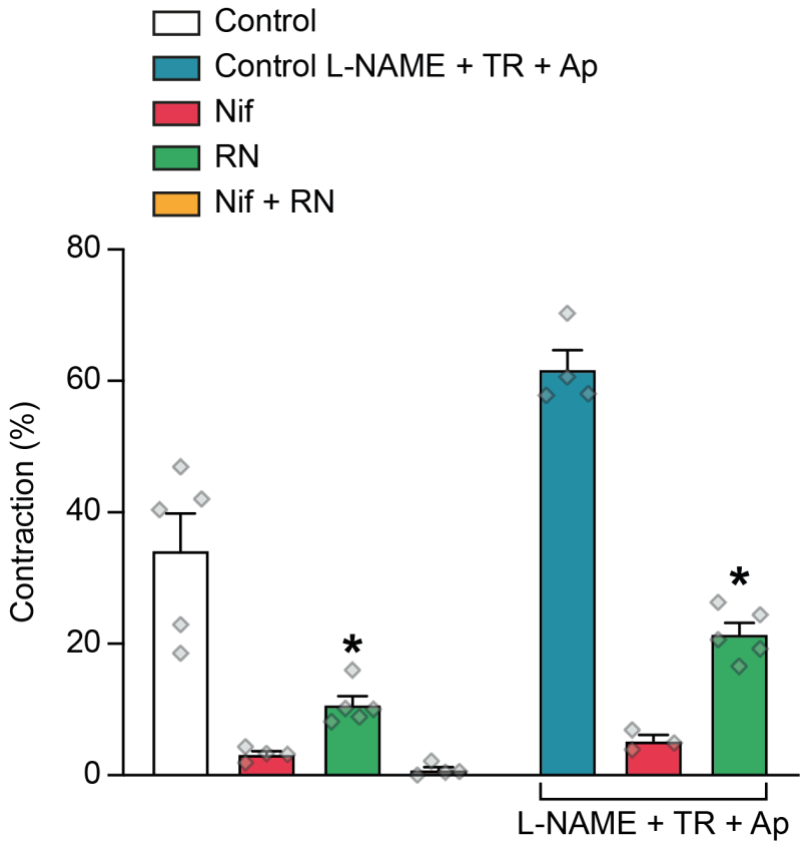


Figure 5.3.7 Effect of Ca_V, TRPV4, NOS, IK_{Ca} and SK_{Ca} inhibition on 45 mM K^+-induced contraction in mesenteric arteries. Bar graph summarizing contraction to isotonic 45 mM K^+ under control conditions; and with 100 µM L-NAME, 1 µM TRAM-34 (TR) and 0.1 µM apamin (Ap); and the additional presence of 1 µM nifedipine (Nif), 30 µM RN 1734 (RN) or Nif + RN. Data are means ± SEM; n = 3-5. *P < 0.05 compared to control.

5.3.8 TRPV4 activation causes contraction during blockade of endothelium-dependent relaxation

To further investigate the contribution of VSM TRPV4 to contraction, experiments were performed with its selective agonist GSK 1016790A. As described previously, 0.3 µM GSK 1016790A caused relaxation in preconstricted arteries under control conditions, but during blockade of endothelium-dependent vasodilation it caused a gradual, but robust contraction (42.0 ± 5.6%, n = 8) (see Figures 5.3.8A and 5.3.8B). GSK 1016790A-induced contraction was not reproducible in the same artery, and when applied the first time, was antagonised by either RN 1734 or nifedipine (Second Exposure, 0.4 ± 0.2%, n = 5; RN, 2.0 ± 0.6%, n = 8; Nif, 5.3 ± 1.4%, n = 3). Furthermore, 0.3 µM GSK 1016790A also caused vasoconstriction in pressurised arteries in the presence of L-NAME, TRAM-34 and apamin (69.6 ± 2.4%, n = 4). These observations suggest cation influx through TRPV4s is able to stimulate contraction by depolarizing the VSM and opening Ca_Vs.

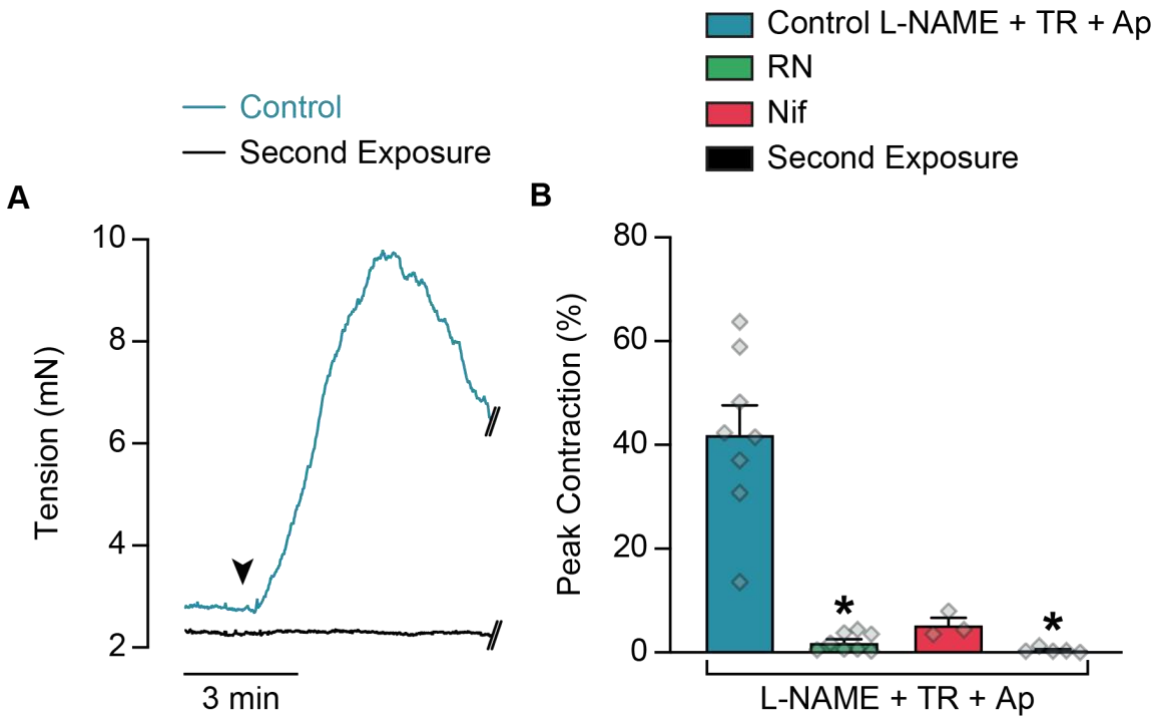


Figure 5.3.8 Effect of TRPV4 and Ca_V blockade on GSK 1016790A-induced contraction during inhibition of endothelium-dependent relaxation. (**A**) Representative traces of VSM tension during stimulation with 0.3 µM GSK 1016790A in the presence of 100 µM L-NAME, 1 µM TRAM-34 (TR) and 0.1 µM apamin (Ap). The teal trace represents a control response, and the black trace represents a response to a second exposure in the same artery. The arrowhead indicates when GSK 1016790A was added to the bath. Traces are representative of at least 5 separate experiments (**B**) Bar graph summarizing contraction to 0.3 µM GSK 1016790A in the presence of L-NAME + TR + Ap; and with 30 µM RN 1734 or 1 µM nifedipine; and contraction to a second exposure of GSK 1016790A under the same conditions. Data are means ± SEM; n = 3-8. *P < 0.05 compared to control.

5.3.9 Myogenic tone and endothelium-dependent vasodilation in coronary arteries are not modulated by NOS inhibition

To assess the role of NO in mediating TRPV4-dependent vasodilation in arteries from the heart, experiments with pressurised coronary arteries were conducted in the presence of L-NAME. The degree of myogenic tone did not differ between arteries before and after the addition of L-NAME (Control; 35.34 ± 3.0%, n = 13; L-NAME, 32.6 ± 6.2%, n = 4). Furthermore, NOS blockade did not affect vasodilation to ACh (0.1 µM; Control, 62.9 ± 9.6%, n = 9; L-NAME, 54.4 ± 15%, n = 4) (see Figure 5.3.9A) or GSK 1016790A (0.3 µM; Control, 92.6 ± 1.7%; L-NAME, 78.1 ± 12.1%; n = 3) (see Figure 5.3.9B). These observations suggest NO production is neither stimulated by pressure-dependent vasoconstriction to limit myogenic tone, nor is it a component of ACh- or GSK 1016790A-induced vasodilation.

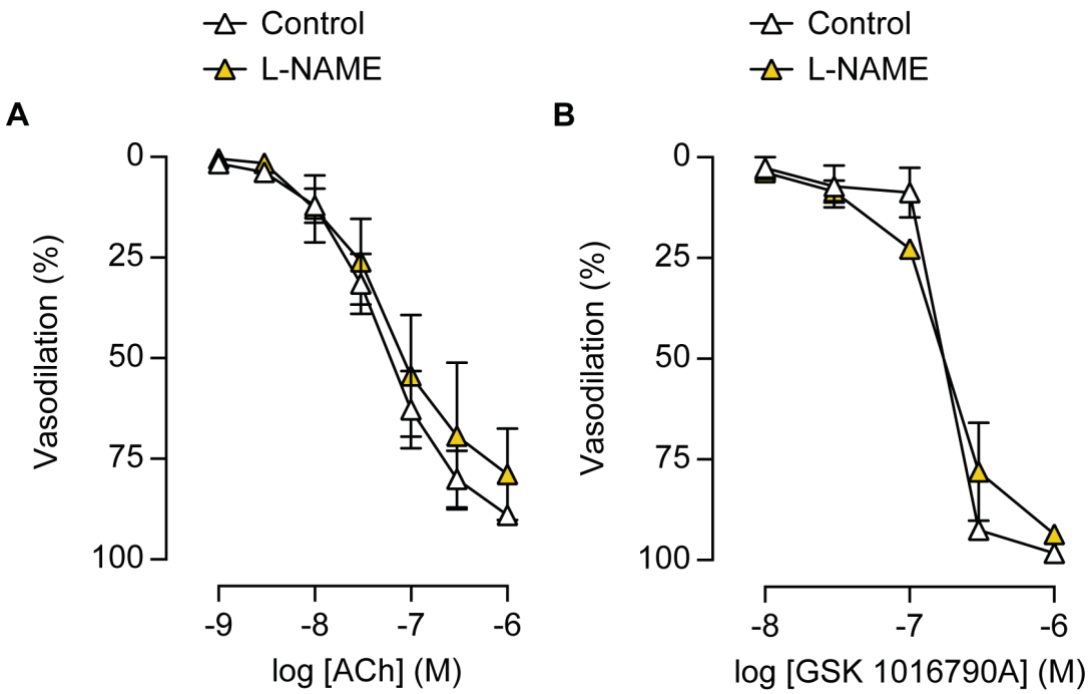


Figure 5.3.9 Effect of NOS inhibition on ACh- and GSK 1016790A-induced relaxation in coronary arteries. (**A**) Cumulative concentration-response curves summarizing relaxation to ACh in the absence and presence of 100 µM L-NAME. (**B**) Cumulative concentration-response curves summarizing relaxation to GSK 1016790A in the absence and presence of L-NAME. Data are means ± SEM; n = 3-9.

5.3.10 TRPV4 activation contributes to myogenic tone in coronary arteries

To determine the contribution of TRPV4s and Ca_Vs to pressure-induced vasoconstriction in coronary arteries, pressurised and myogenically-active coronary vessels were exposed to RN 1734 and, in a subset of experiments, nifedipine. The addition of RN 1734 to the superfusion caused gradual vasodilation from the baseline level of tone (60 min, 60.1 ± 7.8%, n = 6) (see Figure 5.3.10A). The residual myogenic tone was completely attenuated in the additional presence of nifedipine (Control, 35.34 ± 3.0%, n = 13; RN, 16.5 ± 3.2%, n = 8; RN + Nif, 0.6 ± 0.3%, n = 4). This finding suggests cation influx through TRPV4s is a crucial component of myogenic tone development in coronary vessels, alongside Ca^{2+} influx through Ca_Vs.

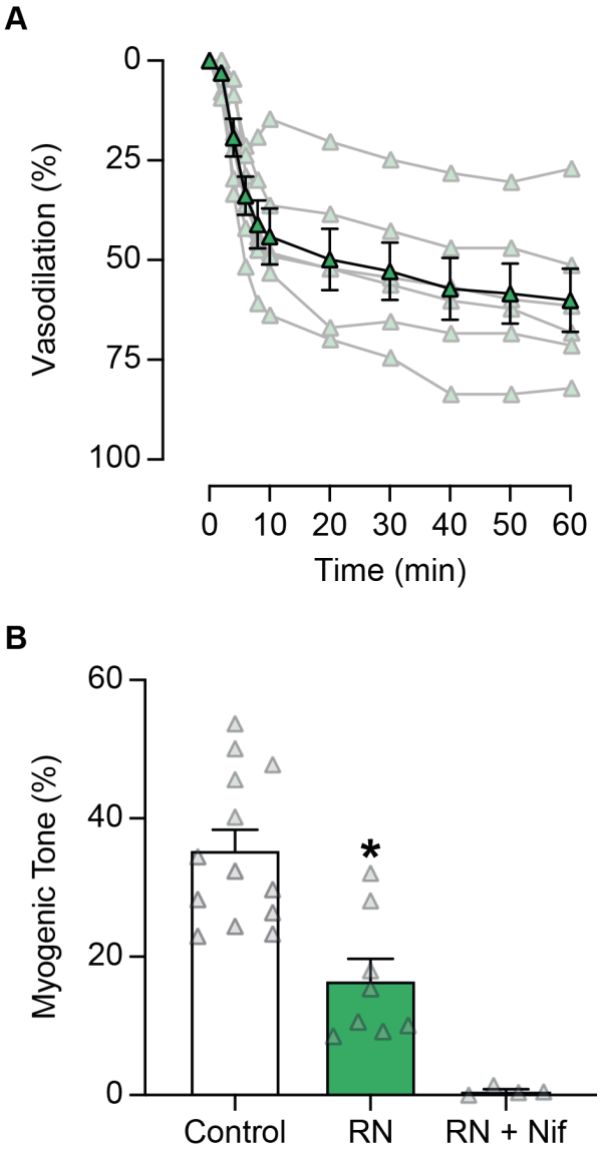


Figure 5.3.10 Effect of TRPV4 and Ca_V blockade on coronary artery myogenic tone. (**A**) Scatter plot summarizing relaxation to 30 µM RN 1734 (RN) over time. RN is added to superfusion at 0 min. The transparent traces represent individual experiments. (**B**) Bar graph summarizing myogenic tone in the absence and presence of RN or RN + 1 µM nifedipine (Nif). Data are means ± SEM; n = 4-13. *$P < 0.05$ compared to control.

5.4 DISCUSSION

The current investigation examined the involvement of TRPV4 in signalling pathways which regulate resistance artery tone. The findings reiterate an essential role for TRPV4 in IK_{Ca} activation during endothelium-dependent vasodilation. However, assessment of TRPV4's contribution to endothelium-dependent and -independent negative feedback mechanisms proved difficult as the TRPV4 antagonist RN 1734 unexpectedly attenuated contraction following both α_1-AR stimulation and direct VSM depolarization. Further exploration revealed direct activation of TRPV4 causes contraction in the absence of NO and EDH production, and RN 1734 partially blocks pressure-induced myogenic tone development in coronary arteries. These observations may reflect a functional association of VSM TRPV4s with Ca_Vs, or an off-target effect of the TRPV4 antagonist RN 1734.

Activation of mAChRs has previously been shown to stimulate TRPV4-dependent Ca^{2+} sparklet activity in ECs at MEP sites characterised by a high density of IK_{Ca}s (Bagher et al., 2012; Sonkusare et al., 2014). Sonkusare et al. (2014) demonstrated AKAP150, which also colocalised with MEPs, facilitated the activation of TRPV4 by PKC upregulated during mAChR activation. In the presence of L-NAME and apamin, the ability for ACh to stimulate relaxation in rat mesenteric arteries was completely abrogated with the addition of either TRAM-34 or RN 1734. This finding confirms TRPV4 mediates agonist-induced activation of IK_{Ca} rather than eNOS or SK_{Ca} (see Figure 5.4.1A).

The TRPV4 agonist GSK 1016790A caused vasodilation of rat coronary arteries which was insensitive to treatment with L-NAME, suggesting TRPV4s on the endothelium of arteries which supply the myocardium are also functionally linked to the production of EDH rather than NO. A similar observation was made in human coronary arteries wherein arachidonic acid, which may directly bind TRPV4, and luminal flow caused TRPV4-dependent vasodilation (Bubolz et al., 2012; Zheng et al., 2013). In contrast, bradykinin-induced relaxation in these arteries was reportedly not affected by RN 1734 (Bubolz et al., 2012). This is an interesting finding considering the bradykinin response is mediated by EC B_2 receptors, which, like mAChRs, are coupled to G proteins containing the G_q α subunit and stimulate PKC (Batenburg et al., 2004).The lack of effect of RN 1734 on bradykinin-induced vasodilation in coronary arteries may reflect differences between the vascular beds studied. Tajada et al. (2017) reported clusters of AKAP150 and TRPV4 were further apart in myocytes isolated from mouse mesenteric arteries than cerebral arteries. Subsequently, AngII stimulated TRPV4-dependent currents and Ca^{2+} sparklets in cerebral myocytes, but not mesenteric myocytes. Therefore, the ability for PKC to activate TRPV4 appears to be dependent on AKAP150 localization, which may differ between mesenteric and coronary arteries. How anchoring protein expression profiles vary between vascular beds is a promising avenue of research as it may also explain some of the variation in mechanisms of endothelium-dependent relaxation.

As well as vasodilation, TRPV4 has been shown to contribute to the intrinsic regulation of VSM contraction. Inhibition or knockdown of TRPV4 potentiated

vasoconstriction to PE in mouse mesenteric arteries (Hong et al., 2018). This was attributed to a flux of VSM IP_3 through MEGJs to the underlying endothelium, where it activated IP_3-sensitive TRPV4s and generated K_{Ca}-dependent EDH. Furthermore, in denuded mouse cerebral arteries, AngII-induced contraction was greater in TRPV4-null vessels, implicating loss of the regulatory TRPV4-RyR-BK_{Ca} axis in VSMCs (Earley et al., 2005; Mercado et al., 2014). In the current investigation, inhibition of endothelium-dependent relaxation potentiated contraction following α_1-AR activation in the presence of nifedipine, and direct depolarization of the VSM with elevated $[K^+]_o$. These observations indicate Ca^{2+} influx through VSM Ca_Vs in sufficient but not essential for stimulation of myoendothelial feedback in rat mesenteric arteries, which is similar to previous findings from our research group made in rat cremasteric arteries (Garland et al., 2017) (see Figure 1.3.2). Additionally, treatment of arteries with ryanodine also increased PE-induced contraction, without affecting relaxation to ACh, supporting a role for VSM RyRs in limiting contraction possibly by activating BK_{Ca}s. However, an involvement of TRPV4 in these feedback mechanisms is difficult to assess due to the unanticipated attenuation of α_1-AR- and voltage-dependent contraction by RN 1734.

An ability for TRPV4 activation to cause contraction was demonstrated during inhibition of NOS, IK_{Ca} and SK_{Ca} wherein GSK 1016790A caused robust contraction, which was sensitive to RN 1734 and nifedipine, and not reproducible within the same artery. The insensitivity to a second exposure likely reflects internalization of the channel, which has been shown by comparing the plasma

membrane expression of TRPV4 in TRPV4-expressing cells before and after stimulation with a maximal concentration of GSK 1016790A (Jin et al., 2011; Baratchi et al., 2019). The effects of RN 1734 and nifedipine on GSK 1016790A-induced contraction indicate cation influx through TRPV4s can depolarize the VSM and mediate Ca_V opening, a mechanism already described for other VSM TRP channels (Earley and Brayden, 2015). A similar effect of GSK 1016790A was reported in denuded rat pulmonary arteries, suggesting TRPV4s localised to the VSM are responsible rather than endothelial TRPV4s which could mediate the release of an endothelium-derived diffusible contractile factor such as endothelin-1 (Hilgers and De Mey, 2009; Sukumaran et al., 2013). TRPV4-dependent contraction is evidence against an association of TRPV4 with the RyR-BK_{Ca} complex in VSMCs, which was previously shown to cause relaxation in denuded rat cerebral arteries following exposure to EET (Earley et al., 2005) and limit contraction to AngII in denuded mouse cerebral arteries (Mercado et al., 2014). This discrepancy may reflect an ability for EET and AngII to activate a sub-population of TRPV4s closely associated with RyRs or represent another example of a difference between vascular beds with regards to TRPV4s function.

Evidence for a role for TRPV4 in mediating contraction to other stimuli was provided by the observation that TRPV4 inhibition with RN 1734 reduced the response to α_1-AR activation. The contraction was attenuated further in the additional presence of nifedipine. A similar trend was observed during direct depolarization of the VSM wherein 45 mM K^+-induced contraction was partially blocked with RN 1734 and completely prevented with the combination of RN 1734

and nifedipine. These data suggest TRPV4 may be activated during depolarization-independent PE-induced contraction and exhibit sensitivity to changes in membrane potential. However, the latter is not usually a characteristic of TRP channels. Moreover, patch-clamp experiments with TRPV4-expressing HEK cells did not report a significant change in current density at positive membrane voltages in the absence of an agonist (Phelps et al., 2010). Alternatively, TRPV4 could be activated by Ca^{2+} influx through Ca_Vs during stimulation with elevated $[K^+]_o$, thus contributing to the increase in $[Ca^{2+}]_i$ and amplifying the contractile response (see Figure 5.4.1B). However, a previous investigation reported contraction to 60 mM K^+ was not different between mesenteric arteries isolated from wild-type and TRPV4-null mice (Zhang et al., 2009). Thus, the possibility that inhibition of contraction may be due to an off-target action of RN 1734 can't be disregarded.

RN 1734 is a commonly used TRPV4 antagonist which inhibited 4α-PDD-induced Ca^{2+} influx in HEK cells expressing rat TRPV4 with an IC_{50} of 3.2 µM, and has been used in the range of 10-30 µM during previous investigations with small resistance arteries (Bagher et al., 2012; Bubolz et al., 2012; Ma et al., 2013; Zheng et al., 2013; Seki et al., 2017). It also exhibited a relatively high selectivity for TRPV4 over a panel of related TRP channels consisting of TRPV1, TRPV3 and transient receptor potential cation channel subfamily M member 8 (Vincent et al., 2009). However, in a study conducted with denuded pulmonary arteries isolated from TRPV4-null mice, 5-30 µM RN 1734 acutely caused vasodilation following preconstriction with 60 mM $[K^+]_o$. The authors of the investigation do not

provide an explanation for this result other than suggesting the antagonist may have an off-target effect which inhibits depolarization-dependent contraction. Subsequently, care must be taken when interpreting the results presented in the current investigation. Moreover, to take this research forward it is essential to confirm the specificity of RN 1734 and consider the use of other TRPV4 antagonists and knockdown approaches.

Reassuringly, our research group has previously demonstrated 30 μM RN 1734 does not reduce Ca_V-dependent myogenic tone in rat cremasteric arteries and increases the degree of intrinsic vasoconstriction at low pressure (Garland et al., 2017). This suggests the association of TRPV4 with Ca_Vs is not present in this tissue or RN 1734 does not have off-target effects against Ca^{2+} influx through Ca_Vs. In the current study RN 1734 attenuated myogenic tone in rat coronary arteries, implicating the involvement of TRPV4 in pressure-induced depolarization. Previous investigations with human coronary arteries reported RN 1734 did not affect basal vascular tone (Bubolz et al., 2012; Zheng et al., 2013). However, these studies also relied on the use of endothelin-1 for preconstriction to study dilatory responses as the level of myogenic tone was never more than 10%. This is in contrast to ~35% tone in rat coronary arteries reported here and may reflect compromised vascular health in arteries from patients requiring coronary bypass procedures. Furthermore, a role for TRPV4 in myogenic tone has previously been identified in renal arteries of neonatal pigs using the TRPV4 blocker HC 0670047, which is structurally distinct from RN 1734 (Soni et al., 2017). Alternatively, the effect of RN 1734 may represent an off-target effect at a

channel involved in pressure-induced contraction in coronary arteries besides the Ca_V which doesn't contribute to cremasteric artery myogenic tone development. Potential candidates include members of the canonical, melastatin or polycistin subfamilies of TRP channels which have also been identified as playing a role in myogenic tone (Baylie and Brayden, 2011). Regardless, the difference in effect of RN 1734 between rat coronary and cremasteric arteries indicates the mechanism of pressure-induced vasoconstriction is variable between tissue beds which warrants further investigation in and of itself.

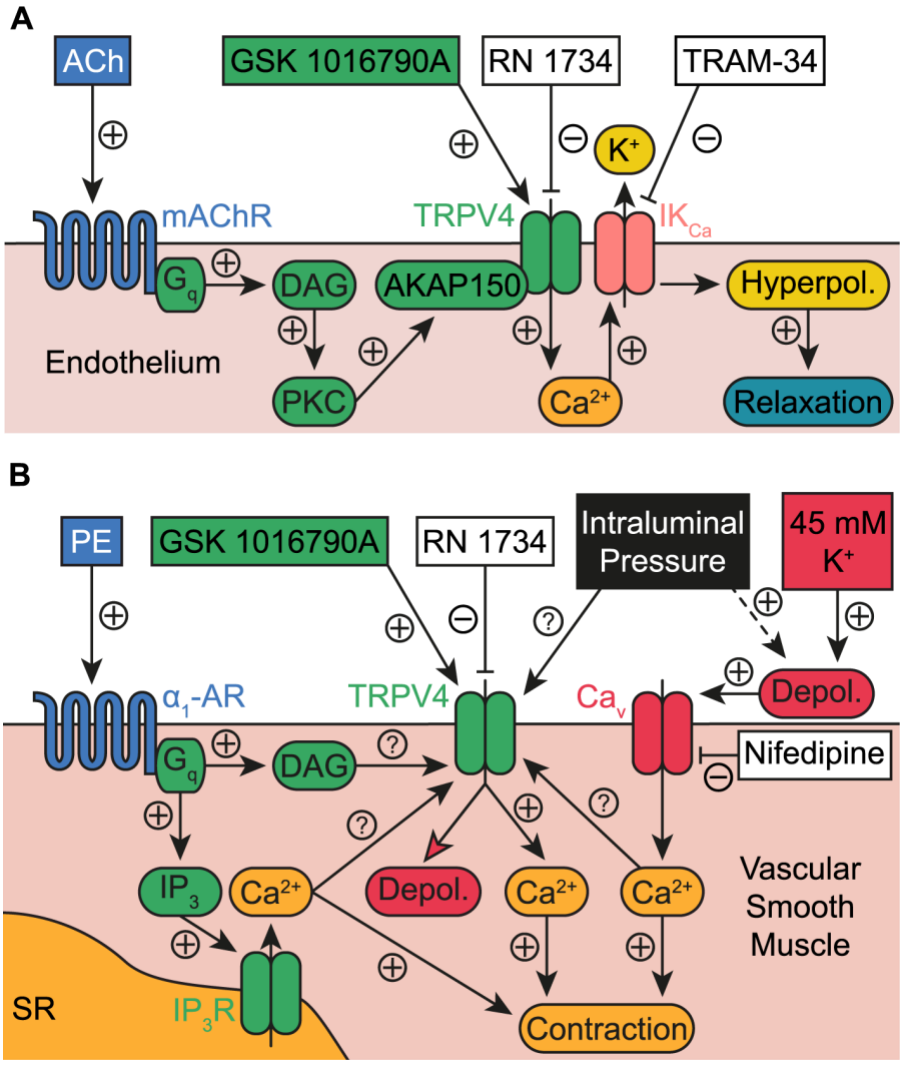


Figure 5.4.1 Proposed mechanism of TRPV4-dependent relaxation (**A**) and contraction (**B**) in the current investigation. Boxes with curved edges represent intracellular signalling components. Boxes with sharp edges represent agonists or antagonists. Arrows with a red arrowhead indicate direction of positive current. Arrows with a dashed line represent an indirect effect.

5.5 CONCLUSION

The findings of the current study partially supported the hypothesis. A role for TRPV4 in mediating IK_{Ca}-dependent relaxation was confirmed, but an evaluation of its contribution to myoendothelial feedback was difficult due to a direct inhibition of VSM TRPV4s, and hence vasoconstriction, by RN 1734. This inhibition may reflect an essential role of TRPV4 in agonist-stimulated and depolarization-dependent contraction, as well as myogenic tone development. However, it may also represent a previously unaccounted for off-target effect of RN 1734 on depolarization-dependent contraction. Both possibilities demand further exploration and have far-reaching implications for the study of vascular TRPV4.

6.0 FUTURE DIRECTIONS

The overarching aim of this thesis was to explore the modulation of vascular tone by myoendothelial feedback and the signalling pathways regulating its activation in resistance arteries (see Section 1.3.2 and Section 1.3.3). The most significant findings of the research presented here pertain to the experimental approaches employed for the study of resistance artery physiology, with the unexpected finding for the potential role for pressure-induced ROCK activation in restricting the influence of the endothelium in feeding back against vasoconstriction. Section 4.0 provides the first evidence that the effect of EC activation during vasoconstriction differs between pressurised arteries and arteries studied isometrically. This observation may offer an explanation for some of the discrepancies reported in studies into myoendothelial feedback.

Previously, ablation of the endothelial input increased the sensitivity of rat mesenteric arteries in the wire myograph to submaximal concentrations of either PE or NAD (Dora et al., 2000; Wei et al., 2018), which is reiterated by the findings reported here using PE (see Section 4.3.1). In contrast, Hong et al. (2018) reported inhibition of NO and EDH production did not affect pressurised mouse mesenteric artery sensitivity to adrenergic stimulation, but rather prevented the vasodilation observed immediately following constriction with maximal concentrations of PE. Similarly, Yashiro and Duling, (2000) reported the magnitude of contraction to PE in pressurised hamster cremasteric arteries was unaffected by blockade of NOS and endothelial K_{Ca}s, but the response was sustained for longer than under control conditions. These observations are synonymous with our pressure myography experiments (see Section 4.3.1) and

suggest under isobaric conditions myoendothelial feedback serves to limit maximal constriction as opposed to regulating artery sensitivity. A similar notion was put forward by our research group during an investigation with pressurised rat cremasteric arteries. We reported PE- and BayK 8644-induced contraction was potentiated in the presence of TRAM-34 due to the loss of EC-dependent dilation, only after the peak response (Garland et al., 2017). Although the overall implication of these studies is similar, in that EC activation regulates contraction, the profile of the feedback response is quite different between experimental approaches and therefore the physiological role of myoendothelial feedback may be misjudged.

A lack of effect of endothelium-derived factors on submaximal contraction in pressurised arteries was also demonstrated in Sections 3.0 and 4.0 as EFS- and ATP-induced vasoconstriction, which were consistently less than 50% of the maximum response, were completely insensitive to NOS and K_{Ca} blockade (see Sections 3.3.3 and 4.3.2). This difference has been eluded to previously in studies examining the effect of elevated vascular tone on responses to ATP (Pakdeechote et al., 2007; Rummery et al., 2007), but not in the context of myoendothelial feedback. The current investigation raised the possibility the difference in vasoreactivity may represent increased activation of ROCK signalling, which has previously been reported to contribute to pressure-induced depolarization and vasoconstriction in rat cerebral and mouse mesenteric arteries. In the pressure myography experiments reported here, ROCKII inhibition attenuated vasoconstriction to PE and increased vasodilation to ACh and

DEA/NO to almost exactly match the responses in the wire myograph (see Sections 4.3.6 and 4.3.7). Based on these findings, it is tempting to speculate ROCK activity is amplified under isobaric conditions, which conveys a reduced sensitivity to NO-dependent myoendothelial feedback. To investigate this hypothesis, the first step is to examine PE-induced EC Ca^{2+} activity in pressurised mesenteric arteries, as previous investigations have done (Schuster et al., 2001; Lamboley et al., 2005; Kansui et al., 2008), and ensure ROCKII inhibition with H1152 does not amplify the Ca^{2+} response. Such a finding would indicate RhoA signalling does not affect the transmission of Ca^{2+} or IP_3 through MEGJs and any observed influence of ROCK inhibition on the feedback response occurs downstream of EC activation. Next, it is crucial to probe the effect of ROCK inhibition on the potentiation of PE-induced contraction following blockade of endothelium-dependent vasodilation. If the hypothesis holds true, L-NAME, TRAM-34 and apamin will increase contraction to submaximal concentrations of PE in the additional presence of H1152, similar to the trend observed under isometric conditions. Moreover, the same experimental conditions could be applied to the studies described in Section 3.0, as ROCK inhibition may also unmask myoendothelial feedback during submaximal contraction during EFS. This is a worthwhile series of experiments to pursue that has implications for research into endothelial regulation of vascular tone and the pathophysiology of hypertension wherein increased ROCK activity reportedly contributes to vascular dysfunction (Yao et al., 2010; Björling et al., 2018).

Another reported difference between pressurised arteries and arteries studied isometrically is the development of myogenic tone, which is essential for the maintenance of blood flow and pressure (Buus et al., 1994; Dunn et al., 1994; Wei et al., 2018). A previous study with rat parenchymal arteries demonstrated ROCK signalling is an essential component of this phenomenon and may be activated by mechanosensitive ROCs. Although a role for activation of ROCK during the myogenic response was not examined in the investigations presented here, TRPV4 inhibition with RN 1734 unexpectedly attenuated the vasoconstriction to pressure in rat coronary arteries (see section 5.3.10). An association between TRPV4 and RhoA-dependent signalling has not been established in the vasculature, but a recent study reported compression of cultured human fibrosarcoma cells caused an increase in ROCK activity which was dependent on Ca^{2+} influx through TRPV4 (He et al., 2018). Considering the mechanosensitive nature of TRPV4 and the ability for its agonist GSK 1016790A to cause voltage-dependent contraction (see Section 5.3.7 and 5.3.8), exploring its involvement in coronary artery vasoconstriction further may partially explain the link between intraluminal pressure and membrane depolarization, which is currently poorly characterised. However, this line of investigation will require a different approach to the techniques utilised in the current investigation as pharmacological blockade of TRPV4 attenuated both contraction and IK_{Ca}-mediated hyperpolarization. That being said, one possible method of avoiding this is to study the effect of RN 1734 on myogenic tone development in denuded coronary arteries, to specifically probe the role of TRPV4 expressed in VSMCs. Additionally, the use of Ca^{2+} imaging would prove insightful, as it would establish

whether pressure-induced TRPV4 activity contributes to the whole-cell Ca^{2+} increase responsible for vasoconstriction or if TRPV4-dependent sparklets can mediate ROCK activation without affecting the global Ca^{2+} response.

It is clear that although much evidence supports the presence of myoendothelial feedback in arteries, an ability to study Ca^{2+} and functional responses in pressurised arteries is the closest *ex vivo* model to that found *in vivo*. An ability to assess changes in models of microvascular dysfunction, and to translate the key observations to humans are the longer-term goals of this study.

7.0 REFERENCES

Aldasoro, M., Martínez, C., Vila, J.M., Medina, P., and Lluch, S. (1996). Influence of endothelial nitric oxide on neurogenic contraction of human cerebral arteries. *J. Cereb. Blood Flow Metab. 16*: 623–628.

Anschütz, S., and Schubert, R. (2005). Modulation of the myogenic response by neurogenic influences in rat small arteries. *Br. J. Pharmacol. 146*: 226–33.

Bagher, P., Beleznai, T., Kansui, Y., Mitchell, R., Garland, C.J., and Dora, K.A. (2012). Low intravascular pressure activates endothelial cell TRPV4 channels, local Ca^{2+} events, and IK_{Ca} channels, reducing arteriolar tone. *Proc. Natl. Acad. Sci. U. S. A. 109*: 18174–18179.

Baratchi, S., Keov, P., Darby, W.G., Lai, A., Khoshmanesh, K., Thurgood, P., Vahidi, P., Ejendal, K., and McIntyre, P. (2019). The TRPV4 agonist GSK1016790A regulates the membrane expression of TRPV4 channels. *Front. Pharmacol. 9*: 6.

Batenburg, W.W., Garrelds, I.M., Kats, J.P. van, Saxena, P.R., and Jan Danser, A.H. (2004). Mediators of bradykinin-induced vasorelaxation in human coronary microarteries. *Hypertension 43*: 488–492.

Baylie, R.L., and Brayden, J.E. (2011). TRPV channels and vascular function. *Acta Physiol. 203*: 99–116.

Bayliss, W.M. (1902). On the local reactions of the arterial wall to changes of internal pressure. *J. Physiol. 28*: 220–231.

Bevan, J.A., and Osher, J. V. (1972). A direct method for recording tension changes in the wall of small blood vessels in vitro. *Agents Actions 2*: 257–260.

Björling, K., Joseph, P.D., Egebjerg, K., Salomonsson, M., Hansen, J.L.,

Ludvigsen, T.P., and Jensen, L.J. (2018). Role of age, Rho-kinase 2 expression, and G protein-mediated signaling in the myogenic response in mouse small mesenteric arteries. *Physiol. Rep. 6*: e13863–e13863.

Boettcher, M., and Wit, C. de (2011). Distinct endothelium-derived hyperpolarizing factors emerge in vitro and in vivo and are mediated in part via connexin 40–dependent myoendothelial coupling. *Hypertension 57*: 802–808.

Bohr, D.F., and Goulet, P.L. (1961). Direct tension recording from smooth muscle of resistance vessels from various organs. *Angiology 12*: 478–485.

Bowles, D.K., Hu, Q., Laughlin, M.H., and Sturek, M. (1997). Heterogeneity of L-type calcium current density in coronary smooth muscle. *Am. J. Physiol. - Hear. Circ. Physiol. 273*: H2083–H2089.

Briones, A.M., Daly, C.J., Jiménez-Altayó, F., Martinez-Revelles, S., Gonzalez, J.M., McGrath, J.C., and Vila, E. (2005). Direct demonstration of β_1- and evidence against β_2- and β_3-adrenoceptors, in smooth muscle cells of rat small mesenteric arteries. *Br. J. Pharmacol. 146*: 679–691.

Brock, J.A., and Helden, D.F. Van (1995). Enhanced excitatory junction potentials in mesenteric arteries from spontaneously hypertensive rats. *Pflugers Arch. Eur. J. Physiol. 430*: 901–908.

Brozovich, F. V., Nicholson, C.J., Degen, C. V., Gao, Y.Z., Aggarwal, M., and Morgan, K.G. (2016). Mechanisms of vascular smooth muscle contraction and the basis for pharmacologic treatment of smooth muscle disorders. *Pharmacol. Rev. 68*: 476–532.

Bubolz, A.H., Mendoza, S.A., Zheng, X., Zinkevich, N.S., Li, R., Gutterman, D.D.,

and Zhang, D.X. (2012). Activation of endothelial TRPV4 channels mediates flow-induced dilation in human coronary arterioles: role of Ca^{2+} entry and mitochondrial ROS signaling. *Am. J. Physiol. Circ. Physiol. 302*: H634–H642.

Buus, N.H., VanBavel, E., and Mulvany, M.J. (1994). Differences in sensitivity of rat mesenteric small arteries to agonists when studied as ring preparations or as cannulated preparations. *Br. J. Pharmacol. 112*: 579–587.

Chadha, P.S., Liu, L., Rikard-Bell, M., Senadheera, S., Howitt, L., Bertrand, R.L., Grayson, T.H., Murphy, T. V., and Sandow, S.L. (2011). Endothelium-dependent vasodilation in human mesenteric artery is primarily mediated by myoendothelial gap junctions intermediate conductance calcium-activated K+ channel and nitric oxide. *J. Pharmacol. Exp. Ther. 336*: 701–708.

Chitaley, K., and Webb, R.C. (2002). Nitric oxide induces dilation of rat aorta via inhibition of Rho-kinase signaling. *Hypertension 39*: 438–442.

Dora, K.A. (2017). Conducted dilatation to ATP and K^+ in rat skeletal muscle arterioles. *Acta Physiol. 219*: 202–218.

Dora, K.A., Doyle, M.P., and Duling, B.R. (1997). Elevation of intracellular calcium in smooth muscle causes endothelial cell generation of NO in arterioles. *Proc. Natl. Acad. Sci. 94*: 6529–6534.

Dora, K.A., Gallagher, N.T., McNeish, A.J., and Garland, C.J. (2008). Modulation of endothelial cell $K_{Ca}3.1$ channels during endothelium-derived hyperpolarizing factor signaling in mesenteric resistance arteries. *Circ. Res. 102*: 1247–1255.

Dora, K.A., Hinton, J.M., Walker, S.D., and Garland, C.J. (2000). An indirect influence of phenylephrine on the release of endothelium-derived

vasodilators in rat small mesenteric artery. *Br. J. Pharmacol. 129*: 381–7.

Dora, K.A., Sandow, S.L., Gallagher, N.T., Takano, H., Rummery, N.M., Hill, C.E., and Garland, C.J. (2003). Myoendothelial gap junctions may provide the pathway for EDHF in mouse mesenteric artery. *J. Vasc. Res. 40*: 480–490.

Du, J., Wang, X., Li, J., Guo, J., Liu, L., Yan, D., Yang, Y., Li, Z., Zhu, J., and Shen, B. (2016). Increasing TRPV4 expression restores flow-induced dilation impaired in mesenteric arteries with aging. *Sci. Rep. 6*:.

Duling, B.R., Gore, R.W., Dacey, R.G., and Damon, D.N. (1981). Methods for isolation, cannulation, and in vitro study of single microvessels. *Am. J. Physiol. - Hear. Circ. Physiol. 10*: H108–H116.

Dunn, W.R., Brock, J.A., and Hardy, T.A. (1999). Electrochemical and electrophysiological characterization of neurotransmitter release from sympathetic nerves supplying rat mesenteric arteries. *Br. J. Pharmacol. 128*: 174–80.

Dunn, W.R., Wellman, G.C., and Bevan, J.A. (1994). Enhanced resistance artery sensitivity to agonists under isobaric compared with isometric conditions. *Am. J. Physiol. 266*: H147–H155.

Earley, S., and Brayden, J.E. (2015). Transient receptor potential channels in the vasculature. *Physiol. Rev. 95*: 645–690.

Earley, S., Heppner, T.J., Nelson, M.T., and Brayden, J.E. (2005). TRPV4 forms a novel Ca^{2+} signaling complex with ryanodine receptors and BK_{Ca} channels. *Circ. Res. 97*: 1270–1279.

Earley, S., Pauyo, T., Drapp, R., Tavares, M.J., Liedtke, W., and Brayden, J.E.

(2009). TRPV4-dependent dilation of peripheral resistance arteries influences arterial pressure. *Am. J. Physiol. Circ. Physiol. 297*: H1096–H1102.

Falloon, B.J., Stephens, N., Tulip, J.R., and Heagerty, A.M. (1995). Comparison of small artery sensitivity and morphology in pressurized and wire-mounted preparations. *Am. J. Physiol. Circ. Physiol. 268*: H670–H678.

Feletou, M., and Vanhoutte, P.M. (1989). Tetrodotoxin-insensitive relaxation of coronary arterial smooth muscle to electrical stimulation: Possible involvement of a dopaminergic mechanism. *J. Vasc. Res. 26*: 213–227.

Fleming, B.P., Barron, K.W., Howes, T.W., and Smith, J.K. (1987). Response of the microcirulation in rat cremaster muscle to peripheral and central sympathetic-stimulation. *Circ Res 61*: 26–31.

Furchgott, R.F., and Zawadzki, J. V. (1980). The obligatory role of endothelial cells in the relaxation of arterial smooth muscle by acetylcholine. *Nature 288*: 373–376.

Gao, F., and Wang, D.H. (2010). Hypotension induced by activation of the transient receptor potential vanilloid 4 channels: Role of Ca^{2+}-activated K^{+} channels and sensory nerves. *J. Hypertens. 28*: 102–110.

Garland, C.J., Bagher, P., Powell, C., Ye, X., Lemmey, H.A.L., Borysova, L., and Dora, K.A. (2017). Voltage-dependent Ca^{2+} entry into smooth muscle during contraction promotes endothelium-mediated feedback vasodilation in arterioles. *Sci. Signal. 10*: eaal3806.

Garland, C.J., Hiley, C.R., and Dora, K.A. (2011a). EDHF: Spreading the influence of the endothelium. *Br. J. Pharmacol. 164*: 839–852.

Garland, C.J., Yarova, P.L., Jiménez-Altayó, F., and Dora, K.A. (2011b). Vascular hyperpolarization to β-adrenoceptor agonists evokes spreading dilatation in rat isolated mesenteric arteries. *Br. J. Pharmacol. 164*: 913–921.

Godfraind, T. (1983). Actions of nifedipine on calcium fluxes and contraction in isolated rat arteries. *J. Pharmacol. Exp. Ther. 224*: 443–450.

Gokina, N.I., Park, K.M., McElroy-Yaggy, K., and Osol, G. (2005). Effects of Rho kinase inhibition on cerebral artery myogenic tone and reactivity. *J. Appl. Physiol. 98*: 1940–1948.

Goonetilleke, L., Ralevic, V., and Dunn, W.R. (2013). Influence of pressure on adenosine triphosphate function as a sympathetic neurotransmitter in small mesenteric arteries from the spontaneously hypertensive rat. *J. Hypertens. 31*: 312–320.

Gündüz, F., Meiselman, H.J., and Başkurt, O.K. (2008). High intravascular pressure attenuates vascular dilation responses of small mesenteric arteries in the rat. *Circ. J. 72*: 482–486.

Hardebo, J.E., Kåhrström, J., and Owman, C. (1989). Characterization of dilation induced by electrical field stimulation in mammalian cerebral and peripheral vessels. *Q. J. Exp. Physiol. 74*: 475–491.

Harrington, L.S., and Mitchell, J.A. (2004). Novel role for P2X receptor activation in endothelium-dependent vasodilation. *Br. J. Pharmacol. 143*: 611–617.

He, L., Tao, J., Maity, D., Si, F., Wu, Y., Wu, T., Prasath, V., Wirtz, D., and Sun, S.X. (2018). Role of membrane-tension gated Ca^{2+} flux in cell mechanosensation. *J. Cell Sci. 131*: jcs208470.

Heathcote, H.R., Lee, M.D., Zhang, X., Saunter, C.D., Wilson, C., and McCarron,

J.G. (2019). Endothelial TRPV4 channels modulate vascular tone by Ca^{2+}-induced Ca^{2+} release at inositol 1,4,5-trisphosphate receptors. *Br. J. Pharmacol.*

Hilgers, R.H.P., and Mey, J.G.R. De (2009). Myoendothelial coupling in the mesenteric arterial bed; Segmental differences and interplay between nitric oxide and endothelin-1. *Br. J. Pharmacol. 156*: 1239–1247.

Hong, K., Cope, E.L., DeLalio, L.J., Marziano, C., Isakson, B.E., and Sonkusare, S.K. (2018). TRPV4 (transient receptor potential vanilloid 4) channel–dependent negative feedback mechanism regulates G_q protein–coupled receptor–induced vasoconstriction. *Arterioscler. Thromb. Vasc. Biol. 38*: 542–554.

Ito, I., Jarajapu, Y.P.R., Grant, M.B., and Knot, H.J. (2007). Characteristics of myogenic tone in the rat ophthalmic artery. *Am. J. Physiol. - Hear. Circ. Physiol. 292*: H360–H368.

Jackson, W.F., Boerman, E.M., Lange, E.J., Lundback, S.S., and Cohen, K.D. (2009). Smooth muscle α_{1D}-adrenoceptors mediate phenylephrine-induced vasoconstriction and increases in endothelial cell Ca^{2+} in hamster cremaster arterioles. *Br. J. Pharmacol. 155*: 514–524.

Jensen, P.E. (1995). Electrical field stimulation of rat mesenteric small arteries: Force and free cytosolic calcium during neurogenic contractions and mechanisms of non-neurogenic relaxations. *Acta Physiol. Scand. 153*: 289–300.

Jin, M., Wu, Z., Chen, L., Jaimes, J., Collins, D., Walters, E.T., and O'Neil, R.G. (2011). Determinants of TRPV4 activity following selective activation by

small molecule agonist GSK1016790A. *PLoS One 6*: e16713.

Kansui, Y., Garland, C.J., and Dora, K.A. (2008). Enhanced spontaneous Ca2+ events in endothelial cells reflect signalling through myoendothelial gap junctions in pressurized mesenteric arteries. *Cell Calcium 44*: 135–146.

Kerr, P.M., Wei, R., Tam, R., Sandow, S.L., Murphy, T. V., Ondrusova, K., Lunn, S.E., Tran, C.H.T., Welsh, D.G., and Plane, F. (2015). Activation of endothelial IK_{Ca} channels underlies NO-dependent myoendothelial feedback. *Vascul. Pharmacol. 74*: 130–138.

Kügelgen, I. von, and Starke, K. (1985). Noradrenaline and adenosine triphosphate as co-transmitters of neurogenic vasoconstriction in rabbit mesenteric artery. *J. Physiol. 367*: 435–455.

Lamboley, M., Pittet, P., Koenigsberger, M., Sauser, R., Bény, J.-L., and Meister, J.-J. (2005). Evidence for signaling via gap junctions from smooth muscle to endothelial cells in rat mesenteric arteries: Possible implication of a second messenger. *Cell Calcium 37*: 311–320.

Lamont, C., Vainorius, E., and Wier, W.G. (2003). Purinergic and adrenergic Ca2+ transients during neurogenic contractions of rat mesenteric small arteries. *J. Physiol. 549*: 801–808.

Lamont, C., Vial, C., Evans, R.J., and Wier, W.G. (2006). $P2X_1$ receptors mediate sympathetic postjunctional Ca^{2+} transients in mesenteric small arteries. *Am J Physiol Hear. Circ Physiol 291*: H3106-13.

Lawton, P.F., Lee, M.D., Saunter, C.D., Girkin, J.M., McCarron, J.G., and Wilson, C. (2019). VasoTracker, a low-cost and open source pressure myograph system for vascular physiology. *Front. Physiol. 10*: 99.

Ledoux, J., Taylor, M.S., Bonev, A.D., Hannah, R.M., Solodushko, V., Shui, B., Tallini, Y., Kotlikoff, M.I., and Nelson, M.T. (2008). Functional architecture of inositol 1,4,5-trisphosphate signaling in restricted spaces of myoendothelial projections. *Proc. Natl. Acad. Sci. 105*: 9627–9632.

Lemmey, H.A.L., Ye, X., Ding, H.C., Triggle, C.R., Garland, C.J., and Dora, K.A. (2018). Hyperglycaemia disrupts conducted vasodilation in the resistance vasculature of db/db mice. *Vascul. Pharmacol. 103–105*: 29–35.

Li, Y., and Brayden, J.E. (2017). Rho kinase activity governs arteriolar myogenic depolarization. *J. Cereb. Blood Flow Metab. 37*: 140–152.

Luksha, L., Agewall, S., and Kublickiene, K. (2009). Endothelium-derived hyperpolarizing factor in vascular physiology and cardiovascular disease. *Atherosclerosis 202*: 330–344.

Ma, X., Du, J., Zhang, P., Deng, J., Liu, J., Lam, F., Li, R., Huang, Y., Jin, J., and Yao, X. (2013). Functional role of TRPV4-K_{Ca}2.3 signaling in vascular endothelial cells in normal and streptozotocin-induced diabetic rats. *Hypertension 62*: 134–9.

Martínez, C., Cases, E., Vila, J.M., Aldasoro, M., Medina, P., Marco, V., and Lluch, S. (1995). Influence of endothelial nitric oxide on neurogenic contraction of human pulmonary arteries. *Eur Respir J 8*: 1328–1332.

Mathewson, A.M., and Dunn, W.R. (2014). A comparison of responses to raised extracellular potassium and endothelium-derived hyperpolarizing factor (EDHF) in rat pressurised mesenteric arteries. *PLoS One 9*: e111977.

Mauban, J.R.H., Lamont, C., Balke, C.W., and Wier, W.G. (2001). Adrenergic stimulation of rat resistance arteries affects Ca^{2+} sparks, Ca^{2+} waves, and

Ca^{2+} oscillations. *AJP Hear. Circ. Physiol. 280*: H2399-405.

McNeish, A.J., Sandow, S.L., Neylon, C.B., Chen, M.X., Dora, K.A., and Garland, C.J. (2006). Evidence for involvement of both IK_{Ca} and SK_{Ca} channels in hyperpolarizing responses of the rat middle cerebral artery. *Stroke 37*: 1277–1282.

McSherry, I.N., Sandow, S.L., Campbell, W.B., Falck, J.R., Hill, M.A., and Dora, K.A. (2006). A role for heterocellular coupling and EETs in dilation of rat cremaster arteries. *Microcirculation 13*: 119–130.

Mercado, J., Baylie, R., Navedo, M.F., Yuan, C., Scott, J.D., Nelson, M.T., Brayden, J.E., and Santana, L.F. (2014). Local control of TRPV4 channels by AKAP150-targeted PKC in arterial smooth muscle. *J. Gen. Physiol. 143*: 559–575.

Moore, D.H., and Ruska, H. (1957). The fine structure of capillaries and small arteries. *J. Biophys. Biochem. Cytol. 3*: 457–462.

Mulvany, M.J., and Halpern, W. (1977). Contractile properties of small arterial resistance vessels in spontaneously hypertensive and normotensive rats. *Circ. Res. 41*: 19–26.

Nausch, L.W.M., Bonev, A., Heppner, T.J., Tallini, Y., Kotlikoff, M.I., and Nelson, M.T. (2012). Sympathetic nerve stimulation induces local endothelial Ca^{2+} signals to oppose vasoconstriction of mouse mesenteric arteries. *AJP Hear. Circ. Physiol. 302*: H594–H602.

Nishijima, Y., Zheng, X., Lund, H., Suzuki, M., Mattson, D.L., and Zhang, D.X. (2014). Characterization of blood pressure and endothelial function in TRPV4-deficient mice with L-NAME- and angiotensin II-induced

hypertension. *Physiol. Rep. 2*: e00199.

Pakdeechote, P., Rummery, N.M., Ralevic, V., and Dunn, W.R. (2007). Raised tone reveals purinergic-mediated responses to sympathetic nerve stimulation in the rat perfused mesenteric vascular bed. *Eur. J. Pharmacol. 563*: 180–186.

Phelps, C.B., Wang, R.R., Choo, S.S., and Gaudet, R. (2010). Differential regulation of TRPV1, TRPV3, and TRPV4 sensitivity through a conserved binding site on the ankyrin repeat domain. *J. Biol. Chem. 285*: 731–740.

Rao, M.Y., Soliman, H., Bankar, G., Lin, G., and MacLeod, K.M. (2013). Contribution of Rho kinase to blood pressure elevation and vasoconstrictor responsiveness in type 2 diabetic Goto-Kakizaki rats. *J. Hypertens. 31*: 1160–1169.

Riper, D.A. Van, and Bevan, J.A. (1991). Evidence that neuropeptide Y and norepinephrine mediate electrical field-stimulated vasoconstriction of rabbit middle cerebral artery. *Circ. Res. 68*: 568–577.

Rummery, N.M., Brock, J.A., Pakdeechote, P., Ralevic, V., and Dunn, W.R. (2007). ATP is the predominant sympathetic neurotransmitter in rat mesenteric arteries at high pressure. *J. Physiol. 582*: 745–54.

Sandow, S.L., Tare, M., Coleman, H.A., Hill, C.E., and Parkington, H.C. (2002). Involvement of myoendothelial gap junctions in the actions of endothelium-derived hyperpolarizing factor. *Circ. Res. 90*: 1108–1113.

Schuster, A., Oishi, H., Bény, J.-L., Stergiopulos, N., and Meister, J.-J. (2001). Simultaneous arterial calcium dynamics and diameter measurements: application to myoendothelial communication. *AJP Hear. Circ. Physiol. 280*:

H1088-96.

Seki, T., Goto, K., Kiyohara, K., Kansui, Y., Murakami, N., Haga, Y., Ohtsubo, T., Matsumura, K., and Kitazono, T. (2017). Downregulation of endothelial transient receptor potential vanilloid type 4 channel and small-conductance of Ca^{2+}-activated K^{+} channels underpins impaired endothelium-dependent hyperpolarization in hypertension. *Hypertension 69*: 143–153.

Shaw, L., O'Neill, S., Jones, C.J.P., Austin, C., and Taggart, M.J. (2009). Comparison of U46619-, endothelin-1- or phenylephrine-induced changes in cellular Ca^{2+} profiles and Ca^{2+} sensitisation of constriction of pressurised rat resistance arteries. *Br. J. Pharmacol. 141*: 678–688.

Søndergaard, A.M., Overgaard, C.B., Mazur, A., Postnov, D.D., Matchkov, V. V., and Aalkjær, C. (2019). Rat mesenteric small artery neurogenic dilatation is predominantly mediated by β_1-adrenoceptors in vivo. *J. Physiol. 597*: 1819–1831.

Soni, H., Peixoto-Neves, D., Matthews, A.T., and Adebiyi, A. (2017). TRPV4 channels contribute to renal myogenic autoregulation in neonatal pigs. *Am. J. Physiol. - Ren. Physiol. 313*: F1136–F1148.

Sonkusare, S.K., Bonev, A.D., Ledoux, J., Liedtke, W., Kotlikoff, M.I., Heppner, T.J., Hill-Eubanks, D.C., and Nelson, M.T. (2012). Elementary Ca^{2+} signals through endothelial TRPV4 channels regulate vascular function. *Science (80-.). 336*: 597–601.

Sonkusare, S.K., Dalsgaard, T., Bonev, A.D., Hill-Eubanks, D.C., Kotlikoff, M.I., Scott, J.D., Santana, L.F., and Nelson, M.T. (2014). AKAP150-dependent cooperative TRPV4 channel gating is central to endothelium-dependent

vasodilation and is disrupted in hypertension. *Sci. Signal. 7*: ra66 LP-ra66.

Straub, A.C., Zeigler, A.C., and Isakson, B.E. (2014). The myoendothelial junction: Connections that deliver the message. *Physiology 29*: 242–249.

Sukumaran, S. V., Singh, T.U., Parida, S., Narasimha Reddy, C.E., Thangamalai, R., Kandasamy, K., Singh, V., and Mishra, S.K. (2013). TRPV4 channel activation leads to endothelium-dependent relaxation mediated by nitric oxide and endothelium-derived hyperpolarizing factor in rat pulmonary artery. *Pharmacol. Res. 78*: 18–27.

Swärd, K., Mita, M., Wilson, D.P., Deng, J.T., Susnjar, M., and Walsh, M.P. (2003). The role of RhoA and Rho-associated kinase in vascular smooth muscle contraction. *Curr. Hypertens. Rep. 5*: 66–72.

Tajada, S., Moreno, C.M., O'Dwyer, S., Woods, S., Sato, D., Navedo, M.F., and Santana, L.F. (2017). Distance constraints on activation of TRPV4 channels by AKAP150-bound PKCα in arterial myocytes. *J. Gen. Physiol. 149*: 639 LP – 659.

Tarasova, O., Sjöblom-Widfeldt, N., and Nilsson, H. (2003). Transmitter characteristics of cutaneous, renal and skeletal muscle small arteries in the rat. *Acta Physiol. Scand. 177*: 157–166.

Tran, C.H.T., Taylor, M.S., Plane, F., Nagaraja, S., Tsoukias, N.M., Solodushko, V., Vigmond, E.J., Furstenhaupt, T., Brigdan, M., and Welsh, D.G. (2012). Endothelial Ca^{2+} wavelets and the induction of myoendothelial feedback. *AJP Cell Physiol. 302*: C1226–C1242.

Tuttle, J.L., and Falcone, J.C. (2001). Nitric oxide release during α_1-adrenoceptor-mediated constriction of arterioles. *AJP Hear. Circ. Physiol.*

281: H873-81.

Tykocki, N.R., Boerman, E.M., and Jackson, W.F. (2017). Smooth muscle ion channels and regulation of vascular tone in resistance arteries and arterioles. *Compr. Physiol. 7*: 485–581.

Vincent, F., Acevedo, A., Nguyen, M.T., Dourado, M., DeFalco, J., Gustafson, A., Spiro, P., Emerling, D.E., Kelly, M.G., and Duncton, M.A.J. (2009). Identification and characterization of novel TRPV4 modulators. *Biochem. Biophys. Res. Commun. 389*: 490–494.

Wei, R., Lunn, S.E., Tam, R., Gust, S.L., Classen, B., Kerr, P.M., and Plane, F. (2018). Vasoconstrictor stimulus determines the functional contribution of myoendothelial feedback to mesenteric arterial tone. *J. Physiol. 596*: 1181–1197.

Westcott, E.B., and Segal, S.S. (2013). Perivascular innervation: A multiplicity of roles in vasomotor control and myoendothelial signaling. *Microcirculation 20*: 217–238.

Winter, P., and Dora, K.A. (2007). Spreading dilatation to luminal perfusion of ATP and UTP in rat isolated small mesenteric arteries. *J. Physiol. 582*: 335–347.

Yang, X.R., Lin, A.H.Y., Hughes, J.M., Flavahan, N.A., Cao, Y.N., Liedtke, W., and Sham, J.S.K. (2012). Upregulation of osmo-mechanosensitive TRPV4 channel facilitates chronic hypoxia-induced myogenic tone and pulmonary hypertension. *Am. J. Physiol. - Lung Cell. Mol. Physiol. 302*: L555–L568.

Yao, L., Romero, M.J., Toque, H.A., Yang, G., Caldwell, R.B., and Caldwell, R.W. (2010). The role of RhoA/Rho kinase pathway in endothelial dysfunction. *J.*

Cardiovasc. Dis. Res. 1: 165–170.

Yarova, P.L., Smirnov, S. V., Dora, K.A., and Garland, C.J. (2013). β_1-Adrenoceptor stimulation suppresses endothelial IK_{Ca}-channel hyperpolarization and associated dilatation in resistance arteries. *Br. J. Pharmacol. 169*: 875–886.

Yashiro, Y., and Duling, B.R. (2000). Integrated Ca^{2+} signaling between smooth muscle and endothelium of resistance vessels. *Circ. Res. 87*: 1048–1054.

Yasuda, N., Kasuya, Y., Yamada, G., Hama, H., Masaki, T., and Goto, K. (1994). Loss of contractile activity of endothelin-1 induced by electrical field stimulation-generated free radicals. *Br. J. Pharmacol. 113*: 21–28.

Zhang, D.X., Mendoza, S.A., Bubolz, A.H., Mizuno, A., Ge, Z.D., Li, R., Warltier, D.C., Suzuki, M., and Gutterman, D.D. (2009). Transient receptor potential vanilloid type 4-deficient mice exhibit impaired endothelium-dependent relaxation induced by acetylcholine in vitro and in vivo. *Hypertension 53*: 532–538.

Zheng, X., Zinkevich, N.S., Gebremedhin, D., Gauthier, K.M., Nishijima, Y., Fang, J., Wilcox, D.A., Campbell, W.B., Gutterman, D.D., and Zhang, D.X. (2013). Arachidonic acid-induced dilation in human coronary arterioles: convergence of signaling mechanisms on endothelial TRPV4-mediated Ca^{2+} entry. *J. Am. Heart Assoc. 2*: e000080.

Zhong, Y., Feng, X., Xu, T., Yang, C., Zhang, W., Chen, X., Fan, X., Lu, L., Zhang, M., Li, L., and Xu, Z. (2019). Inherited risk plus prenatal insult caused malignant dysfunction in mesenteric arteries in adolescent SHR offspring. *PLoS One 14*: e0215994.